

2003

Controls on the delivery of fluvial sediment to the coastal ocean: The Salinas River, California

Katherine L. Farnsworth

College of William and Mary - Virginia Institute of Marine Science

Follow this and additional works at: <https://scholarworks.wm.edu/etd>



Part of the [Geology Commons](#), and the [Hydrology Commons](#)

Recommended Citation

Farnsworth, Katherine L., "Controls on the delivery of fluvial sediment to the coastal ocean: The Salinas River, California" (2003). *Dissertations, Theses, and Masters Projects*. Paper 1539616643.

<https://dx.doi.org/doi:10.25773/v5-m27h-qr85>

This Dissertation is brought to you for free and open access by the Theses, Dissertations, & Master Projects at W&M ScholarWorks. It has been accepted for inclusion in Dissertations, Theses, and Masters Projects by an authorized administrator of W&M ScholarWorks. For more information, please contact scholarworks@wm.edu.

Controls on the Delivery of Fluvial Sediment to the Coastal Ocean:
The Salinas River, California

A Dissertation
Presented to
The Faculty of the School of Marine Science
The College of William and Mary in Virginia

In Partial Fulfillment
Of the Requirements for the Degree of
Doctor of Philosophy

By

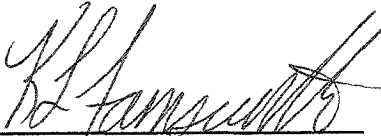
Katherine L. Farnsworth 2003

APPROVAL SHEET

This dissertation is submitted in partial fulfillment of

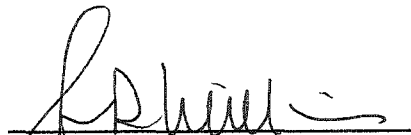
The requirements for the degree of

Doctor of Philosophy

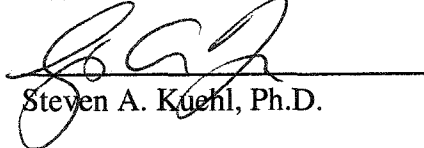


Katherine L. Farnsworth

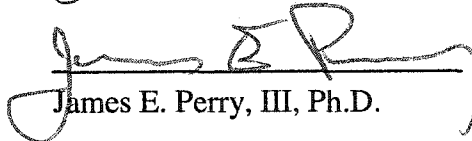
Approved July, 2003



John D. Milliman, Ph.D.
Committee Chairman/Advisor



Steven A. Kuehl, Ph.D.



James E. Perry, III, Ph.D.



Gregory S. Hancock, Ph.D.
Department of Geology
College of William and Mary



Jonathan A. Warrick, Ph.D.
United States Geological Survey
Menlo Park, CA

DEDICATION

I dedicate this dissertation to my nephews,
Derin and Adem Dogu.

As I near the end of being a student, they are just beginning.

Thanks for helping me to still see the wonder in the world,
from the sand on the beach to the beauty of a flower,
and of course the life changing thrill of catching your first fish.
I think we still have a lot to learn from each other.

I also want to thank them for still thinking I am 'cool',
even though I am a "Mud Doctor" not a "Dinosaur Doctor".

"The real voyage of discovery is not in seeking new landscapes but in having new eyes"
~ Marcel Proust

TABLE OF CONTENTS

	Page
Acknowledgements	vi
List of Tables	vii
List of Figures	viii
Abstract	x
Chapter 1: Introduction	2
1.1 Introduction	3
1.2 Aims and Organization	6
1.3 Global Estimates	6
1.3.1 Data and Methods	7
1.3.1.1 Global Freshwater Flux	8
1.3.1.2 Global Dissolved Solid Flux	8
1.3.1.3 Global Suspended Sediment Flux	12
1.3.2 Global Patterns	15
1.4 Character of Dryland Rivers	20
1.4.1 Sediment Delivery from Rivers	25
1.5 References	31
Chapter 2: Effects of Climatic and Anthropogenic Change on Small Mountainous Rivers: The Salinas River Example	36
2.1 Introduction	37
2.1.1 Variability in Sediment Discharge	40
2.1.2 Climate Change	41
2.1.3 Anthropogenic Impact	46
2.2 Problems with Estimating Sediment Discharge	48
2.3 Response to Change and Episodic Events: the Salinas River Example	49
2.4 Discussion	61
2.5 Acknowledgements	62
2.6 References	64
Chapter 3: Local and Global Controls on the Magnitude and Timing of Fluvial Delivery from the Salinas River	67
3.1 Introduction	68
3.2 General Hydrology of the Watershed	71
3.2.1 Hydrologic Data and Methods	73
3.2.1.1 Discharge	73
3.2.1.2 Sediment	79
3.3 Local Controls	83

3.3.1	Groundwater System	83
3.3.2	Precipitation Distribution	88
3.3.3	Salinas Lagoon	91
3.3.4	Human Impact	91
3.4	Global Controls	94
3.4.1	El Niño/Southern Oscillation	96
3.4.2	Pacific Decadal Oscillation	98
3.4.3	Interactions with Salinas River	99
3.5	Events	106
3.5.1	Hyperpycnal Flows	114
3.6	Summary	115
3.7	References	119
Chapter 4: Long-term Sediment Storage on the Monterey		
	Bay Continental Shelf	124
4.1	Introduction	125
4.1.1	Salinas Shelf	125
4.1.2	Delivery System	129
4.2	Methods	132
4.3	Results and Discussion	134
4.3.1	Long-term Sediment Storage	134
4.3.2	Short-term Sediment Storage	141
4.4	Summary	148
4.5	References	151
Chapter 5: Summary		154
5.1	Summary	155
5.2	References	159
Vita	160

ACKNOWLEDGMENTS

Over the many years I have spent here at the Virginia Institute of Marine Science, so many people have helped me and made this experience an enjoyable one.

First I must thank Dr. John Milliman, my advisor, for all of his support, advice and guidance through the years. He has provided me with the freedom and means to explore many corners of this earth and diverse aspects of this field. His insight and thought provoking questions always seemed to point me in interesting new directions, like he knew the answers were just around the corner, if I would only look. I am glad that I listened (well, most of the time!). I would also like to thank the other members of my committee for their thoughtful comments and questions throughout my studies and research. Dr. Steve Kuehl's comments and discussion have helped to strengthen this manuscript and others to come. Dr. Jon Warrick provided a window into the rivers of Southern California and the opportunity to see them flooding firsthand. I also want to thank him for his great discussions on rivers and the coastal ocean, events and all things great and small. Dr. Greg Hancock provided my first real solid background in hydrology, and I look forward to continuing discussions on the role of events in controlling the geomorphic nature of rivers. Dr. Jim Perry I would like to thank for providing me the opportunity to work with him not only with regard to my research, but also for the opportunity to work on a project involving GIS education. Dr. Perry, along with Dr. Mike Newman, provided me the opportunity to develop an online GIS tutorial, which was a wonderful learning opportunity – in so many ways.

My time here at VIMS was made much easier by the invaluable support provided to me by Beth Marshall, Cynthia Harris and Cindy Hornsby. Without them, nothing would have gotten done. Thanks too to the staff of the Dean of Graduate Studies office, without them I would never have remembered to register for classes or file any of my necessary paperwork – THANKS! I would also like to thank Marilyn Lewis and the rest of the library staff for helping me acquire all the resource material I needed through this process.

Thanks are also due to the many wonderful students I have interacted with over the years. The help you have provided me, not only personally, but also professionally will never be forgotten. Specifically to Paul Liu for your many discussions involving sea level, GIS, seismic profile interpretation and pretty much everything else. Thanks also go to former VIMS geology students Steve Goodbred and Tim Dellapenna for helping me to see the fun in this field and giving me encouragement to stick it out to the end. Tara Kniskern also deserves kudos for the long discussions and debates we have had on many a scientific, and non-scientific topic, and for helping me have fun through the whole process.

Lastly I must thank my family for putting up with me through this process and providing encouragement through their patience and love.

LIST OF TABLES

<u>Table</u>		<u>Page</u>
Chapter 1		
1-1	Distribution of estimated global flux by oceanic basin	22
Chapter 2		
2-1	Major 24-hour sediment loads from United States Rivers	45
Chapter 3		
3-1	Hydrologic statistics for USGS stations in the Salinas Watershed	72
3-2	Linear regression relationships between Salinas Watershed gauges	90
3-3	Reservoirs in the Salinas Watershed	93
3-4	Classification of water years defined by PDO and SOI	100
3-5	Recurrence intervals for gauges within the watershed	111
Chapter 4		
4-1	Long-term sediment storage and delivery to Monterey Bay	140
4-2	Short-term sediment accumulation in Monterey Bay	145
4-3	Hyperpycnal River Plume travel velocity estimates	147

LIST OF FIGURES

<u>Figure</u>		<u>Page</u>
Chapter 1		
1-1	Example of GIS polygon for global estimates	9
1-2	Dissolved Yield vs. Basin Area for Global Database	11
1-3	Total Suspended Sediment vs. Area for Global Database	13
1-4	Distribution by continent of water and sediment discharge	16
1-5	Global Estimate Maps	18
1-6	Southeast Asia Regional Estimate Map	21
1-7	Commonly cited relationships of Precipitation vs. Yield	26
1-8	Sediment Yield and concentration vs. Runoff	28
1-9	Sediment Concentration vs. Basin Area	30
Chapter 2		
2-1	Sediment Yield vs. Basin Area	38
2-2	Annual deviation from the 50-yr mean of various sized rivers	42
2-3	Daily load comparison of the Mississippi and the Eel rivers	44
2-4	Salinas River drainage basin characteristics	51
2-5	Annual runoff throughout the Salinas Basin	53
2-6	River discharge above and below Nacimiento Dam	55
2-7	Annual number of low-flow days at Spreckels	56
2-8	Annual load of the Salinas	57
2-9	Annual load of the Salinas vs. SOI	58
2-10	Loss of water to groundwater recharge along the course of the river ...	60
Chapter 3		
3-1	Topography of the Salinas Basin	69
3-2	Length of gauging station records	75
3-3	Monthly distribution of runoff and mean and maximum flows.	76
3-4	Historical maximum and minimum daily flows at Spreckels	78
3-5	Runoff duration curves for Salinas stations	80
3-6	Sediment rating curve for Salinas River at Spreckels	84
3-7	Comparison of estimated annual loads and USGS published annual loads	85
3-8	Water loss along the Arroyo Seco	87
3-9	Annual precipitation map of the Salinas River watershed	89
3-10	Historical reservoir water storage	95
3-11	SOI and PDO time series	97
3-12	Correlation of SOI with annual discharge	101

3-13	ENSO and PDO relationships with annual discharge	102
3-14	Annual residual runoff throughout the basin	104
3-15	Annual discharge for six PDO/ENSO categories	105
3-16	Annual discharge and the ratio of maximum to mean flow	107
3-17	Event and non-event discharge vs. Annual discharge	108
3-18	Grouping of water years by annual discharge and number of event days	109
3-19	Event definition example	113
3-20	Historic cumulative sediment and water discharge	116
3-21	Historical water loss	118

Chapter 4

4-1	Bathymetry of Monterey Bay	126
4-2	Representative seismic reflection profile	128
4-3	Historical locations of the Salinas River Mouth	131
4-4	Trackline locations	133
4-5	Bathymetric profiles from the mouth of the Salinas River	135
4-6	Profiles of bathymetry and angular unconformity	137
4-7	Holocene isopach map of the southern shelf	138
4-8	Box core locations on the southern shelf	143

ABSTRACT

Understanding the controls on the magnitude and timing of sediment delivery to the coastal ocean is important when interpreting the role of rivers in the biological, chemical, physical and geological coastal zone systems. A global database (1500 rivers) was assembled to estimate global fluvial delivery of water and sediment to the coastal ocean. I estimate an annual delivery of 35,000 km³ of freshwater, $4 * 10^6$ tonnes of dissolved solids and $18.6 * 10^6$ tonnes of suspended sediment. The global delivery of fluvial water and sediment, both suspended and dissolved, is dominated by southeast Asia, due to the unique climatic, geologic and geomorphic character of the rivers in this region. Over 30% of the global freshwater discharge to the oceans is estimated to originate in southeast Asia and Oceania. This same region of the world is responsible for over 30% of the dissolved solid input and an astounding 70% of the suspended sediment.

The Salinas River, central California, was the focus of an in-depth study on the controls on sediment delivery from a small (11,000 km²), semi-arid watershed. The Salinas River was chosen because there is a significant historical dataset from monitoring efforts throughout the basin, and it was thought to react to El Niño conditions in a similar manner to the rivers of southern California. This river discharges into the Monterey Bay (Central California) an average of 0.4 km³ of water and 3.3 tonnes of sediment per year. Basin scale control on the discharge of the river is dominated by the underlying geology as well as the anthropogenic changes to the watershed (e.g., damming of 2 large tributaries and high concentration of agriculture). Despite the highly altered nature of the Salinas River, the fluvial discharge is dominated by short-lived, intense meteorological events. The frequency of these events is determined by the oceanic and atmospheric conditions present offshore. Historically, large flood events on the Salinas River almost entirely correlate with El Niño events. However, not all El Niño years produce large flood events. It was determined that the probability of a large flood on the Salinas River is determined not only by the presence of El Niño conditions, but also by the interaction between the Pacific Decadal Oscillation with the ENSO. The coinciding of warm phases of both of these large-scale phenomena produces significantly higher annual discharges than any other combination of the climatic phenomena.

Estimating the sediment load of the river from historical gauging records allows us to determine the role the Salinas River plays in the sediment budget of the Monterey Bay. The Monterey Submarine Canyon bisects the bay, restricting the shelf space and creating 2 separate sedimentary environments. The southern shelf bypasses most modern fluvial sediment to the canyon, whereas the northern shelf stores most of the sediment delivered. The estimate of Holocene sediment discharge from the rivers and creeks of the bay indicate that > 60% of fluvially delivered sediment is lost to the canyon and deep ocean. The transport pathways of this removal are currently unknown, but hyperpycnal flow from the mouth of the Salinas River is hypothesized.

**Controls on the Delivery of Fluvial Sediment
to the Coastal Ocean:
The Salinas River, California**

Chapter 1: Introduction

1.1 Introduction

The coastal margin is an important boundary connecting the terrestrial and marine environments. Rivers are the most important link between these two systems in terms of the delivery of water, dissolved constituents, and suspended matter. The coastal zone (defined by LOICZ¹ as the region +/- 200m in elevation from the ocean-land interface) is naturally a dynamic location; however, humans have significantly modified it. According to the United Nations World Water Assessment Programme, humans “withdraw 8 % of the total annual renewable freshwater, and appropriate 26 % of annual evapotranspiration and 54 % of accessible runoff” (United Nations World Water Assessment Programme, 2003). As such, we have become a major part of the hydrologic cycle (Vörösmarty and Sahagian, 2000), and that, coupled with Hooke’s (2000) assessment of humans as geomorphic agents, underlines our global impact on riverine flow, and sediment delivery. Rivers link land and oceans on continental scales, with large river basins draining the interior of the continents. However, the impact of anthropogenic changes in the terrestrial coastal zone has a much more immediate impact on the coastal ocean.

Human activities have affected the riverine systems by worldwide modification of hydrologic pathways via damming, land use change

¹ Land-Ocean Interactions in the Coastal Zone (LOICZ) is a project of the International Geosphere-Biosphere Programme (IGBP) of the International Council of Scientific Unions.

(e.g., deforestation and mining) and other water diversions (Vörösmarty and Sahagian, 2000). The pollution of rivers by toxins and excess nutrients has also occurred worldwide, leading to the inability to claim any rivers as “pristine”. Due to local human impacts, such as agricultural runoff and wastewater release, coupled with global dispersal of atmospheric pollutants (Wania and MacKay, 1996). The interception and storage of riverborne sediment is also altering natural fluvial systems worldwide. It is estimated that the global sediment trapping efficiency of large dams is between 16 – 30 % (Vörösmarty and Sahagian, 2000). This not only has effects directly downstream of the dam (e.g., loss of flood plain and changes in riparian ecosystems), but also in the coastal ocean as many nutrients are transported via the sediment (e.g., trapping of carbon behind dams; Stallard, 1998).

The coastal shelf environment is heavily influenced by both the terrestrial systems, and the open-ocean. On land, the coastal zone is the site of rapid change, with rapid population growth and urban development, as well as large human-induced changes to landscape and riverine processes. The open-ocean’s input is mainly in the form of physical interaction and chemical/biological contributions. Along eastern boundary coastal systems this includes input from the deep ocean via upwelling. Sedimentologically, the influence to the coastal shelf is usually dominated by the terrestrial system.

The past few centuries have been a time of enormous alteration of the landscape by humans, leading to extreme changes in fluvial character (e.g., Gregory and Walling, 1973; Meade, 1982; Trimble, 1981; Said, 1993; Stanley and Wingerath,

1996; Hooke, 2000; Kondolf et al., 2002). Increased population densities along major river drainages, as well as along the coast, have changed the quantity of water discharge and the character of solid and dissolved loads to the coastal waters. The perturbations of the natural cycling of water, as well as nutrients such as carbon, nitrogen and phosphorous, have greatly changed ecosystems in the coastal zone. Quantification of the delivery of water, sediment and dissolved constituents is important in understanding the consequences of anthropogenic and natural changes to the landscape.

The rivers of California provide particularly interesting examples of the impact of climate and anthropogenic change on fluvial discharge to the coastal ocean. Mount describes these Californian systems as ones of extremes: “extremely wet or extremely dry” (Mount, 1995). The semi-arid climate of southern and central California rivers is punctuated by periodic, intense bursts of precipitation. Combined with the small size of the coastal watersheds, these weather events are quickly translated into floods that deliver large amounts of water and sediment to the coastal ocean. The Salinas River is located in central California, and is the third largest river in the state. Unlike most small rivers, the Salinas has a 70-year historical gauging record, allowing for a more robust assessment of water and sediment discharge. The river discharges into Monterey Bay, an interesting system with the Monterey Submarine Canyon dividing the bay in half, and little sediment exchange with the shelves to the north and south. The combination of the availability of historical records and the semi-closed sediment system of the bay allowed for a more complete study of the link between the Salinas River and the Monterey Bay.

1.2 Aims and Organization

The aims of this dissertation are to:

- Illuminate the role of variability in rivers in response to various forcings, particularly basin size and climate;
- Elucidate the many problems facing estimates of sediment delivery on both the global and local scale;
- Define the local aspects of the Salinas River watershed which lead to sediment and water flux;
- Determine the global and local forcings at play in the Salinas River watershed, and how this affects sediment delivery to the Monterey Bay;
- Estimate the volumetric flux of sediment from the Salinas River and compare this with long-term sediment storage on the shelf.

This dissertation consists of five chapters, starting with this introductory chapter that includes global estimates of delivery to the coastal ocean and information on dryland rivers. In Chapter two, I discuss the climatic and anthropogenic variability that can occur in river basins, and use the Salinas River (Central California, USA) as an example. Chapter three focuses on the modern terrestrial system, with a detailed look at the character of the Salinas River as well as delivery from the other rivers entering into Monterey Bay. Chapter four looks at long term shelf sedimentation on the southern shelf of Monterey Bay and the role of the Salinas River in the sediment budget. A final chapter synthesizes conclusions from all the chapters, and suggests directions for future research.

1.3 Global Estimates

The relationship between upland erosion and sediment yield from the mouth of a river is complicated by storage of sediment in the channel and floodplain (Trimble, 1981; Walling and Webb, 1983; Trimble, 1999; Goodbred and Kuehl,

1999). Local basin affects significantly complicate the attempt at generating global estimates of sediment yield. Many authors have created maps of global sediment yield (Fournier, 1960; Strakhov, 1967; Milliman and Meade, 1983; Walling and Webb, 1983; Jansson, 1988 and Ludwig and Probst, 1998), using a variety of techniques, from multiple regressions to point interpolation, with the results varying widely.

1.3.1 Data and Methods

To improve on these estimates we began by assembling a large database of global river data (Milliman and Farnsworth, in prep). These approximately 1500 rivers account for over 87 % of the total land area draining to the ocean (~ 100 million km²); however, although there is water discharge data for all of the rivers, less than half have been documented for suspended or dissolved sediment. To estimate global discharges, an extrapolation of the data from monitored rivers to unmonitored rivers was necessary. We used a method that allowed values measured at the mouths of rivers to be distributed over the entire watershed then extrapolated to proximal unmonitored basins with similar climate, geology and relief. Global land area draining to the ocean was divided into 188 polygons based on drainage basins, with the grouping of monitored and unmonitored rivers together into polygons with similar geology, elevation and climate regimes (Milliman and Farnsworth, in prep). This was done using ArcView GIS (v.3.1), and digitizing of the polygon boundaries by hand.

Sediment load and yield are defined here for clarity, as many fields use the same terms, but with different meanings. Load is defined as the total quantity of sediment, dissolved or suspended, moving out of a watershed in a given time interval,

and is usually expressed as tons per year ($t\ yr^{-1}$). Yield is defined as the quantity of sediment from a watershed relative to the watershed area, expressed as $t\ km^{-2}\ yr^{-1}$. Most sediment load calculations only include suspended load, as bed load is difficult to measure and therefore is not routinely measured. Bed load was generally assumed to be approximately 10% of the suspended load (Milliman and Meade, 1983).

1.3.1.1 Global Freshwater Flux

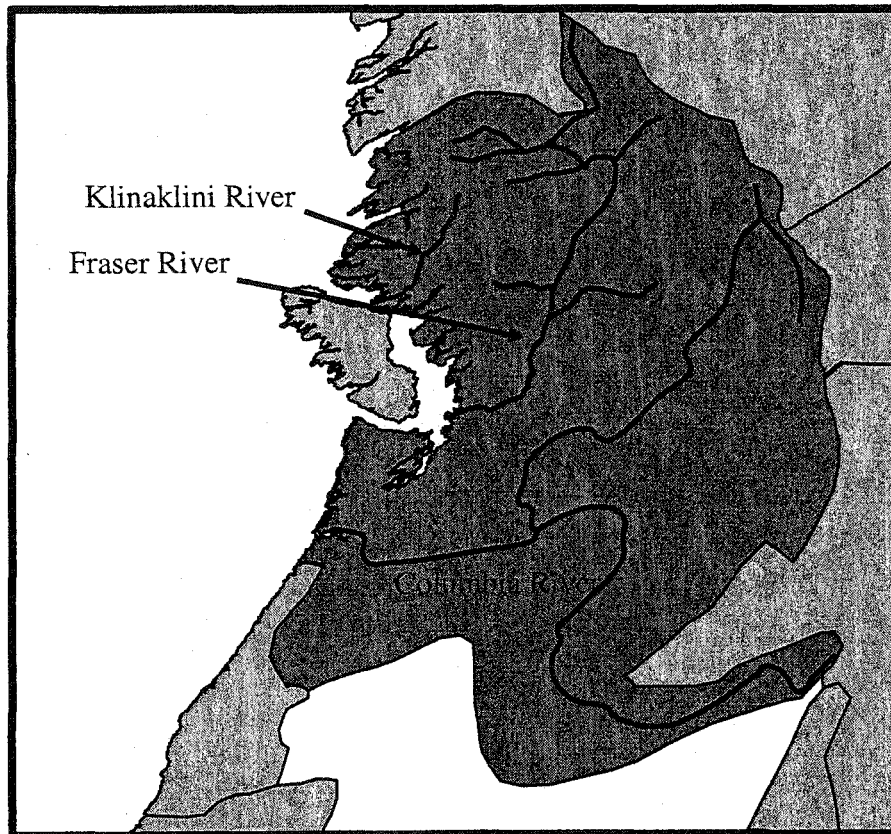
The relationship between freshwater discharge and basin area is a relatively straightforward one, with discharge increasing with basin area (Milliman and Syvitski, 1992). Thus, for a specific climatic (Baumgartner and Reichel, 1975) and geomorphic region (Larsen and Pittman, 1985), hydrologic runoff (freshwater discharge normalized by basin area) can be assumed to be constant (Figure 1-1). This allows for the extrapolation of runoff data from larger rivers to smaller rivers of similar climatic regimes (i.e., in the same polygon). The estimated discharge volume (Q_P) for each polygon was then calculated using the following formula:

$$Q_P = (Q_M/A_M)*A_P \quad [1]$$

with Q_M being the discharge of monitored rivers within that polygon, A_M the area of the monitored rivers (Q_M/A_M thereby being hydrologic runoff) and A_P the total area of the polygon. This distributes the hydrologic runoff characteristics of the monitored rivers, to others in the region that have not been measured.

1.3.1.2 Global Dissolved Solid Flux

In the database, we have numbers for dissolved flux from 25% of the 1500 rivers (365 rivers), with the majority of these values coming from Meybeck and Ragu (1996). Meybeck (1994) indicates that the dissolved load of a basin is a function of



River	Area (km ²)	Q (km ³)	Runoff (mm/yr)
Fraser	260,000	110	423
Klinaklini	6,500	1	154
Columbia	670,000	240	358

Figure 1-1: Example of polygon in western North America. Total polygon area is 961,000 km² and monitored rivers account for most of this. All rivers in polygon have similar geology, climate and relief.

basin area, local geology and climate, not the simple relationship based almost entirely on basin area that we saw with freshwater flux. Thus, when examining the relationship between dissolved discharge and basin area, regional character must be considered.

The dissolved yield values from the larger monitored rivers must be scaled to the smaller unmonitored rivers. Usually this requires an increase in the yield, as many smaller rivers have a higher dissolved yield than their larger counterparts (Figure 1-2). This is similar to the relationship seen with suspended sediment, as chemical weathering rates are strongly coupled with physical erosion rates (Stallard and Edmond, 1983). The 40 highest ranked rivers for dissolved load account for over 75 % of the total measured dissolved load in our database. These rivers were the large rivers found predominantly in Asia, Europe, North America and northeast South America. It would appear that the dissolved loads from these areas dominate the global estimate; however, with the work of Milliman and Syvitski (1992), we see that smaller rivers may have significantly higher yields than those of the larger rivers. This is reiterated in the fact that of the top 40 dissolved loads, only three of them (Rhine, Weser and the Po) are in the top 40 dissolved yields. It was imperative to scale the yield values in regions of high dissolved loads to the smaller rivers, to not severely underestimate the global dissolved solid load. The top 40 yields occur in the same regions as the top ranked loads, with Europe, Southeast Asia and North America dominating. The reasons for such high dissolved loads in these areas vary considerably. The northern European rivers, though flowing through low-lying terrain, have been altered for years by mining and industrial activities. This has

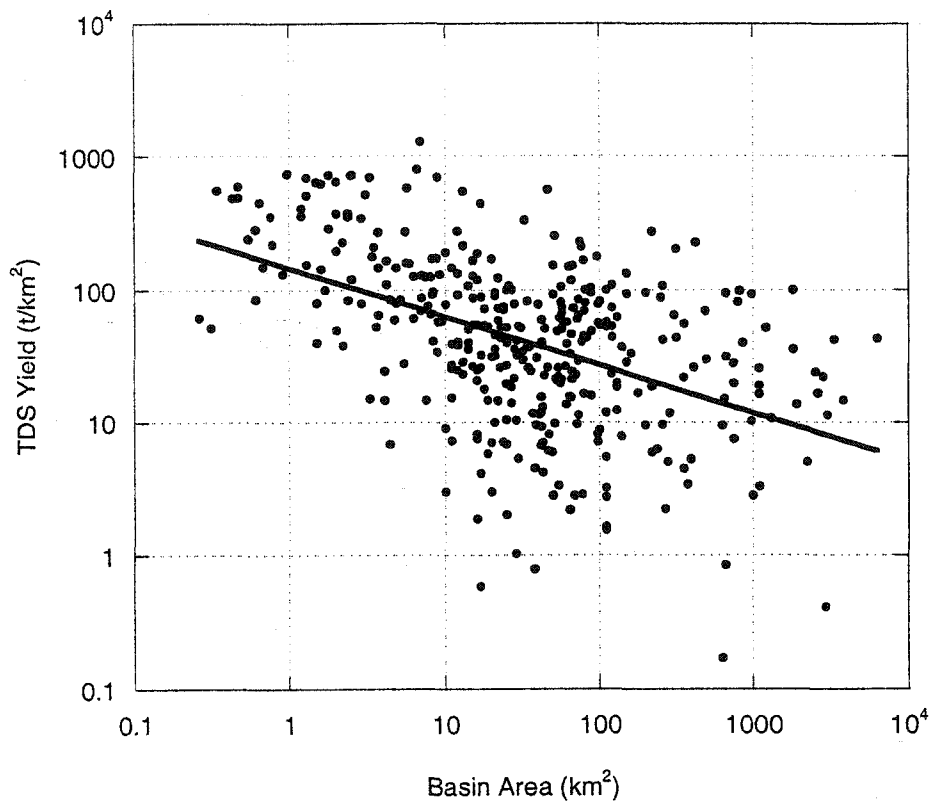


Figure 1-2: Dissolved yield vs. basin area for approximately 360 rivers in the Global Rivers Database (Milliman and Farnsworth, in prep.). Shows the same relationship of increasing dissolved yield with decreasing basin area as Milliman and Syvitski, 1992.

increased the dissolved load of some constituents by orders of magnitude (Meybeck, 1994). The North American rivers (particularly those in the eastern U.S. and Canada) have been similarly altered through human interaction. The Southeast Asian and Oceania rivers in high standing, tropical areas are exposed to extensive erosion, both physical and chemical (Stallard and Edmond, 1983). This is also a region with an abundance of small watersheds draining to the ocean.

For those regions lacking high loads, the simple extrapolation method was used to simplify the calculations. This was done by extending the yields of monitored rivers to unmonitored rivers using the same method as for riverine discharge. The estimated flux of dissolved material (D_P) from each polygon to the coastal oceans was then calculated using the following formula:

$$D_P = (D_M/A_M)*A_P \quad [2]$$

with D_M being the flux of dissolved material from monitored rivers within that polygon, A_M the area of the monitored rivers and A_P the total area of the polygon. This distributes the dissolved material flux of the monitored rivers, to others in the region that have not been measured.

1.3.1.3 Global Suspended Solid Flux

Looking at the relationship between basin area and suspended sediment load for all rivers in the database, there is a positive relationship ($r^2 = 0.33$), with a large amount of scatter, as rivers of the same area have up to 5 orders of magnitude difference in their sediment load (Figure 1-3). Milliman and Syvitski (1992) reported this same relationship between basin area and sediment load, and an inverse one between basin area and yield. Similar to dissolved yield, we must take into account

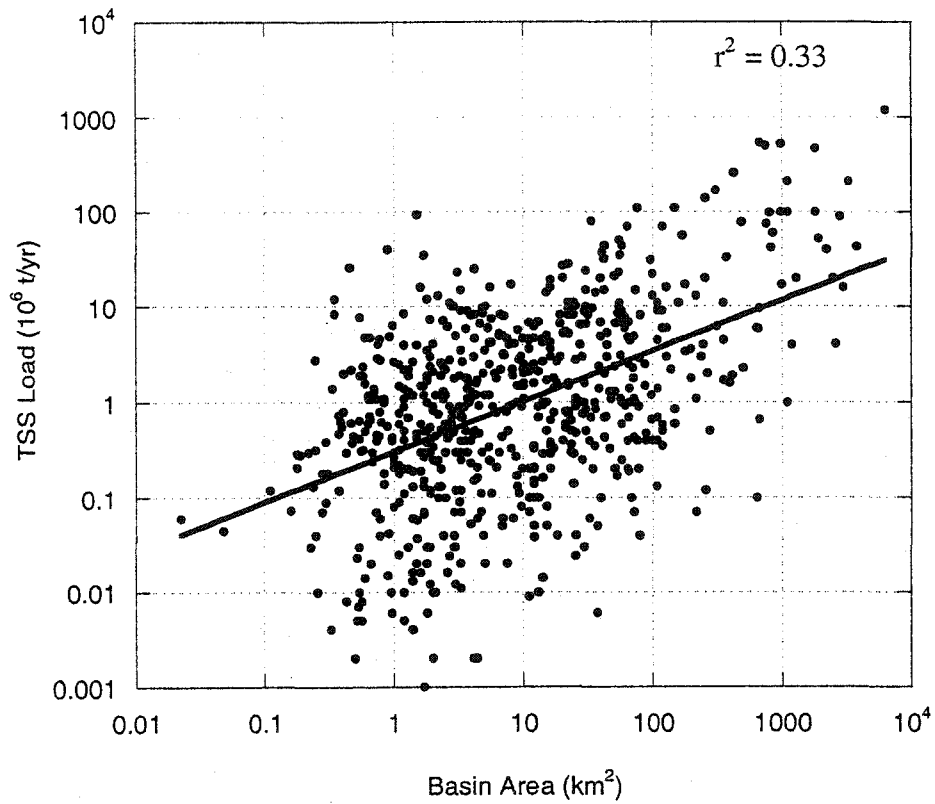


Figure1-3: Total suspended solids vs. basin area for approximately 675 rivers from the Global Rivers Database (Milliman and Farnsworth, in prep.). Illustrates the large variation in suspended load with basin area, sometimes up to five orders of magnitude in the smaller basins, and three orders of magnitude in the larger basins.

basin geology and climate, as well as basin morphology. As the polygons were created with these variables in mind, much of this has been accounted for, however, just like dissolved yield, scaling to smaller unmonitored rivers needs to occur. The top 40 ranked suspended solid loads accounted for over 75 % of the total measured load in our database. These, of course, are the large rivers, as basin area is a key component of determining sediment load. However basin yield increases with a decrease in basin area (Milliman and Syvitski, 1992). Therefore, to calculate the global flux of suspended solids from land, we must scale the yields rather than just extrapolating over the entire polygon. This relationship is most pronounced in mountainous regions with small watersheds draining young, erodable rock. Because their sediment loads are typically very small and there is no clear change in sediment yield with varying basin area, scaling was not applied in regions of low-lying old rocks such as eastern North America, northern Europe, the Arctic and most of Africa. An increase in the sediment yields was applied for smaller unmonitored rivers in southern Europe (draining the southern Alps), Oceania, New Zealand, Southeast Asia as well as western North and South America. The regions where scaling was not applied, polygon suspended solid estimates were computed in the same method as freshwater flux. The estimated flux of suspended material (S_P) from each polygon to the coastal oceans is then calculated using the following formula:

$$S_P = (S_M/A_M)*A_P \quad [3]$$

with S_M being the load of suspended material from monitored rivers within that polygon, A_M the area of the monitored rivers, and A_P the total area of the polygon.

This distributes the suspended material flux of the monitored rivers, to others in the region that have not been measured.

1.3.2 Global Patterns

The delivery to the coastal ocean of freshwater and sediment, both dissolved and suspended, is globally distributed (Figure 1-4). As stated previously, the flux of water and sediment is controlled by basin area, leading to continental flux estimates strongly correlated to drainage area. The extremely high suspended flux from Asia/Oceania and the low fluxes from Africa are indicative of regions where climate and geomorphic forcings play important roles. Southeast Asia and Oceania have high sediment yields, as in this region wet climate and high relief dominate. Africa on the other hand, has sediment yields dominated by geology and the arid climate.

Specific examples are seen when we compare the Amazon River with the smaller rivers of Indonesia. The Amazon, with a basin area of $6.3 \times 10^6 \text{ km}^2$, accounts for 7 % of global land area draining to the ocean. If all rivers were considered equal, we would then expect 7 % of the global discharge of water, suspended and dissolved sediment to be attributed to the Amazon. In reality, it accounts for approximately 18 % of the global freshwater discharge, and 7 % of both the suspended and dissolved fluxes. This is in stark contrast to the sediment loads of the six high-standing islands of Indonesia. The rivers on the islands of Sumatra, Java, Borneo, Celebes, Timor and New Guinea, whose collective areas total $2.3 \times 10^6 \text{ km}^2$, discharge approximately 3300 km^3 of water and $4.2 \times 10^9 \text{ t}$ of sediment annually. This means that an area occupying only 2 % of the global land area draining to the

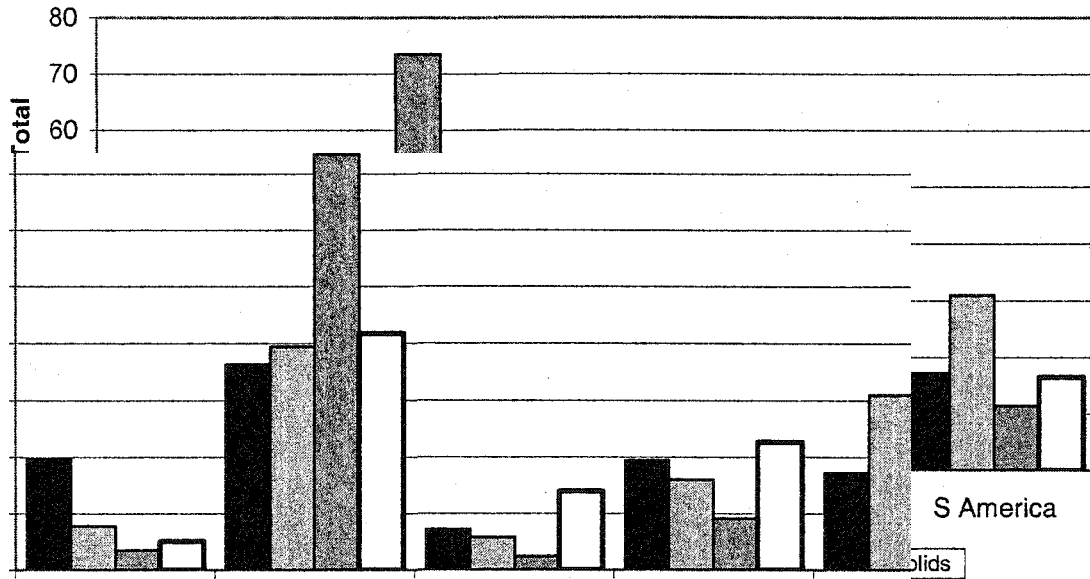


Figure 1-4: Distribution of total continent area, freshwater flux, suspended and dissolved solid fluxes by continent. Asia/Oceania has a significantly larger flux of suspended solids than expected by area, with Africa having much lower fluxes, both due to their climatic and geologic settings.

oceans discharges approximately 9 % of the freshwater and 20 % of the total sediment load (Milliman et al., 1999).

Global flux estimates of water, suspended sediment and dissolved material to the coastal ocean are presented here (Figure 1-5). These estimates are the most extensive to date, as they use the largest database of measured values. However, the error associated with them is quite unknown, as error is introduced not only during estimation, but also from the original measurements. All of the numbers in our database have been reviewed for quality, but with limited data for comparison, some errors are sure to be included.

Our freshwater estimate of 35,000 km³/yr (Figure 1-5a) is similar to that of others (e.g., Baumgartner and Reichel, 1975; Berner and Berner, 1987) and appears well constrained given continental precipitation and temperature patterns. Calculations of delivery of dissolved and suspended material to the coastal ocean is much more difficult. Our estimation of global dissolved load to the ocean of 4 billion t/yr (Figure 1-5b) is similar to that of Meybeck (1988), but the amount of extrapolation which was done to achieve these estimates suggests possible estimation errors. Only 25% of the rivers in the database contain measurements for dissolved load, although most of these are the large rivers. We therefore have dissolved flux data for approximately 73 % of the total land area draining to the oceans. Delivery of suspended sediment to the coastal zone has been studied in great detail on local scales. Our estimate of $18.6 * 10^9$ t/yr of sediment (Figure 1-5c) is plagued by the same problems as dissolved load, but is similar to other estimates (e.g., Holeman, 1968).

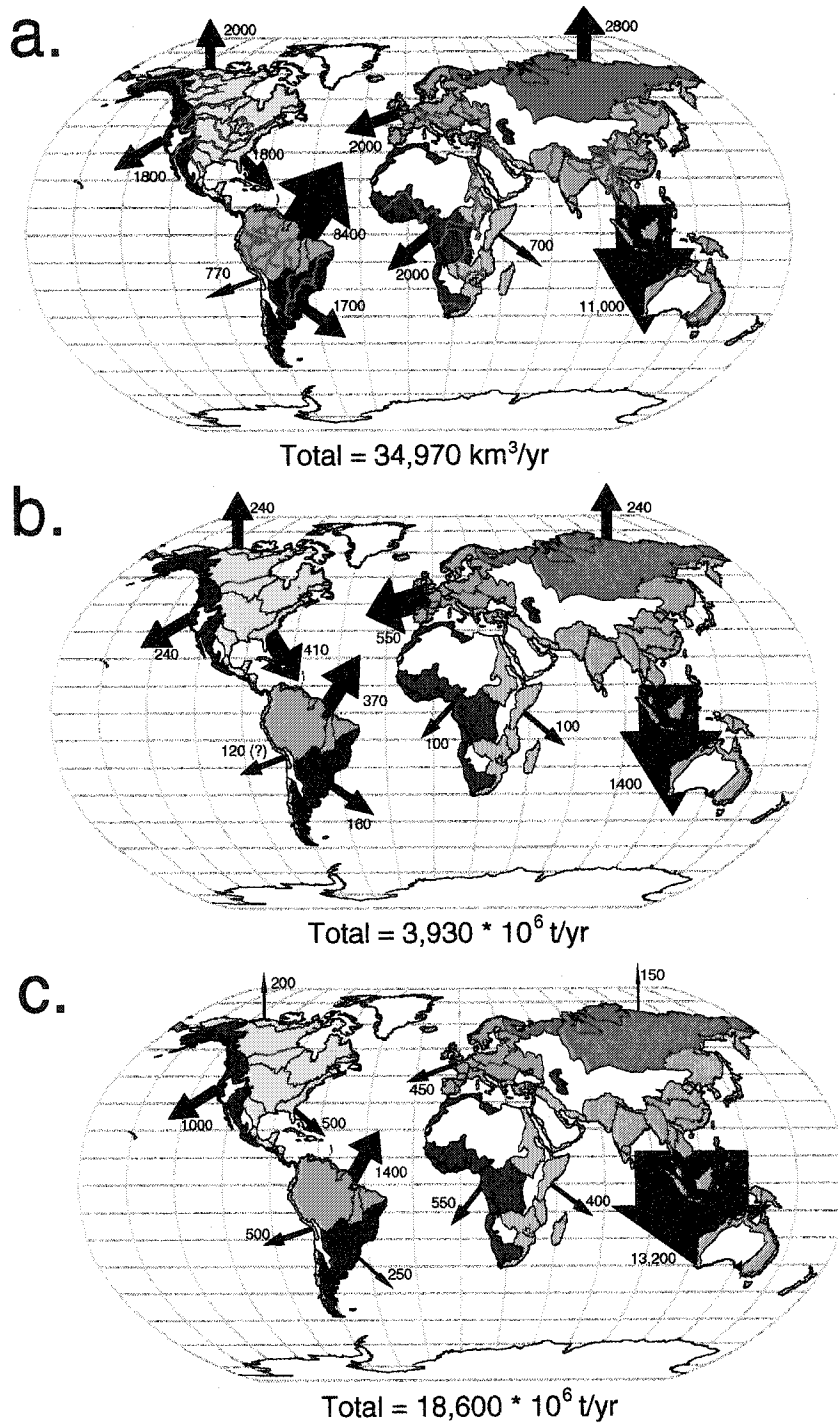


Figure 1-5: Global estimates of a) Fluvial Freshwater Flux, b) Total Dissolved Flux and c) Total Suspended Solids Flux

The errors associated with estimating the global fluxes of sediment fall into two categories, data measurement errors and estimation errors. The data measurement errors are where a large amount of the error arises. First is the lack of extensive monitoring of small rivers. Smaller rivers have been shown to have higher yields than their larger counterparts (Milliman and Syvitski, 1992), and not having these data leads to an underestimation of the flux. Coupled with this is error associated with the numbers we have for smaller rivers. Small rivers are much more episodic in nature than larger rivers. If the monitoring of the river was conducted sporadically, or only for a short time period, events that dominate the sediment transport regime may have been missed, leading to erroneous numbers.

Another large source of potential error is unaccounted storage in the floodplain below the measurement location. Measurements are made at the last gauging station before the tidal influence; for some rivers this may be sufficiently far enough upstream that significant storage or erosion may take place below this location.

An ever-changing source of error is associated with rapid human-induced change in the watersheds. Most of the numbers used in these estimates are pre-1980, with some of them being much older than that. Much change has occurred since then, whether it be an increase in sediment fluxes due to clear cutting in remote areas or decreases in sediment flux due to the construction of dams (Vörösmarty et al., 1997). These affects may negate each other, however they have yet to be quantified on a global scale.

Southeast Asia contributes more than half of the sediment delivered to the coastal oceans. We can examine this area more thoroughly by looking at the contribution from local regions (Figure 1-6). The small role Australia plays in freshwater and sediment delivery is apparent, even with a land area of almost 8 million km². This is due to the interplay of arid climate and old, stable geology, causing most rivers to be both transport and supply limited. Indonesia and Papua New Guinea, as mentioned before, have large sediment fluxes. The rest of mainland Southeast Asia is dominated by the Himalayan Mountains. Their sheer magnitude and high elevation, lead to high sediment loads from all of the major rivers in the region.

Overall, the regions of the globe where high volcanic mountains are located in close proximity to the coastline account for a large amount of sediment that is delivered to the coastal ocean. This is represented by the distribution of water and sediment flux to the Atlantic and Pacific oceans (Table 1-1). The Pacific and Indian Oceans receive equal proportions of water and dissolved sediment, unlike the relationship seen with suspended sediment. The large amount of sediment entering the Pacific and Indian oceans comes from active margin regions. This reinforces the role of small rivers in mountainous regions being extremely important to the global budgets.

1.4 Character of Dryland Rivers

Dryland rivers are considered those which are in semi-arid to hyper-arid regions (Middleton and Thomas, 1997). These climatic conditions are found throughout the world. The Salinas River is considered a semi-arid river with rainfall

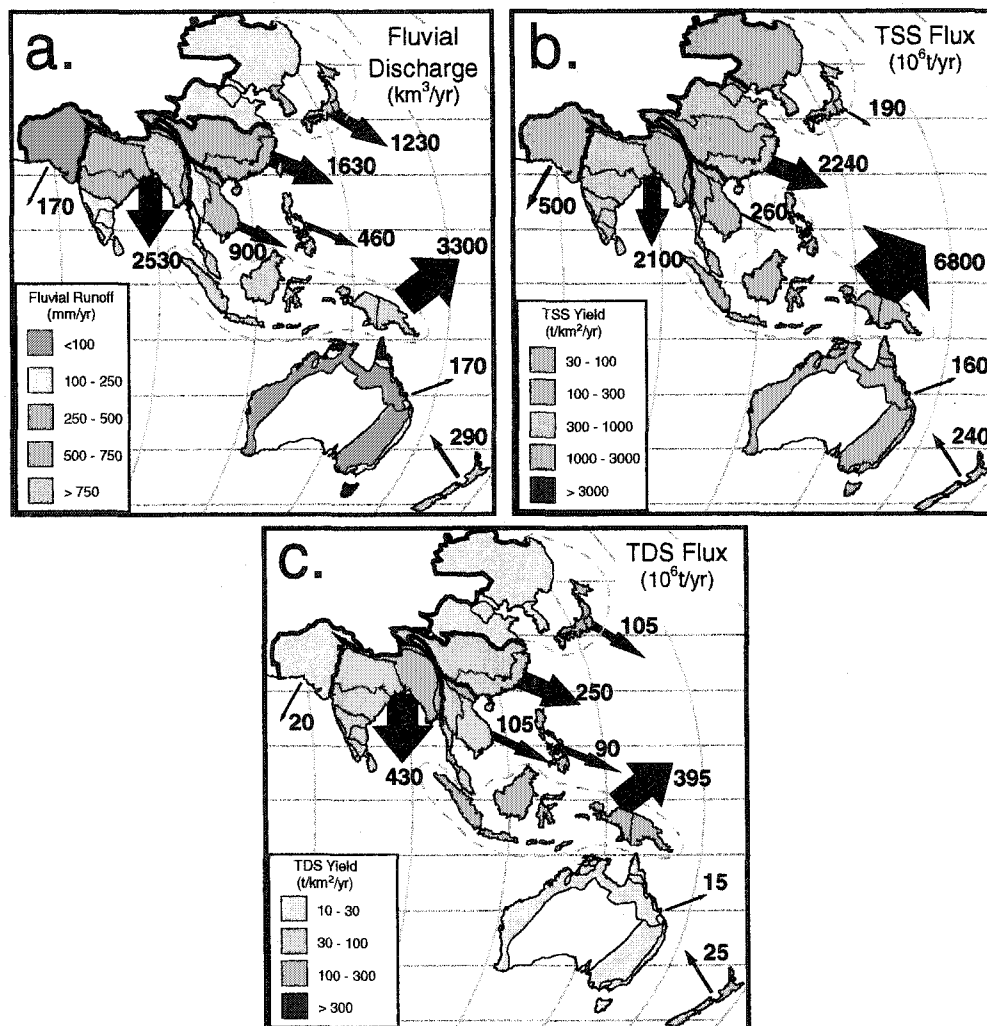


Figure 1-6: Regional estimates of a) Fluvial Discharge, b) Total Suspended Solids Flux and c) Total Dissolved Solids Flux for Southeast Asia-Oceania-Australia.

Table 1-1: Distribution of estimated global fluxes by oceanic basin, including percentage of total. Shows anomalously high suspended sediment flux into the Pacific and Indian Oceans.

	Freshwater Flux (km ³ /yr)	Dissolved Solid Flux (*10 ⁶ t/yr)	Suspended Solid Flux (*10 ⁶ t/yr)
Pacific – Indian	14,270 (42%)	1,860 (47%)	15,100 (81%)
Arctic	4,800 (13%)	480 (12%)	350 (2%)
Atlantic	15,900 (45%)	1,590 (41%)	3,150 (17%)

only during the winter months. The rivers of southern California represent a spectrum of precipitation regimes, ranging from semi-arid in the northern central coast region (e.g., Salinas River) to arid in the far south (e.g., Tijuana River). In the south, the high levels of aridity are mainly due to global atmospheric patterns (Hadley Cell), creating arid regions in the sub-tropics with scarce and irregular rainfall. The region to the north is semi-arid, due to the proximity to this highly arid region, and the Salinas River in particular is considered semi-arid because of local orographic effects. As the storms come ashore, the rain is left in the coastal ranges to the west, and the inland valley is in a rain shadow.

Although dryland regions often receive little rain, their surface features are mostly produced by the action of rivers (Graf, 1988a). Surface runoff is important, though usually only occurring episodically (with return rates in some extremely dry areas of 10's of years). Rivers in these areas may be ephemeral, intermittent or perennial. The common definitions of these terms as they relate to dryland rivers is as follows:

- Ephemeral – transitory, short-lived, flowing briefly and rarely, returning to dry conditions between precipitation events
- Intermittent – flows occasionally and irregularly, usually has small amount of flow contribution from groundwater as well as the precipitation events
- Perennial – typically when flow is sourced from outside the dryland region

Most rivers in humid regions rarely stop flowing, whereas dryland rivers are rarely perennial unless they receive water from outside the arid region, or have water

released from manmade storage reservoirs during dry periods. Much of the Salinas River is classified as intermittent, with some of the smaller tributaries ephemeral.

Although episodic in nature, the magnitudes of dryland river floods are much larger than those experienced in humid-region rivers of comparable size, and the discharge of the largest flood is very much larger than the mean annual flood discharge (McMahon, 1979). An arid river can have a 50-year flood event that is 280 times the mean annual discharge (Graf, 1988b), while humid rivers such as those found on the east coast of the US have flood magnitudes about 2.5 times the mean discharge (Wall and Englot, 1985). According to Costa (1987), of the 12 largest floods ever measured in the United States, all occurred in semi-arid to arid regions, and 10 of those occurred in regions with less than 400 mm of annual rainfall.

In these dryland regions, many of the morphological changes, and therefore sediment transport, occur during these rare large magnitude floods. This is seen in humid regions (Nanson, 1986; Maizels, 1993), but is magnified in arid regions due to the large ratio of the episodic flood to the mean discharge (Patton et al., 1993; Baker, 1988; Osterkamp and Costa, 1987; Pickup, 1991).

In riverine systems, there is commonly a connection between the surface and subsurface (groundwater) flow, through which rivers can either receive contributions from (influent river) or lose water to (effluent river) the groundwater system. It is possible for this hydraulic connection to be lost when the water table completely disconnects from the river, leaving an area of partly unsaturated soil between the two, and seepage from the riverbed to the surface aquifer is the only connection (Winter et al., 1998). In arid regions, rivers are usually either effluent rivers or disconnected

from the water table altogether. This is quite different than humid regions where rivers are usually influent rivers, receiving a base flow from the groundwater, causing an increase in discharge downstream. This can lead to a lack of connection between small precipitation events in the upper-watershed and the delivery from the mouth of the river.

1.4.1 Sediment Delivery from Rivers

A key study by Langbein and Schumm (1958) has provided the basis for considering dryland rivers for more than 40 years (e.g., Dorn, 1996; Knighton and Nanson, 1997; Kochel et al., 1997). Using data from 94 sampling stations in the Southwest United States, they developed a relationship that shows maximum sediment yields occurring in semi-arid regions, with an annual precipitation of approximately 300 mm. (Figure 1-7a). Langbein and Schumm concluded that when precipitation exceeds this value, vegetation increases, thereby increasing surface protection and reducing sediment production. In regions with less than 300 mm of annual precipitation, even though there is a lack of vegetation, there isn't enough hydraulic power to erode and transport the materials produced, in other words, the system is transport limited. This relationship was developed by group-averaging the stations with similar precipitation values, which thereby ignored the roles of basin area, geology and morphology within each of these groups.

Many authors have since shown exception to this rule (e.g., Douglas, 1967; Wilson, 1973; Walling and Webb, 1983), but have yet to fully explain the problems associated with the Langbein and Schumm relationship. For example, Walling and Webb (1983) used a global database and found a second peak around 1400 mm

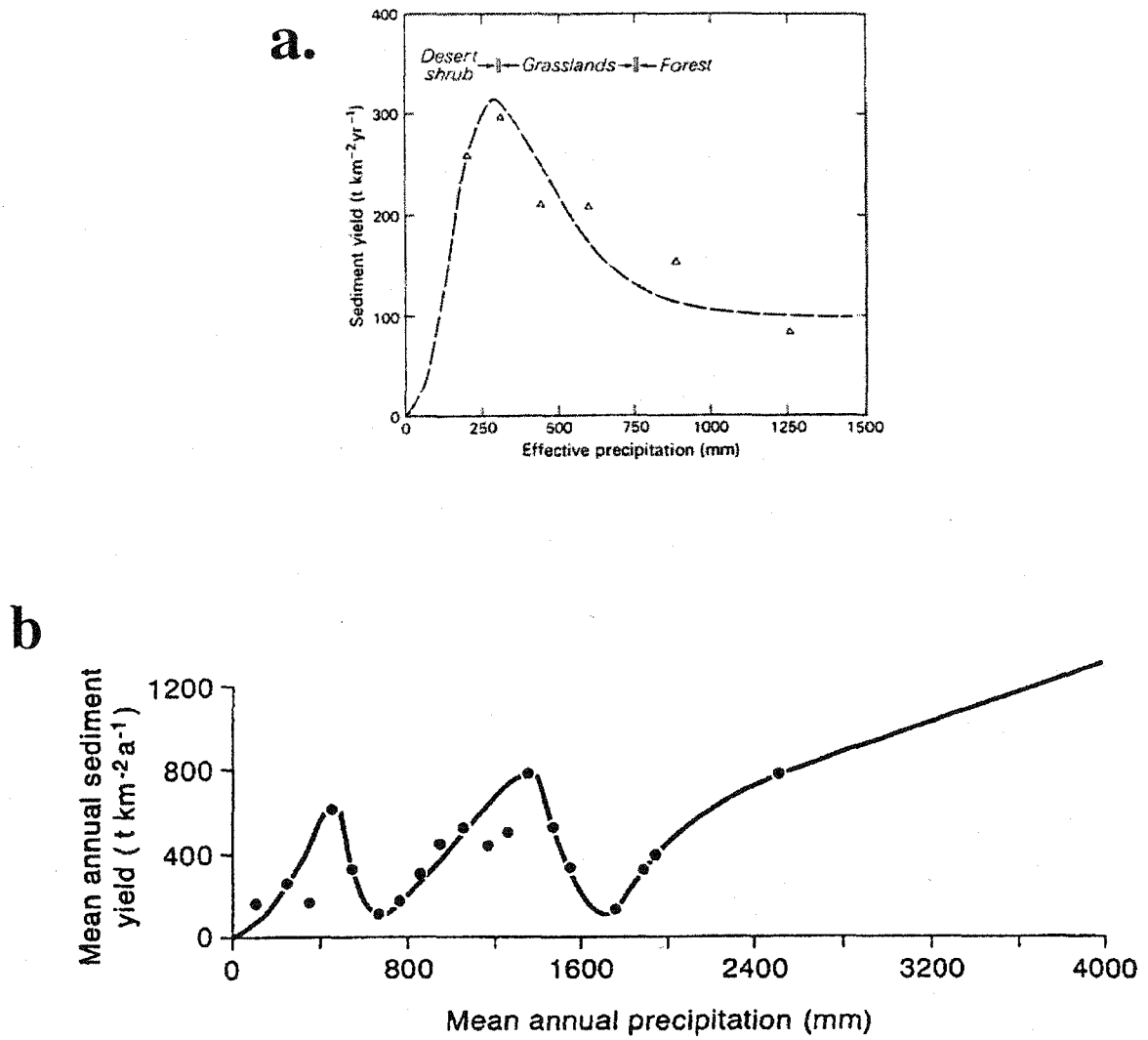


Figure 1-7: Two commonly cited relationships between precipitation and Sediment Yield; A) Langbein and Schumm, 1958 and B) Walling and Webb, 1983. These relationships have been disputed by the work done here and seen in Figure 1-8.

precipitation (Figure 1-7b). They also used a group averaging technique, which ignored other factors that account for much of the difference in sediment delivery. Walling and Webb (1983) agreed, however, that vegetation appears to be the key in this relationship. In the wet regions, the high yields seem to be due to the fact that during the most intense storms the protective role of vegetative cover decreases when the canopy is damaged and streams overflow their banks.

By not considering the other important factors that play a role in sediment yield (geology, morphology and area), these published relationships appear flawed. For example, we have examined rivers from mountainous regions, with basin areas between 1000 and 5000 km². These rivers were chosen due to their importance for delivering large amounts of sediment to the coastal ocean (Milliman and Syvitski, 1992). Classification by the main lithologic character of the basins (i.e. poorly erodible vs. easily erodible bedrock) allowed for an even clearer view of the role of runoff. There is a steady increase in sediment yield from low runoff to higher runoff (Figure 1-8a), until approximately 700 - 800 mm/yr. With increasing annual runoff, sediment yield increases dramatically. The basins with more easily erodible rocks (mudstones and poorly cemented sandstones) have higher sediment yields than basins dominated by less erodible rocks (granites and basalts), as would be expected. The main difference seen between this analysis and those of Langbein and Schumm (1958) and Walling and Webb (1983) is the lack of any distinct maxima in the yield, which may only be due to the limited amount of data available.

Basins appear to be transport limited in areas of low runoff, meaning that sediment is in ample supply in arid regions, as seen by the high sediment

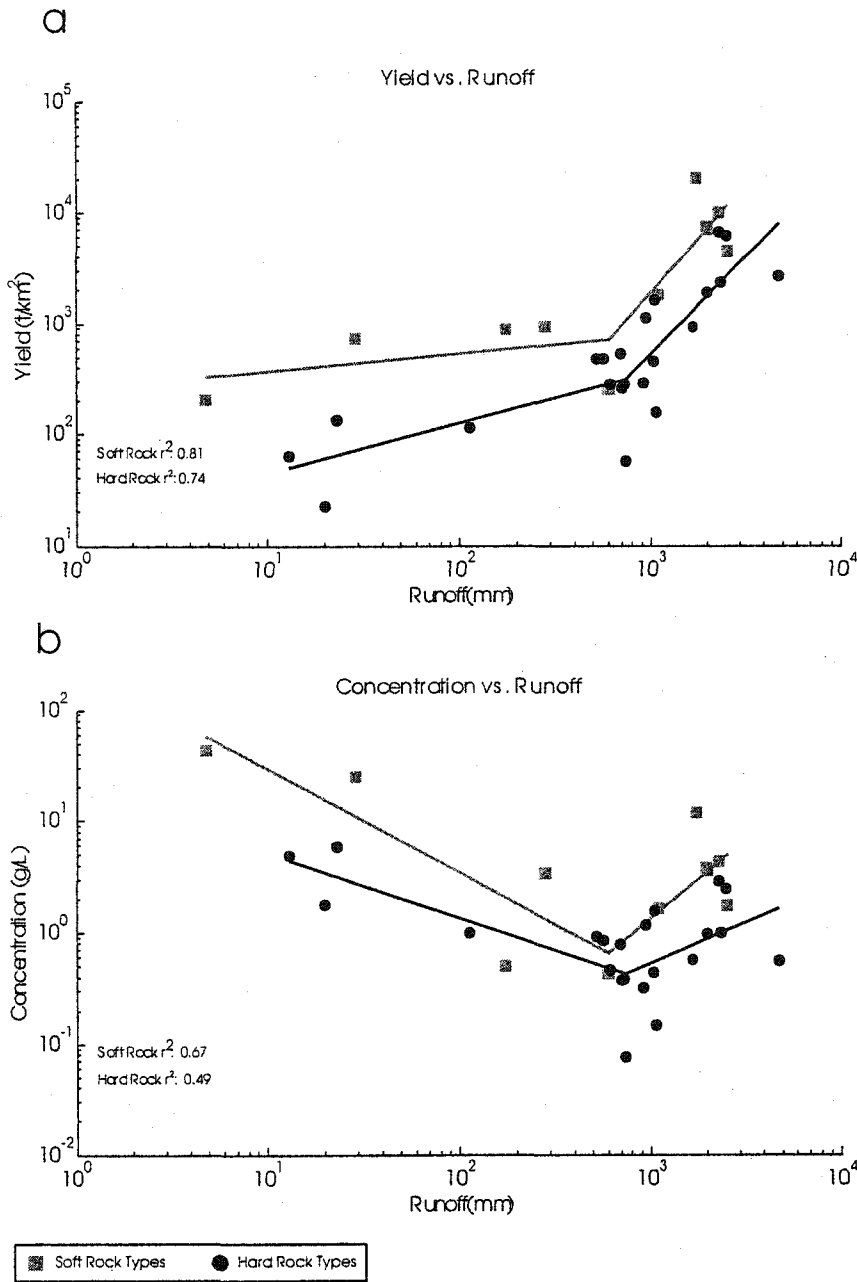


Figure 1-8: Sediment yield (a) and sediment concentration (b) in wet, tropical mountainous rivers with relation to annual runoff (cm). Shows transport limiting conditions in areas of low runoff, transitioning to sediment limited as 600 mm/year annual runoff is approached. Following this threshold, there is neither transport nor sediment limitation. In this region, with an increase in annual runoff, there is an increase in both yield and concentration. Segmented linear regression fit using methods outlined by Chappell (1989).

concentrations (Figure 1-8b), but the lack of running water limits yield. This then transitions into a sediment-limited system in areas approaching 700 mm/yr of annual runoff. However, there appears to be some threshold (approximately 700 – 800 mm/yr) where the precipitation overwhelms even the established vegetation (this may take the form of mass movements in some of these mountainous regions), and at this point yields rise dramatically with increased runoff (concentrations also increase).

A threshold level also has been seen on event scales. Hopley et al. (1990) measured sediment concentrations in the North Queensland tropical rainforest during normal rainfall conditions to be 5 – 20 mg/L. During the first of two intensive rain events, with 24-hour rainfall totals of 100 mm, fluvial concentrations were 100 – 200 mg/L, and after the second, with 300 mm of rain in 24 hours, the concentrations were 180-260 mg/L. Even on this short-duration event scale, these intense short-lived storms can cause extensive erosion, and play key roles in the transport and delivery of sediment to the coastal ocean.

Dryland rivers generate higher sediment concentrations than other climatic regimes. We see this throughout our global database, with significantly higher sediment concentrations in the arid rivers, relative to the wet rivers, regardless of classification by other geomorphic factors (e.g., basin area or general geology) (Figure 1-9). The caveat is once again that these dryland rivers are transport limited, and therefore, delivery to the coastal ocean is limited by this lack of water for transport. There may also be a disconnect during smaller events between the headwaters and the mouth of the river due to the loss of riverine water to the groundwater system. When these rivers do actually flow and deliver to the coast, the loads can be extreme.

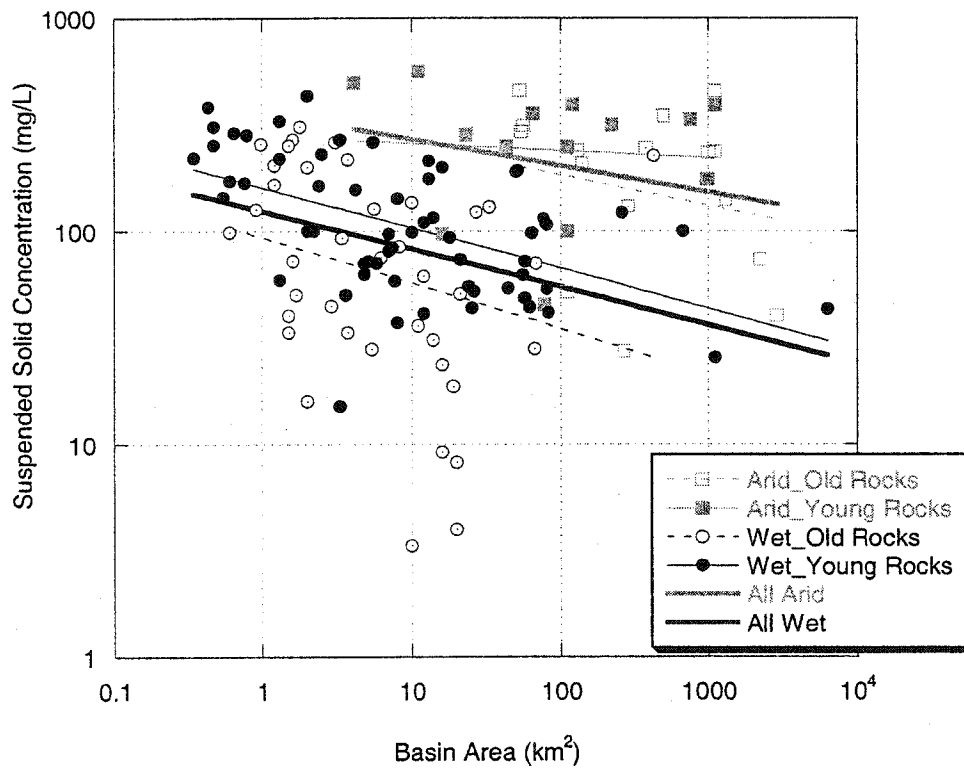


Figure 1-9: Concentrations of arid rivers (regardless of size) are generally higher than those of wet rivers of the same drainage area.

1.5 References:

- Baker, V.R., 1988. Flood Erosion. In: V.R. Baker, R.C. Kochel and P.C. Patton (Editors), *Flood Geomorphology*. John Wiley & Sons, New York, pp. 81-95.
- Baumgartner, A. and Reichel, E., 1975. *The world water balance; mean annual global, continental and maritime precipitation, evaporation, and runoff*. Elsevier Sci. Publ. Co., New York, NY, 179 pp.
- Berner, E.L. and Berner, R.A., 1987. *The Global Water Cycle: Geochemistry and Environment*. Prentice-Hall, Englewood Cliffs, N.J., 397 pp.
- Chappell, R., 1989. Fitting Bent Lines to Data, with Applications to Allometry. *Journal of Theoretical Biology*, 138: 235-256.
- Costa, J.E., 1987. Hydraulics and basin morphometry of the largest flash floods in the coterminous United States. *Journal of Hydrology*, 93: 313-338.
- Dorn, R.I., 1996. Climatic Hypotheses of Alluvial-fan Evolution in Death Valley Are Not Testable. In: B.L. Rhoads and C.E. Thorn (Editors), *The Scientific Nature of Geomorphology: Proceedings of the 27th Binghamton Symposium in Geomorphology*. John Wiley & Sons.
- Douglas, I., 1967. Man, vegetation and the sediment yields of rivers. *Nature*, 215(5104): 925-928.
- Fournier, F., 1960. *Climat et Erosion*. Presses Universitaires de France, Paris, 201 pp.
- Goodbred, S.L. and Kuehl, S.A., 1999. Holocene and modern sediment budgets for the Ganges-Brahmaputra river system: Evidence for highstand dispersal to flood-plain, shelf and deep-sea depocenters. *Geology*, 27(6): 559 - 562.
- Graf, W.L., 1988a. Definition of flood plains along arid-region rivers. In: V.R. Baker, R.C. Kochel and P.C. Patton (Editors), *Flood Geomorphology*. Wiley, New York, pp. 231-242.
- Graf, W.L., 1988b. *Fluvial Processes in Dryland Rivers*. Springer-Verlag, Berlin, 143 pp.
- Gregory, K.J. and Walling, D.E., 1973. *Drainage Basin Form and Process*. Edward Arnold, London, 458 pp.
- Holeman, J.N., 1968. The Sediment Yield of Major Rivers of the World. *Water Resources Research*, 4(4): 737-746.

- Hooke, R.L., 2000. On the history of humans as geomorphic agents. *Geology*, 28(9): 843-846.
- Hopley, D., Van Woesik, R., Hoyal, D.C.J.P. and Steven, A.D.L., 1990. The effect of disturbing tropical rainforest catchments adjacent to fringing coral reefs through the development of a road: Cape Tribulation, Great Barrier Reef, Congress on Coastal and Marine Tourism. 2, Honolulu, Hawaii, pp. 328-33.
- Jansson, M.B., 1988. A global survey of sediment yield. *Geograf. Ann.*, 70: 81-98.
- Knighton, A.D. and Nanson, G.C., 1997. Distinctiveness, diversity and uniqueness in arid zone river systems. In: D.S.G. Thomas (Editor), *Arid Zone Geomorphology: Process, Form and Change in Drylands*. Wiley, Chichester, pp. 185-203.
- Kochel, R.C., Miller, J.R. and Ritter, D.F., 1997. Geomorphic response to minor cyclic climate changes, San Diego County, California. *Geomorphology*, 19: 277-302.
- Kondolf, G.M., Piégay, H. and Landon, N., 2002. Channel response to increased and decreased bedload supply from land use change: contrasts between two catchments. *Geomorphology*, 45: 35-51.
- Langbein, W.B. and Schumm, S.A., 1958. Yield of Sediment in Relation to Mean Annual Precipitation. *AGU Transactions*, 39: 1076 - 1084.
- Larsen, R.L. and Pittman, W.C.I., 1985. *The Bedrock Geology of the World*. W.H. Freeman and Company, Inc., New York.
- Ludwig, W. and Probst, J.L., 1998. River sediment discharge to the oceans; present-day controls and global budgets. *American Journal of Science*, 298(4): 265-295.
- Maizels, J.K., 1993. Lithofacies variations within sandur deposits: the role of runoff regime, flow dynamics and sediment supply characteristics. *Sedimentary Geology*, 85: 299-325.
- McMahon, T.A., 1979. Hydrological characteristics of arid zones. *IAHS Publication*, 128: 105-123.
- Meade, R.H., 1982. Sources, sinks, and storage of river sediment in the Atlantic drainage of the United States. *Journal of Geology*, 90(3): 235-252.
- Meybeck, M., 1988. How to establish and use world budgets of riverine materials. In: A. Lerman and M. Meybeck (Editors), *Physical and Chemical Weathering in Geochemical Cycles*. Kluwer Academic Publisher, pp. 247 - 272.

- Meybeck, M., 1994. Origin and variable composition of present day riverborne material, Material Fluxes on the Surface of the Earth. Nat. Acad. Press, Washington, DC, pp. 61-73.
- Meybeck, M. and Ragu, A., 1996. GEMS/Water Contribution to the Global Register of River Inputs (GLORI), GEMS/Water Programme (UNEP/WHO/UNESCO).
- Middleton, N.J. and Thomas, D.S.G., 1997. World Atlas of Desertification. UNEP / Edward Arnold, London.
- Milliman, J.D. and Farnsworth, K.L., in prep. Flux and Fate of Fluvial Sediment to the Coastal Oceans. Oxford University Press.
- Milliman, J.D., Farnsworth, K.L. and Albertin, C.S., 1999. Flux and fate of fluvial sediments leaving large islands in the East Indies. *Journal of Sea Research*, 41: 97 - 107.
- Milliman, J.D. and Meade, R.H., 1983. World-wide delivery of river sediment to the oceans. *Journal of Geology*, 91(1): 1-21.
- Milliman, J.D. and Syvitski, J.P.M., 1992. Geomorphic/Tectonic Control of Sediment Discharge to the Ocean: The Importance of Small Mountainous Rivers. *Journal of Geology*, 100: 525 - 544.
- Mount, J.F., 1995. California Rivers and Streams. University of California Press, Berkeley, CA, 359 pp.
- Nanson, G.C., 1986. Episodes of vertical accretion and catastrophic stripping: a model of disequilibrium flood plain development. *Geological Society of America Bulletin*, 97: 1467-1475.
- Osterkamp, W.R. and Costa, J.E., 1987. Changes accompanying and extraordinary flood on a sand-bed stream. In: L. Mayer and D. Nash (Editors), *Catastrophic Flooding: Binghampton Symposium in Geomorphology*. Allen and Unwin, Boston, pp. 201-224.
- Patton, P.C., Pickup, G. and Price, D.M., 1993. Holocene palaeofloods of the Ross River, central Australia. *Quaternary Research*, 40: 201-212.
- Pickup, G., 1991. Event frequency and landscape stability on the floodplain systems of arid central Australia. *Quaternary Science Reviews*, 10: 463-473.
- Said, R., 1993. The River Nile: geology, hydrology and utilization. Pergamon Press, Oxford, United Kingdom, 320 pp.

- Stallard, R.F., 1998. Terrestrial sedimentation and the carbon cycle: Coupling weathering and erosion to carbon burial. *Global Biogeochemical Cycles*, 12: 231-257.
- Stallard, R.F. and Edmond, J.M., 1983. Geochemistry of the Amazon 2. The influence of geology and weathering environment on the dissolved load. *Journal of Geophysical Research*, 88: 9671-9688.
- Stanley, D.J. and Wingerath, J.G., 1996. Nile sediment dispersal altered by the Aswan High Dam: The kaolinite trace. *Marine Geology*, 133: 1 - 9.
- Strakhov, N.M., 1967. *Principles of lithogenesis*, 1. Oliver and Boyd, London, 245 pp.
- Trimble, S.W., 1981. Changes in sediment storage in the Coon Creek basin, Driftless Area, Wisconsin, 1853-1975. *Science*, 214(4517): 181-183.
- Trimble, S.W., 1999. Decreased Rates of Alluvial Sediment Storage in the Coon Creek Basin, Wisconsin, 1975-93. *Science*, 285: 1244-1246.
- United Nations World Water Assessment Programme, 2003. Executive Summary, The World Water Development Report : Water for People, Water for Life. United Nations.
- Vörösmarty, C.J., Meybeck, M., Fekete, B. and Sharma, K., 1997. The potential impact of neo-castorization of sediment transport by the global network of rivers. *IAHS Publication*, 245: 261-273.
- Vörösmarty, C.J. and Sahagian, D., 2000. Anthropogenic Disturbance of the Terrestrial Water Cycle. *BioScience*, 50(9): 753-765.
- Wall, D.J. and Englot, M.E., 1985. Correlation of annual peak flows for Pennsylvania streams. *Water Resources Bulletin*, 21: 459-464.
- Walling, D.E. and Webb, B.W., 1983. Patterns of Sediment Yield. In: K.J. Gregory (Editor), *Background to Paleohydrology*. John Wiley and Sons, Ltd., pp. 69 - 100.
- Wania, F. and MacKay, D., 1996. Tracking the Distribution of Persistent Organic Pollutants. *Environmental Science & Technology*, 30(9): 390A-396A.
- Wilson, L., 1973. Variations in mean annual sediment yield as a function of mean annual precipitation. *American Journal of Science*, 273(4): 335-349.

Winter, T.C., Harvey, J.W., Franke, O.L. and Alley, W.M., 1998. Ground Water and Surface Water, A single resource. USGS Circular 1139, U.S. Geological Survey, Denver, CO.

Chapter 2: Effects of Climatic and Anthropogenic Change on Small Mountainous Rivers: The Salinas River Example

[Published as: Farnsworth, K.L. and J.D. Milliman, 2003, "Effects of Climatic and Anthropogenic Change on Small Mountainous Rivers: The Salinas River Example", Global and Planetary Change.]

2.1 Introduction

Rivers form the major link between the terrestrial and marine systems, discharging more than $35 \times 10^3 \text{ km}^3$ of water and $20 \times 10^9 \text{ t}$ of suspended and dissolved solids annually (Milliman and Farnsworth, in prep). Suspended sediment delivery to the global ocean has been calculated to be between 15 and $18 \times 10^9 \text{ t/yr}$ (Holeman, 1968; Milliman and Meade, 1983; Milliman and Syvitski, 1992; Ludwig and Probst, 1998), a disproportional amount being discharged by rivers draining active mountains in southern Asia, Oceania, and North and South America. The importance of small mountainous rivers only became obvious when the database was sufficient (e.g. Li, 1976; Griffiths and Glasby, 1985) to indicate the extreme sediment yields from high-standing islands. Holeman (1968) essentially ignored the sediment flux from Oceania, whereas we presently estimate that these high-standing islands discharge more than 40% of the sediment reaching the global ocean (e.g., Milliman et al., 1999).

Erosion and delivery of sediment are a function of river runoff, basin morphology, tectonics, bedrock lithology, human activity, and basin area. For example, sediment yield (load normalized for basin area - e.g., $\text{t/km}^2/\text{yr}$) is an inverse function of basin area (Milliman and Syvitski, 1992). In the case of Southeast Asian and Oceanic rivers draining young mountains, watersheds smaller than 10^3 km^2 have about an order of magnitude greater sediment yield than those rivers having watersheds greater than 10^5 km^2 (Figure. 2-1). Smaller rivers have less basin area in which to store flood-driven sediment (Milliman and Syvitski, 1992), and they also are more likely to respond to event-driven floods (Warrick and Milliman, submitted). As

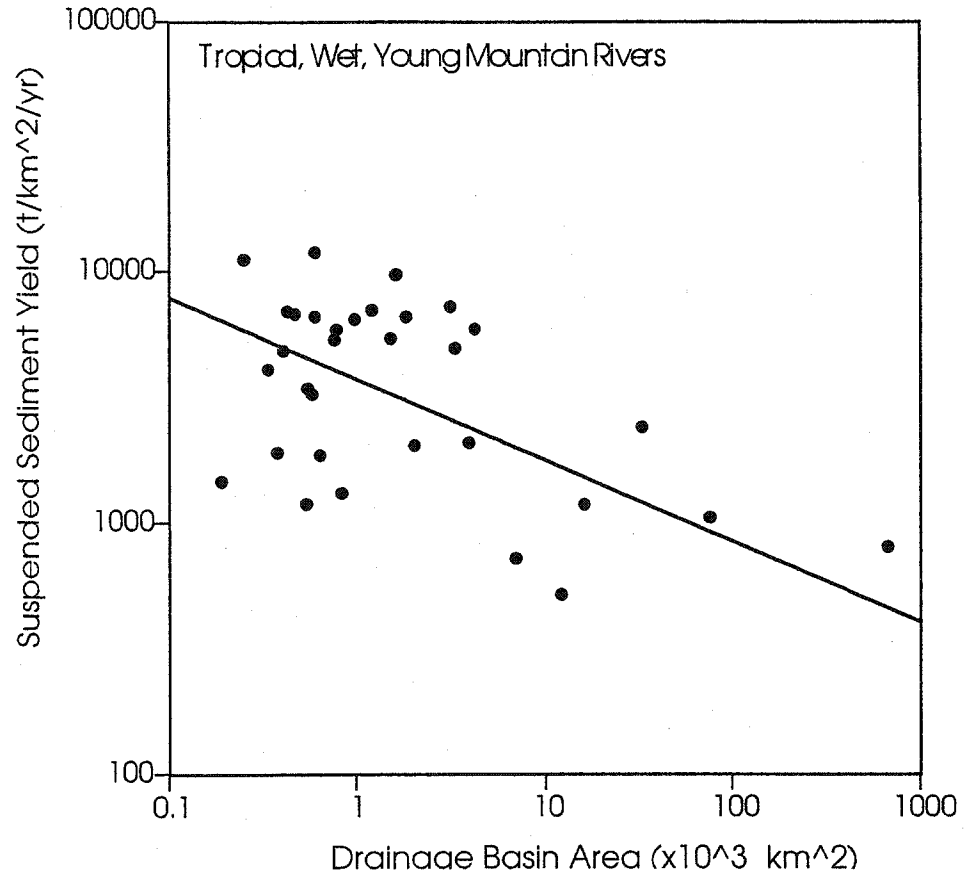


Figure 2-1: Sediment yield ($\text{t}/\text{km}^2/\text{yr}$) for tropical wet rivers draining young mountains in southeastern Asia and the high-standing islands of Oceania. Note the order of magnitude increase in yield with decreasing basin size. Data from Milliman and Farnsworth (in prep.).

the number of small rivers far exceeds the number of large rivers, collectively these smaller rivers are responsible for a much larger amount of sediment delivery to the global ocean than one might intuitively imagine. The 460 mountainous rivers draining six high-standing islands in the East Indies (Sumatra, Java, Borneo, Celebes, Timor and New Guinea), for example, collectively drain less than 1/3 the area of the Amazon River (1.8 vs. 6.3×10^6 km²), but their estimated sediment load is nearly 4 times greater than the Amazon (4.2 vs. 1.1×10^9 t/yr) (Milliman et al., 1999).

The dispersal and fate of sediment derived from small rivers also can be different than that discharged from large rivers. Most large rivers have large flood plains, deltas and/or estuaries in which much of the sediment load is stored for long time periods. Because many large rivers (e.g., Amazon, Orinoco, Congo, Yangtze, etc.) discharge onto broad passive margins, much of the sediment escaping the river or estuary mouth is deposited on the inner shelf; on a global scale relatively little escapes the shelf edge to the deep sea (Meade, 1996). Most small mountainous rivers draining to the oceans, in contrast, are concentrated along active margins and they discharge sediment as a line source (e.g., Mertes and Warrick, 2001), rather than point-source dispersal seen in larger rivers. Moreover, discharge from many of these smaller systems periodically can discharge hyperpycnal concentrations of sediment to the coastal zone, whose transport path and depositional fate may be far different than that for hypopycnal plumes (Mulder and Syvitski, 1995; Warrick and Milliman, submitted).

2.1.1 Variability in Sediment Discharge

Present fluxes of water and sediment from rivers to the coastal ocean are controlled by both natural and anthropogenic influences. Variability in river discharge reflects the influence of both long-term (century to millennial) and short-term (annual and inter-annual) climatic cycles. Superimposed on these are the effects of anthropogenic change on both the watershed and the river itself. Examples of "pristine" rivers, in fact, are difficult to find; most being restricted to sparsely inhabited Arctic watersheds.

Human-induced changes to a drainage basin and the river's flow regime also can affect the transport and delivery of such things as pollutants, pesticides and nutrients. The impact on the coastal ocean from these anthropogenic effects may be subtle but far-reaching. For example, silicate uptake in reservoir waters trapped behind the Danube River's Iron Gates Dam has decreased the silicate delivery and thus shifted the dominant primary producers in NW Black Sea coastal waters from diatoms to dinoflagellates and coccolithorophorids; one result of this shift in ecosystems has been an increase in the occurrence of anoxic conditions (Humborg et al., 1997).

The Yellow River, in northern China is a particularly stark example of natural cycles and anthropogenic change. This river is normally considered an arid river, runoff only being about 40 mm/yr. During the last glaciation, in fact, the river may have been dry, in response to the diminished SW Monsoon and enhanced NE monsoon (Xia et al., 1993). Over the past 100 years, annual precipitation throughout the Yellow River's drainage basin has decreased by about 15% (Galler, 1999), and in

the past decade discharge has dropped by more than 50% in response to both a particularly dry period and the corresponding increase in water removal for irrigation and industrial consumption. As a result, in 1997 the lower Yellow River virtually ceased to exist, being dry for more than 300 days. In contrast to a mean annual load of 1.1×10^9 t/yr documented in the 1950s through late 70s (Qian and Dai, 1980), during the past decade the Yellow River's sediment load has averaged less than 0.2×10^9 , and in 1997 it was only 0.03×10^9 t (Yang et al., 1998; Galler, 1999).

2.1.2 Climate Change

Climatic change is manifested in changes in solar radiation, wind patterns, precipitation, evaporation, and temperature (e.g., storage in glaciers). The hydrologic cycle presumably can absorb small changes in climate, but larger and longer shifts in climate disrupt this balance. Moreover, the long-held image of gradual, long-term change has been modified in light of ice-core and pollen data that show dramatic climate changes occurring on time scales as short as several decades (Dansgaard et al., 1993). Regional weather changes can lead to quick responses in the character (type and density) of vegetation, particularly in arid and semi-arid watersheds, which in turn can have large effects on the erosion and transport of sediment.

Because of the modulation of meteorological events through their watersheds, many large river systems tend to experience relatively little seasonal or inter-annual variability in their discharge. Smaller watersheds, in contrast, are more likely to reflect inter-annual variability (Figure 2-2). Small basins also are more responsive to episodic events and therefore can deliver large portions of their fluvial discharge and sediment loads in relatively short periods of time. In North America, for instance,

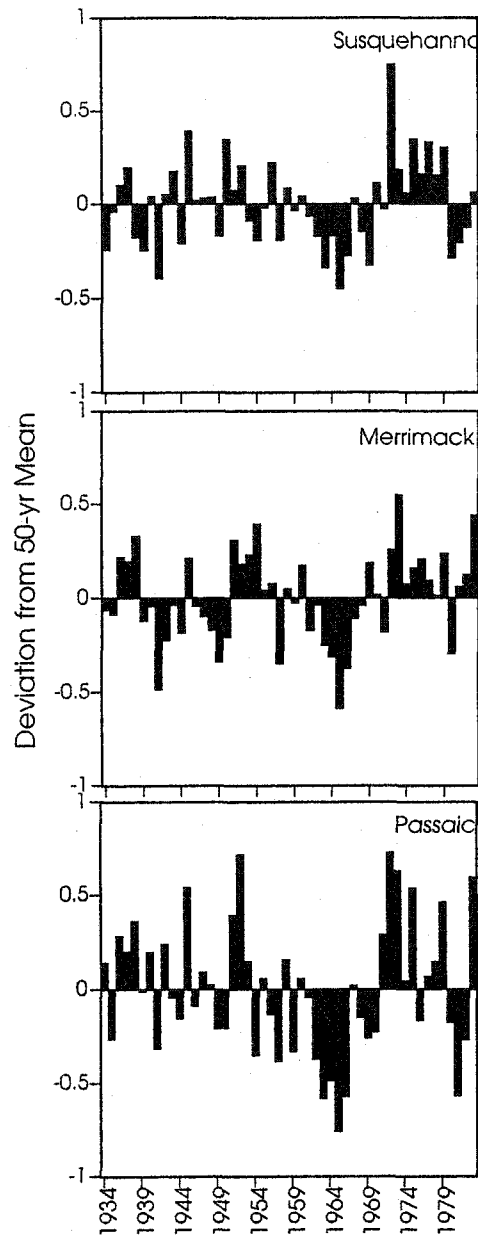


Figure 2-2: Annual deviations from the 50-yr mean discharge of the Susquehanna (drainage basin area = 71,000 km²), Merrimack (12,000 km²) and Passaic (1900 km²) rivers in the northeastern U.S. Deviations in Susquehanna flow are mostly less than 25% of the 50-yr mean, and only one year (1972, a 100-yr event) exceeded 50%. The smaller Merrimack experienced two years in which the annual discharge exceeded 50% of the mean, but the much smaller Passaic experienced ten significant deviations from its 50-yr mean. Data from the U.S. Geological Survey.

peak 24-hr loads of small rivers such as the Santa Clara (near Santa Barbara, California) can exceed that of the Mississippi. The Eel River, in northern California, experienced a peak discharge in December 1964 that was more than an order of magnitude greater than the peak 24-hour load measured on the Mississippi, even though its drainage basin occupies less than 1/400th the area (Figure 2-3). In fact, a search of the extensive USGS data base indicates that only three Californian rivers (Eel, Salinas and Santa Clara) have recorded daily sediment loads greater than 5×10^6 t/day, with sediment yields often exceeding $1000 \text{ t/km}^2/\text{day}$ during particularly large events (Table 2-1). It is important to note that while the Mississippi has no recorded load approaching 5×10^6 t/day, "floods" can extend for hundreds of days (compared to the 2-7 day length for most small-river floods) (Figure 2-3). As a result total flood-derived discharge in a large river like the Mississippi can exceed 400×10^6 t, whereas the flashy peak events in small rivers generally deliver only a fraction as much sediment (Figure 2-3).

The concentrated delivery of sediment during these peak events (not infrequently hyperpycnal; Warrick and Milliman, submitted), however, can affect the dispersal and fate of the event-derived sediment discharged by small rivers (e.g., Morehead and Syvitski, 1999). Peak concentration of suspended sediment in the Santa Clara, Salinas and Eel rivers, for example, can reach 20 to 100 g/l (Table 2-1), whereas peak concentrations in the Mississippi rarely exceed 2 g/l. The importance

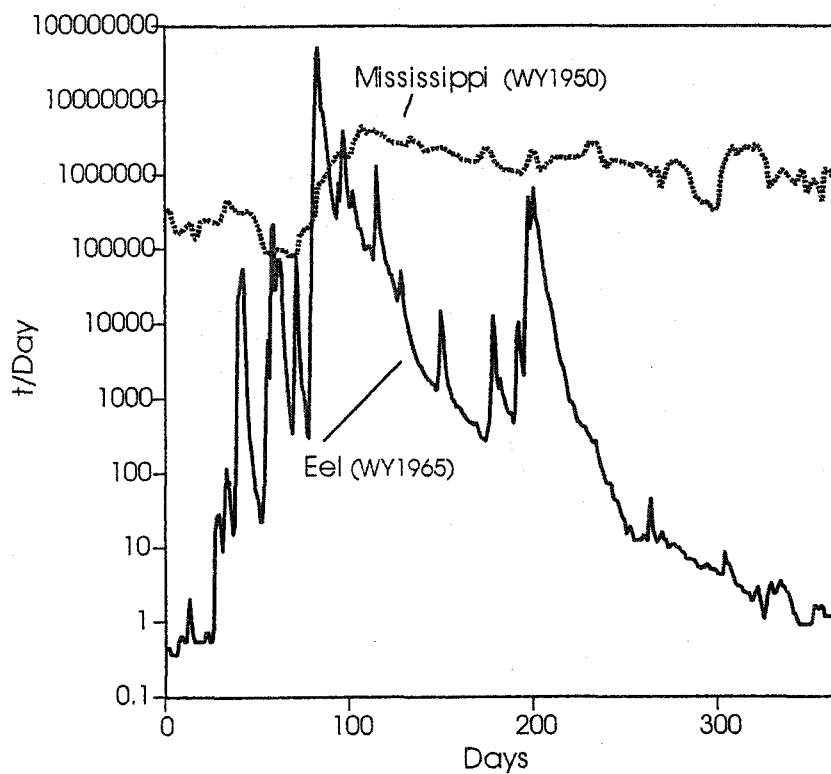


Figure 2-3: Daily sediment loads for the Mississippi and Eel rivers during years of peak discharge, water years 1950 and 1965, respectively. The daily load of the Mississippi was consistently greater than 10^5 t/day throughout the entire year, total annual load being 500×10^6 t. In contrast, the Eel's load exceeded 10^5 t for only 46 days and its total annual load was about 150×10^6 t, but most of the load (110×10^6 t) was transported in three days. During this 3-day period, average sediment concentration was 28 g/l, more than an order of magnitude greater than in the Mississippi (1.2-2 g/l). Data from the U.S. Geological Survey.

Table 2-1. Major 24-hr sediment loads at or near the mouths of U.S. rivers, 1950-90.

River	Basin Area (x10 ³ km ²)	Date	Q (m ³ s ⁻¹)	Sed. Concentration (mg/L)	Sed. Load (x10 ⁶ t/day)	Sed. Yield (t/km ² /day)
Eel	8	12/23/64	18,300	32	51.8	6,470
Eel	8	12/22/64	14,800	28	36.4	4,550
Eel	8	12/22/56	12,000	23	24	3,000
S. Clara	4.1	2/25/69	2,610	69	18.5	4,510
Eel	8	12/24/64	8,810	23	17.3	2,160
S. Clara	4.1	1/25/69	2,100	61	12.9	3,150
Eel	8	12/23/64	8,140	17	12	1,500
S. Clara	4.1	3/4/78	1,720	108	10.7	2,610
Eel	8	1/27/83	6,360	17	9.4	1,170
Salinas	11	2/26/69	1,835	53	9.4	854
Eel	8	12/20/81	6,440	15	8.7	1,080
Salinas	11	3/3/83	1,693	34	7.9	987
Eel	8	12/25/64	5,380	6.2	7.7	962
S. Clara	4.1	2/10/78	1,260	50	6.9	1,680
Eel	8	12/26/64	4,980	16	6.8	850
Eel	8	12/19/81	5,460	14	6.5	812
S. Clara	4.1	3/1/83	1,470	44	6.4	1,560
Eel	8	1/16/74	7,600	7.6	6.2	775
Salinas	11	1/27/69	1,510	43	6.2	563
Eel	8	1/4/66	5,470	13	6.1	762
Eel	8	1/5/66	7,250	9.4	6	750
Eel	8	2/16/82	4,860	13	5.5	687
Eel	8	12/19/56	3,720	16	5.1	637

of such infrequent events in small rivers makes them both interesting and frustrating to study because the long-term sediment discharge can depend on a few scattered events, in some cases no more than a few times every decade.

2.1.3 Anthropogenic Impact

Man has proved to be an effective geologic agent in altering the landscape and therefore river erosion and delivery. Hooke (2000) estimates earth-moving activity related to human actions to be about 100×10^9 t/yr, 5-fold greater than the total fluvial delivery to the global ocean. While the anthropogenic impact on global fluvial sediment fluxes cannot yet be calculated with any degree of accuracy, humans may be directly or indirectly responsible for 80-90% of the fluvial delivery to the coastal ocean (Milliman et al., 1987; Douglas, 1996; Milliman and Farnsworth, in prep). Yet any global pattern of sediment delivery belies recent and ongoing changes that are occurring on local and regional scales. Changing agricultural patterns and reforestation over the past 50 – 100 years have resulted in decreased erosion throughout much of Europe and North America. Decreased sediment loads “augmented” by river-bed mining for sand and gravel, for example, has resulted in the progressive scour of many Italian river beds in recent years, one result being decreased sediment delivery to the coastal zone and thereby increased coastal erosion (Simeoni and Bondesan, 1997; Coltorti, 1997). In contrast to the decreased erosion and sediment transport by rivers in much of the developed western world, erosion is increasing throughout many developing countries. Although definitive data are still lacking, increased deforestation in the mountainous regions of southern Asia and in Oceania (whose rivers, by virtue of their relatively youthful morphology and geology,

as well as the seasonally heavy rains, have high sediment yields) almost certainly have lead to greater fluvial erosion.

The degree to which fluvial water and sediment reach the coastal ocean, of course, depends upon other human activities, namely the construction of structures for flood control, water diversion, power generation and recreation. Reservoirs and irrigation channels can retain a large proportion of the fluvial sediment load, sometimes without actually affecting the amount of annual water discharge. Barrage construction to facilitate irrigation along the lower Indus River in the late 1940s, for example, resulted in a 75% decrease in the river's fluvial sediment load, but only a slight decrease in average annual water discharge; subsequent construction of a series of high dams in the Indus headwaters in the early 1960s subsequently reduced annual discharge of the river by nearly 80% (Milliman et al., 1985). Vörösmarty et al. (1997) have calculated that the 633 dams with large reservoirs (storage capacity greater than 0.5 km^3) globally store about 5000 km^3 of water (nearly 15% of the global fluvial discharge). Collectively they intercept about 40% of the world's freshwater discharge and may trap 25% of the global sediment delivery to the ocean. Woodward (1995) lists five major rivers draining into the Mediterranean whose total sediment discharge has decreased from nearly $190 \times 10^6 \text{ t/yr}$ to less than $10 \times 10^6 \text{ t/yr}$.

Dam construction in North America and Europe essentially has ceased, both because most economic and suitable dam sites already have been occupied and because of increasing concern about weighing the environmental impact against economic benefit. Data from the International Commission on Large Dams (ICOLD) show that as of 1999 Canada had no large dams (defined as being higher than 15 m)

under construction, whereas China and India had 330 and 650, respectively. The recent acceleration of dam construction in Africa and southern Asia can be illustrated in the following: of the 43 countries responding to an ICOLD questionnaire in 1999 (Australia and most countries in South America and within the former Soviet Union were notable in their absence), a total of 47,425 dams were listed, of which China accounted for more than half, a remarkable number considering that in 1949 China had only 3 large dams! Moreover, of the more than 10,000 dams higher than 30 m, China is responsible for 45%. Continuing dam construction throughout Africa and southern Asia therefore may affect significantly the amount of water and sediment delivery to the global ocean.

2.2 Problems in Estimating Sediment Delivery

As discussed in the preceding paragraphs, calculating or even estimating the sediment load of a river is complicated by the impact of natural forcings (climate, morphology, geology), watershed utilization and water management. Because of the changing climate and continually shifting anthropogenic impact, fluvial data must be continually updated. Relying on old data becomes increasingly risky as the character of the watershed and its climate changes. This continued need - in fact increasing need - for river data stands in stark comparison with the decreasing number of rivers that are presently monitored. Vörösmarty et al. (2001) estimate that hundreds of hydrologic stations are closed each year, and the data from many of those rivers that continued to be monitored are difficult to obtain. The various existing global data

banks, for instance, have few data from African rivers more recent than 1984, and French river data since 1980 are almost impossible to obtain.

While U.S. fluvial data are ever easier to access over the U.S. Geological Survey's web page, the number of new data decreases each year. Lanfear and Hirsch (1999) estimate that since the early 1990s more than 100 U.S. hydrologic stations annually have been closed. And the story for water quality is even grimmer: only the Mississippi, Colorado, Columbia and Rio Grande (and their tributaries) are monitored regularly, even though the Colorado and Rio Grande presently effectively discharge little water and no sediment to the coastal ocean. This contrasts strongly with the 20-yr period from the mid-1960s to the mid-80s when essentially all of the large U.S. rivers and many of the smaller rivers were monitored for sediment discharge. Luckily, major events occurred in many of these rivers (Table 2-1), so that we can gather some insight as to their effect.

2.3 Response to Change and Episodic Events: The Salinas River Example

The rivers of California provide particularly interesting examples of the impact of climate and anthropogenic change on fluvial discharge to the coastal ocean. Precipitation patterns throughout the state vary greatly, from less than 100 mm/yr in many of the central valleys to more than 2000 mm/yr in the northern mountains. These regional precipitation patterns are reflected in river runoff: the Tijuana River along the Mexican border has an annual runoff of 10 mm/yr compared to the Mad River in the north with a runoff of 1100 mm/yr. But mean annual precipitation and runoff tell only part of the story because California weather is also one of extremes:

extremely wet or extremely dry” (Mount, 1995). The generally arid weather in many drainage basins is punctuated by periodic, intense bursts of precipitation, often lasting only a few days. Moreover, with few exceptions, most Californian rivers have drainage basins less than 10,000 km² in area, so that the rivers tend to be more responsive to both natural and human-induced change.

Southern and central Californian weather patterns are strongly controlled by the El Niño/Southern Oscillation (ENSO). Warmer sea-surface temperatures in the NW Pacific during El Niño periods result in the northward movement of moisture-laden air, often resulting in heavy rains, although they tend to be episodic. North of San Francisco Bay the ENSO influence is diminished and more weather patterns roll in from Alaska and Canada and the adjacent northern ocean.

Discharging into Monterey Bay, about 100 km south of San Francisco Bay, the Salinas River is the northernmost Californian river that responds strongly to the ENSO signal. With a watershed area of 11,000 km², the basin is 240 km long and has an average width of 65 km. The river flows almost entirely within a northwest-trending structural trough defined by two parts of the NW-SE-trending Coast Range Province, the Sierra de Salinas (maximum elevations 900-1500 m) in the southwest and the Gabilan Range (750 – 1200 m) in the northeast (Figure 2-4a). The mountains bounding the Salinas basin were formed by late Cenozoic uplift and deformation and are underlain by marine sedimentary, intrusive igneous and metamorphic rocks. Generally older consolidated rocks are exposed in the mountains, whereas a cover of recent alluvium and floodplain deposits characterizes the valleys and lowlands.

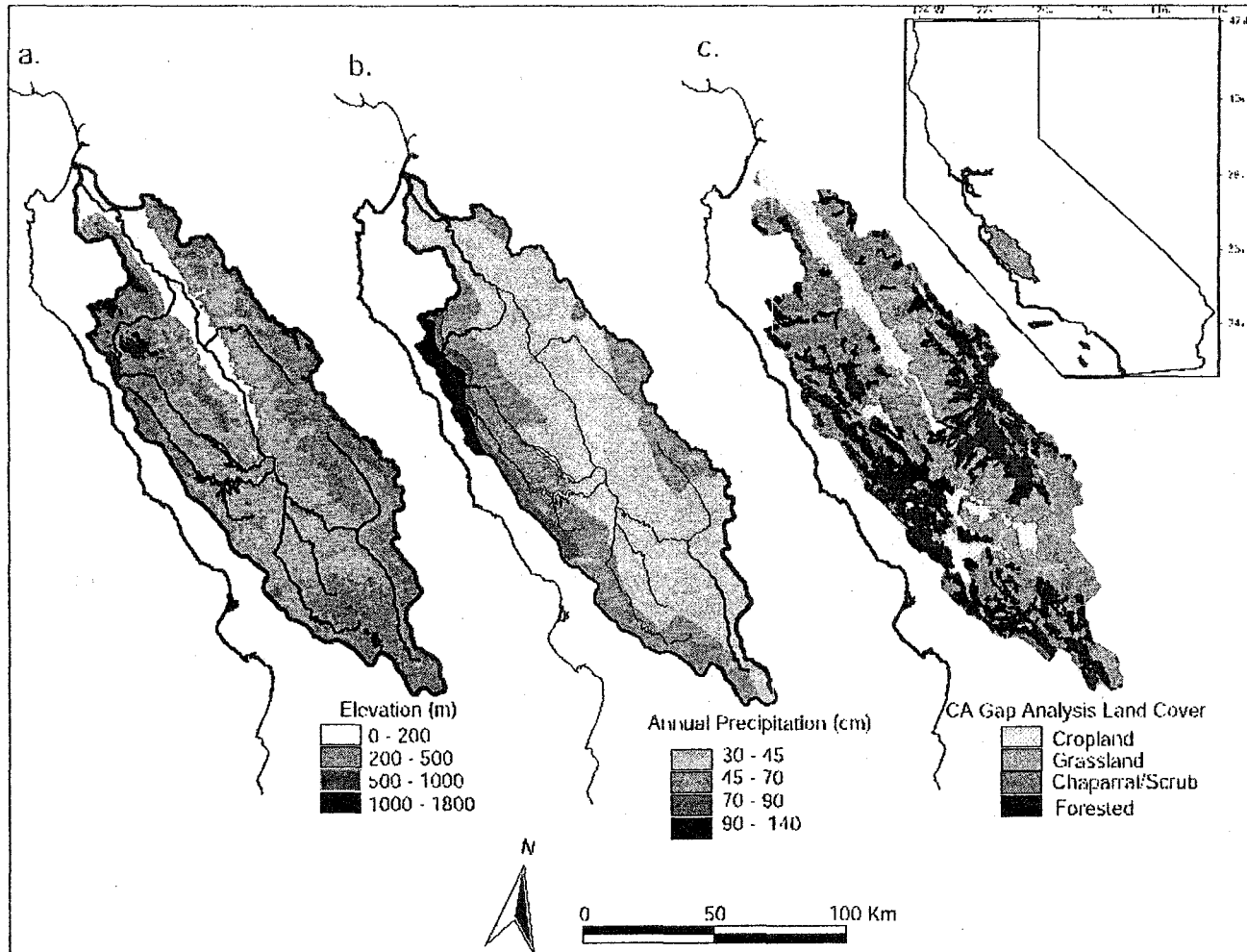


Figure 2-4: Salinas River drainage basin characteristics including elevation (a), annual precipitation (b) and land cover (c). The western mountain ranges receive much greater levels of precipitation than the central valley, although the rich river-derived valley alluvium is the major area for agriculture within the watershed.

Possessing a Mediterranean climate, nearly 90% of the annual precipitation in the Salinas basin falls between November and April, resulting in highly seasonal delivery of both water and sediment to the coastal ocean. Orographically induced rainfall causes heavy annual precipitation (1000 mm/yr) along the southeastern boundary of the watershed, and a rain shadow (<300 mm/yr) in the valley and northern mountains (Figure 2-4b). Because precipitation in the Salinas watershed is influenced by the passing of mid-latitude Pacific storms rather than northern storms, it is relatively warm, falling mostly as rain rather than snow.

The Salinas River has a limited base flow, with many years reporting runoff less than 100 mm/yr (Figure 2-5). The Nacimiento River, San Antonio River and Arroyo Seco drain the wetter western coastal ranges, while the San Lorenzo and Estrella are the main tributaries draining the drier eastern range. Although equal in area to the San Lorenzo, the Arroyo Seco has a 15-fold greater discharge (Figure 2-5).

Three large dams along tributaries have changed the natural variability and timing of flow. The Salinas Dam (Lake Santa Margarita) was constructed by the U.S. Army Corps of Engineers in 1941. Monterey County built the Nacimiento and San Antonio dams on the Nacimiento and San Antonio rivers in 1956 and 1965, respectively, both with storage capacities of approximately 0.4 km³. Water is released from these dams for irrigation and groundwater recharge during the dry summers (USGS, 2000). The amount of water released by the Nacimiento Dam during normal years is similar to that entering the reservoir. However, during extreme years, the hydrograph is highly altered by the presence of the dam. During small precipitation events in 1969, for instance, the reservoir was able to absorb most

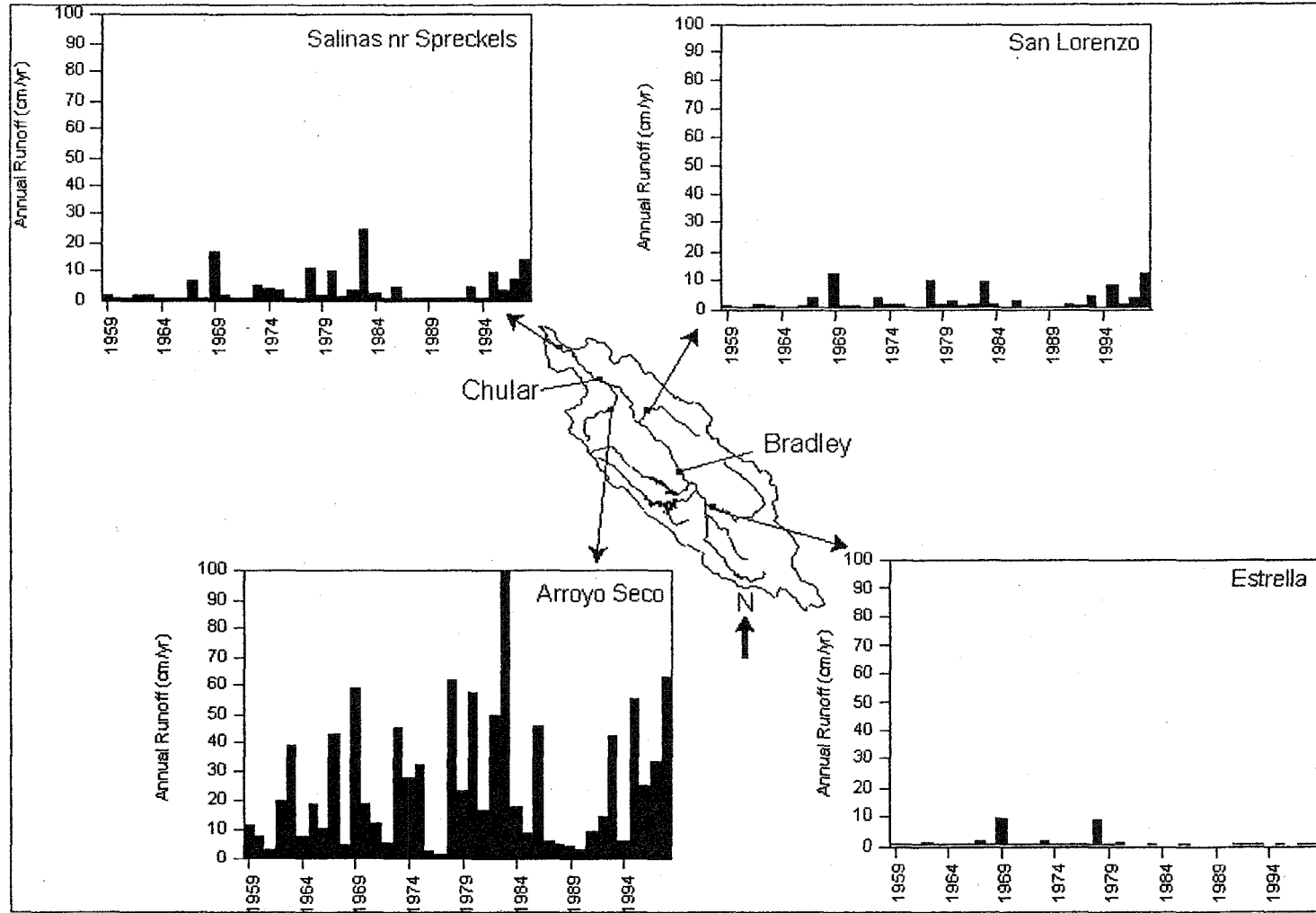


Figure 2-5: Annual runoff for four stations within the Salinas River Basin. The major source of water to the Salinas River is from the western mountain ranges, specifically the unrestricted Arroyo Seco.

of the discharge, but larger storms during that year filled the reservoir and water had to be released (Figure 2-6).

The number of no/low-flow days (< 1cfs) has changed dramatically over the past 70 years. Between 1930 and 1960, the number of no/low-flow days was generally inversely proportional to the amount of precipitation (Figure 2-7). But by 1960, the incremental release of water from the Nacimiento Dam and the San Antonio Dam regulated discharge of reservoir water, thereby modulating down-stream flow and drastically reducing the number of no/low-flow days. During the past decade, however, the pattern has changed again: even though annual precipitation throughout much of the 1990s was high, due to a number of severe El Niño years, the number of low-flow days at the Spreckels gauging station increased, presumably reflecting the increased removal of upstream water for agricultural use.

During the 70 years of monitoring, the Salinas has delivered approximately 2.3×10^8 tons of sediment to Monterey Bay. Mean annual water discharge is $4 \text{ km}^3/\text{yr}$ ($120 \text{ m}^3/\text{sec}$) and mean annual sediment load is $3.3 \text{ t}/\text{yr}$, but in only 18 of those years did the annual load actually approach or exceed the 70-yr mean (Figure 2-8). In 31 of the 70 years, the river delivered less than $0.1 \times 10^6 \text{ t}/\text{yr}$, whereas in 6 years the load exceeded $15 \times 10^6 \text{ t}/\text{yr}$ (Figure 2-8). Total high-discharge time, however, was less than 5 weeks. Four of the 6 high-load years occurred during El Niño years, and 2 during "Nada Niño" years; no significant delivery events occurred during La Niña years (Figure 2-9).

The Salinas Valley has been called the "Salad Bowl of America" due to the large amounts of intense agriculture within its watershed. Land-use throughout the

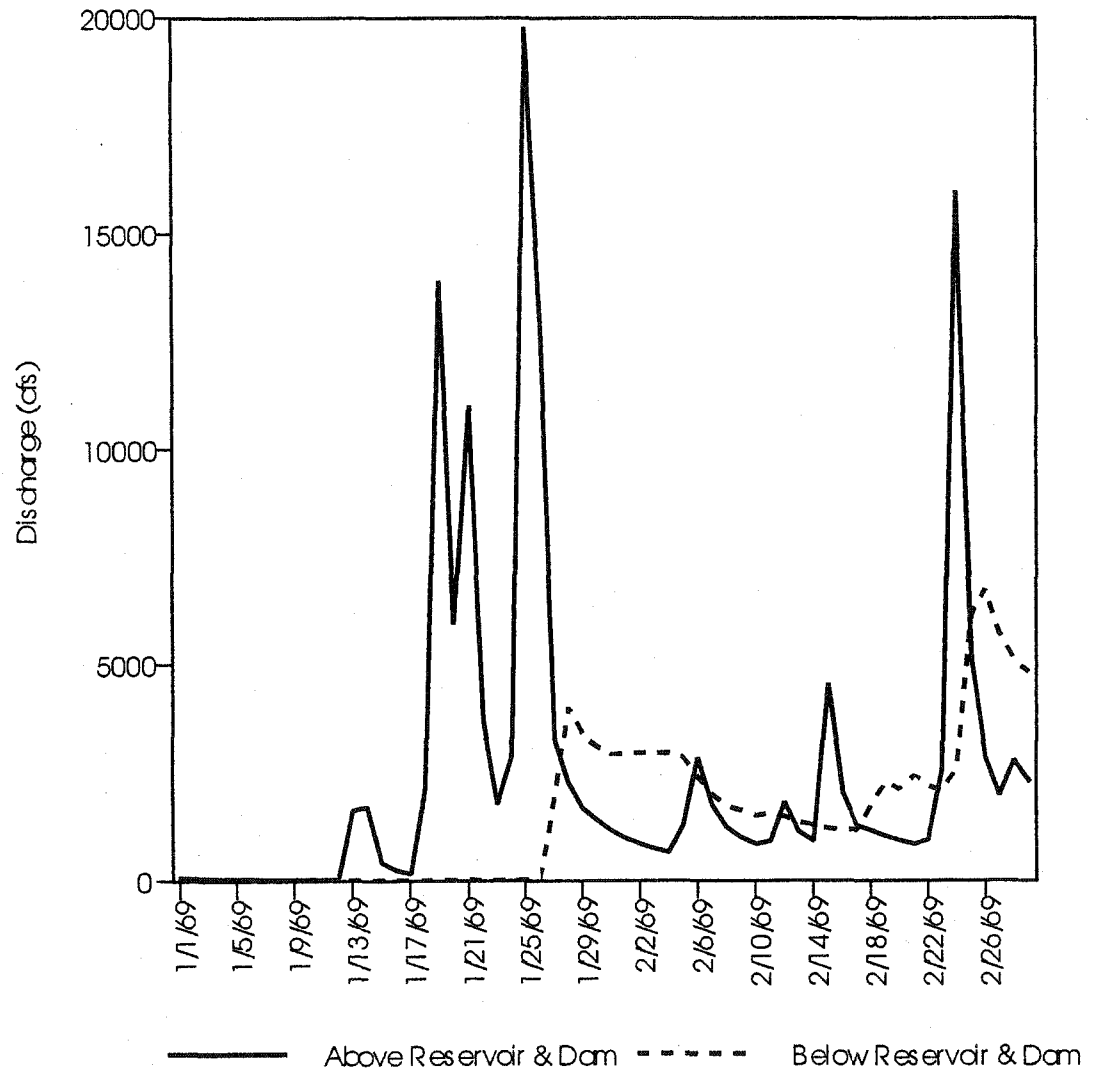


Figure 2-6: River discharge data from the USGS gauging stations above and below Nacimiento Dam. Gauging stations used were USGS 11148800 Nacimiento River near Bryson and 11149400 Nacimiento River near Bradley. There is a significant alteration to the natural hydrograph of the Nacimiento River, which would naturally be a large source of water and sediment to the Salinas River.

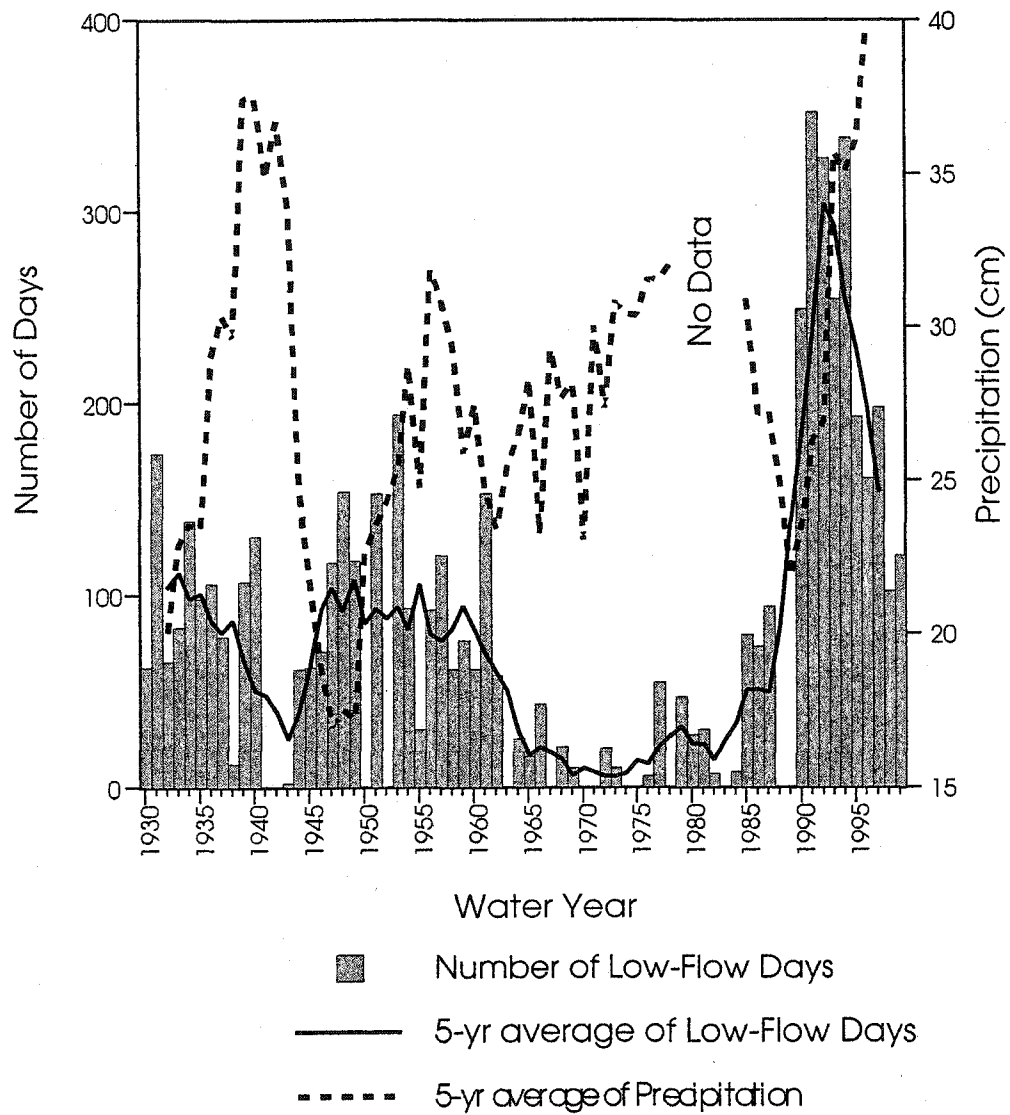


Figure 2-7: Annual number of no- to low-flow days at the Spreckels gauging station near the mouth of the Salinas River. The inverse relationship between precipitation and the number of days with essentially no flow is seen until the 1990s, when water use within the drainage basin changed.

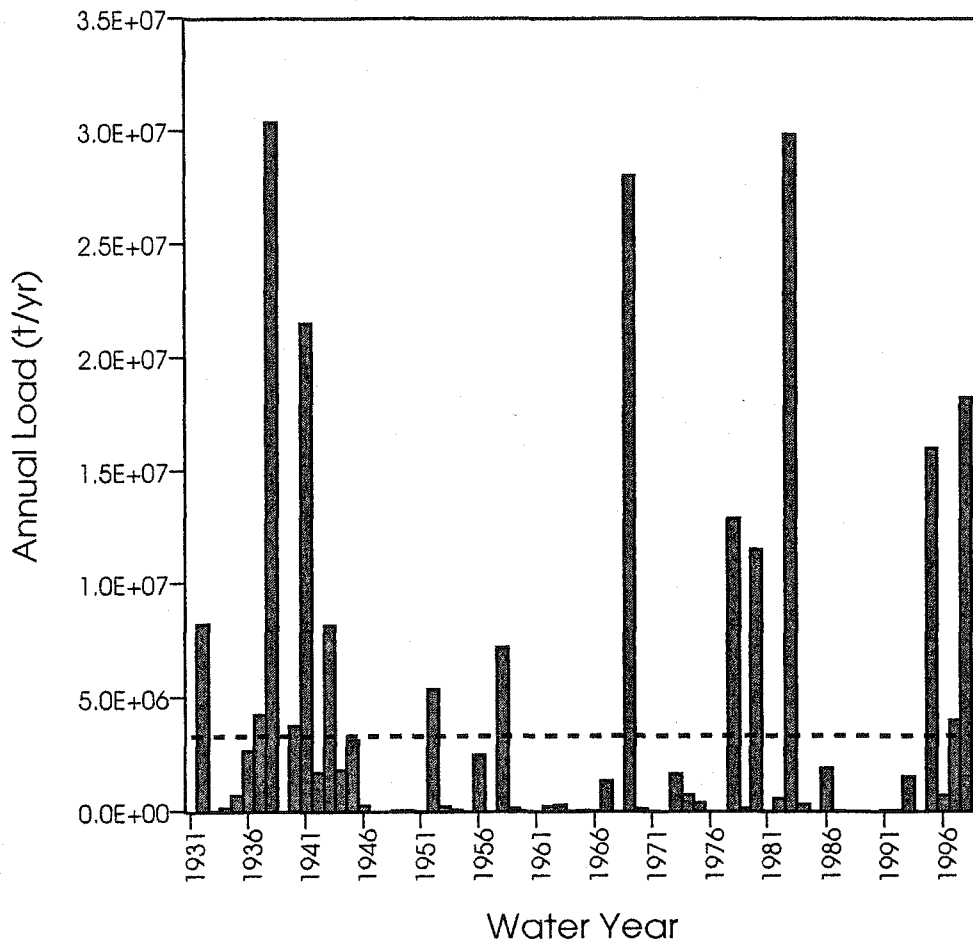


Figure 2-8: Calculated annual load of the Salinas River at Spreckels, using a rating curve developed from 10 years of suspended sediment measurements. The mean annual load is indicated, but due to the episodic nature of this river, is rarely approached.

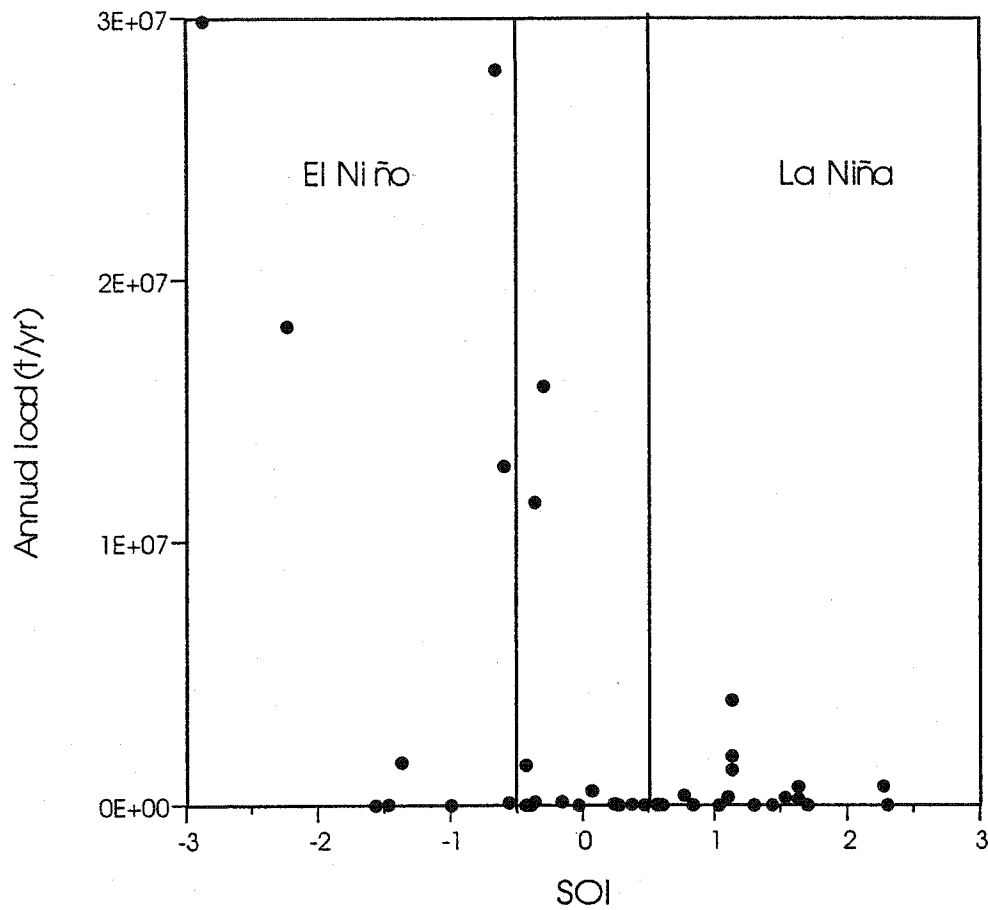


Figure 2-9: The influence of the El Niño Southern Oscillation (ENSO) is seen in the relationship between the Southern Oscillation Index (SOI) and the annual load of the river. There have been no high load (high flow) years during La Niña years, and the largest events have been during El Niño years. Note, however, that the magnitude of the annual load shows little quantitative relation to the SOI

basin, however, is varied, with agriculture dominating the valley floor, rangeland in the hills and forested regions on the steep slopes (Figure 2-4c). In recent years land use within the watershed has changed with the marked increase in viticulture; we assume this change in land use also has affected erosion rates, although suspended sediment in the river has not been sampled since 1979. Water removal from the system is mainly for agricultural use and some years have less water passing Spreckels than in the upper reaches of the river (Figure 2-10). In 1993, for instance, Spreckels (location of the most downstream gauging station) monitored about 30% less discharge than the Salinas tributaries. Even this, however, does not indicate the entire magnitude of water withdrawal, since agricultural activity is also intense downstream from Spreckels.

Rivers are assumed to be the dominant source for California beach sand (Hicks and Inman, 1987). While event delivery to coastal ocean is periodic, littoral drift is continuous. The low- to no- flows in the summer, combined with the wave-dominated coastline, result in sandbar extension across the river mouth, changing the Salinas estuary into a closed lagoon. Therefore for much of the year the Salinas does not discharge to Monterey Bay. Breaching of the sandbar occurs during flood events, and more recently has been "helped" by bulldozers from the Monterey County Water Resources Agency, in large part to prevent flood damage to surrounding areas and to prevent heavy silt loads from entering the Moss Landing Harbor. Thus sediment input to the bay from the Salinas River occurs only when the sand bar has been breached during high flow periods. During these high-flow events the amount of sediment in the river water may exceed hyperpycnal concentrations. The 1978

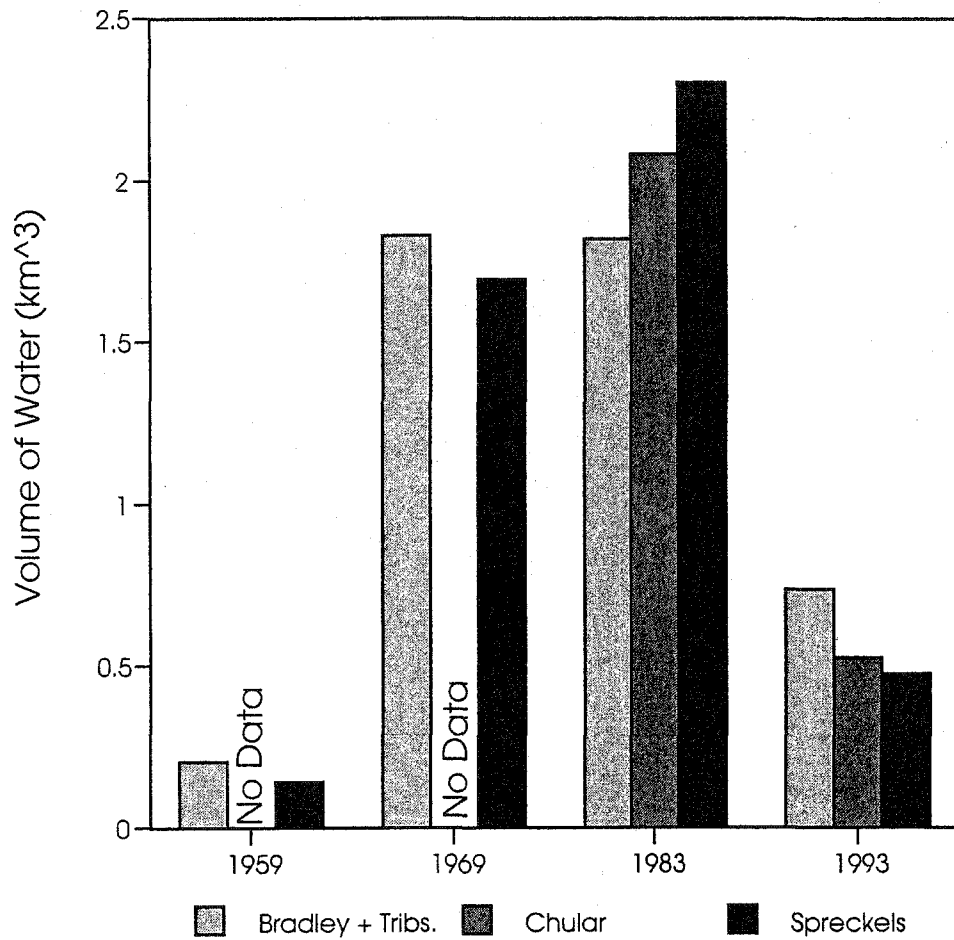


Figure 2-10: Water use within the basin has created a negative water balance within the river itself. The withdrawal of water along the course of the river has caused the volume of water passing a station to be less than that of the station a few km upstream. This is seen in the gauging stations at Bradley, Chular, and Spreckels, in the lower Salinas basin (see Fig. 4 for locations). Although the volume of water passing Chular should be sum of water flowing past Bradley and the San Lorenzo and Arroyo Seco tributaries, in 3 of the 4 years shown in this figure the volume decreases downstream, the result of water withdrawal for agricultural use.

measured concentrations exceeded 24 g/l, suggesting that during major events, such as those during the 1969 and 1983 floods, sediment concentrations may have reached hyperpycnal levels. The fate of sediment derived from episodic hyperpycnal events in the Salinas River at present is difficult to ascertain. Does it accumulate off the river mouth or does most of it escape offshore; if the latter, how does it mobilize and where does it go? The effect of such episodic sediment discharges to the shoreline, benthos, water column and the coastal zone must be immense.

2.4 Discussion

The Salinas River is not that different from many other small rivers throughout the world, which periodically can discharge large volumes of water and sediment to the coastal ocean but whose fluvial and land-use character continue to change. Unfortunately, as changes in land-use and climate continue it will be increasingly difficult to rely on previously collected data to characterize or quantify the amount of sediment discharged to the coastal ocean. Because the Salinas River was monitored for suspended sediment by the USGS only until the late 1970s, rating curves based on these data cannot adequately indicate sediment loads prior to dam construction in the 1950s and 60s or changing land and water use in the past 20 years. The Nacimiento and San Antonio dams almost certainly reduced sediment delivery from the Salinas. Therefore, calculations based on a rating curve from the 1970s will underestimate the historical sediment load of the river prior to 1965. The increased recent agricultural use of the lower Salinas watershed has led to increased water withdrawal from the river for irrigation, thereby altering the river's hydrograph

(Figure 2-7). Present-day sediment flux therefore is probably less than would be calculated using the 1970s-based rating curve. Nevertheless, the lack of more recent data means that we must continue to use this antiquated rating curve: there is nothing else, nor will there be in the foreseeable future.

Small mountainous rivers draining to the coastal ocean play a vital role in the global sediment budget, but the problems associated with using mean values derived from short records need to be addressed and better understood to be able to more accurately estimate the global sediment budget, as well as to study the role of these small rivers locally in control of coastal sedimentation and erosion. It is particularly important that episodic events are closely monitored on these smaller rivers. Both because these often represent the major (perhaps only) period of significant sediment discharge, but also because suspended sediment concentration (at least in some rivers) may reach or exceed hyperpycnal levels, suggesting that they may move offshore via density flows, thereby avoiding the coastal circulation cells (Warrick and Milliman, submitted). Our ability to understand present conditions and predict future conditions will be made increasingly difficult as we rely on increasingly antiquated data. To understand the impact of future change, be it in terms of climate or land-use, we must first understand natural variability of fluvial systems. Mean annual trends derived from an increasingly old database will not be adequate.

2.5 Acknowledgements

Research funds for this and related papers have come from a series of grants from the Marine Geology and Geophysics program of the National Science

Foundation. We thank our colleagues, particularly Jonathan Warrick, Des Walling and James Syvitski for continuing dialog as well as comments on a previous draft of this paper. Many thanks also to Mark Morehead and an anonymous reviewer for their constructive comments.

2.6 References:

- Coltorti, M., 1997. Human impact in the Holocene fluvial and coastal evolution of the Marche region, Central Italy. *Catena*, 30: 311-335.
- Dansgaard, W. et al., 1993. Evidence for general instability of past climate from a 250-kyr ice-core record. *Nature*, 364(6434): 218-220.
- Douglas, I., 1996. The impact of land-use changes, especially logging, shifting cultivation, mining and urbanization on sediment yields in humid tropical Southeast Asia: a review with special reference to Borneo. *IAHS Publication*, 236: 463-471.
- Galler, J.J., 1999. Medium- and long-term changes in fluvial discharge to the sea: the Yellow River case study. M.Sc., College of William and Mary, Williamsburg, VA, 78 pp.
- Griffiths, G.A. and Glasby, G.P., 1985. Input of river-derived Sediment to the New Zealand Continental Shelf: I. Mass. *Estuarine, Coastal and Shelf Science*, 21: 773-787.
- Hicks, D.M. and Inman, D.L., 1987. Sand Dispersion from an Ephemeral River Delta on the Central California Coast. *Marine Geology*, 77: 305-318.
- Holeman, J.N., 1968. The Sediment Yield of Major Rivers of the World. *Water Resources Research*, 4(4): 737-746.
- Hooke, R.L., 2000. On the history of humans as geomorphic agents. *Geology*, 28(9): 843-846.
- Humborg, C., Ittekkot, V., Coclasu, A. and Bodungen, B., 1997. Effect of Danube River dam on Black Sea biogeochemistry and ecosystem structure. *Nature*, 386: 385-388.
- Lanfear, K.J. and Hirsch, R.M., 1999. USGS Study Reveals a Decline in Long-record Streamgages. *EOS*, 80(50): 605-607.
- Li, Y.-H., 1976. Denuadation of Taiwan Island since the Pliocene epoch. *Geology*, 4: 105-107.
- Ludwig, W. and Probst, J.L., 1998. River sediment discharge to the oceans; present-day controls and global budgets. *American Journal of Science*, 298(4): 265-295.

- Meade, R.H., 1996. River-sediment inputs to major deltas. In: J.D. Milliman and B.U. Haq (Editors), *Sea-Level Rise and Coastal Subsidence*. Kluwer Academic Publishers, Boston, pp. 63-85.
- Mertes, L.A.K. and Warrick, J.A., 2001. Measuring flood output from 110 coastal watersheds in California with field measurements and SeaWiFS. *Geology*, 29(7): 659-662.
- Milliman, J.D. and Farnsworth, K.L., in prep. *Flux and Fate of Fluvial Sediment to the Coastal Oceans*. Oxford University Press.
- Milliman, J.D., Farnsworth, K.L. and Albertin, C.S., 1999. Flux and fate of fluvial sediments leaving large islands in the East Indies. *Journal of Sea Research*, 41: 97 - 107.
- Milliman, J.D. and Meade, R.H., 1983. World-wide delivery of river sediment to the oceans. *Journal of Geology*, 91(1): 1-21.
- Milliman, J.D., Shen, H.-T., Yang, Z.-S. and Meade, R.H., 1985. Transport and deposition of river sediment in the Changjiang Estuary and adjacent continental shelf. *Cont. Shelf Res.*, 4(1-2): 37-44.
- Milliman, J.D. and Syvitski, J.P.M., 1992. Geomorphic/Tectonic Control of Sediment Discharge to the Ocean: The Importance of Small Mountainous Rivers. *Journal of Geology*, 100: 525 - 544.
- Milliman, J.D., Yun-Shun, Q., Mei-E, R. and Saito, Y., 1987. Man's influence on the erosion and transport of sediment by Asian rivers; the Yellow River (Huanghe) example. *Journal of Geology*, 95(6): 751-762.
- Morehead, M.D. and Syvitski, J.P., 1999. River-plume sedimentation modeling for sequence stratigraphy; application to the Eel margin, Northern California. *Marine Geology*, 154(1-4): 29-41.
- Mount, J.F., 1995. *California Rivers and Streams*. University of California Press, Berkeley, CA, 359 pp.
- Mulder, T. and Syvitski, J.P.M., 1995. Turbidity currents generated at river mouths during exceptional discharges to the world oceans. *Journal of Geology*, 103(3): 285-299.
- Qian, N. and Dai, D.Z., 1980. The problems of river sedimentation and the present status of research in China, *Symp. River Sedimentation*. China Hydraul. Eng., pp. 1-39.

- Simeoni, U. and Bondesan, M., 1997. The role and responsibility of man in the evolution of the Italian Adriatic coast. *Bull. Inst. Oceanog. Monaco*, 18: 111-132.
- USGS, 2000. National Water Information System. <http://waterdata.usgs.gov/nwis-w/CA>.
- Vörösmarty, C.J. et al., 2001. Global Water Data: A Newly Endangered Species. *EOS*, 82 (5): 54-58.
- Vörösmarty, C.J., Meybeck, M., Fekete, B. and Sharma, K., 1997. The potential impact of neo-castorization of sediment transport by the global network of rivers. *IAHS Publication*, 245: 261-273.
- Warrick, J.A. and Milliman, J.D., submitted. Event-Driven Hyperpycnal Discharge from Southern California Rivers. *Geology*.
- Woodward, J.C., 1995. Patterns of erosion and suspended sediment yield in Mediterranean river basins. In: I.D.L. Foster, A.M. Gurnell and B.W. Webb (Editors), *Sediment and Water Quality in River Catchments*. John Wiley and Sons, Chichester, pp. 365-389.
- Xia, D.X., Wu, S.Y. and Yu, Z., 1993. Changes of the Yellow River since the last glacial age. *Marine Geology and Quaternary Geology*, 13: 83-88.
- Yang, Z.S., Milliman, J.D., Galler, J., Liu, J.P. and Sun, X.G., 1998. Yellow River's Water and Sediment Discharge Decreasing Steadily. *EOS, Transactions, American Geophysical Union*, 79(48): 589,592.

Chapter 3: Local and Global Controls on the Magnitude and Timing of Fluvial Delivery from the Salinas River

3.1 Introduction

The dominant source of freshwater and sediment to the coastal oceans is rivers. In general, relationships between freshwater runoff and sediment yield (load normalized to basin area) decrease with increased basin area (Fread, 1993; Milliman and Syvitski, 1992; Mosley and McKerchar, 1993). This is due to the inability of small watersheds to moderate the impact of storms and to store significant amounts of water and sediment. As such, small rivers draining mountainous coastlines are important sources of sediment to the coastal zone. Unfortunately, many of these small rivers have not been studied or monitored.

One exception is the Salinas River of California, which has been monitored for seventy years. The work presented here addresses the magnitude and timing of historical sediment delivery from the Salinas River to the Monterey Bay. Understanding the character of discharge to the coastal ocean plays an important role in delineating not only the ultimate fate of the sediment, but also the transport pathways.

The Salinas River, the largest river along the Central Coast of California and third largest in the state, originates in the mountains east of the city of San Luis Obispo and flows northwestward into Monterey Bay (Figure 3-1). The Salinas Valley is approximately 30 km wide and 250 km long, and is oriented parallel to the coast along a north-northwest to south-southeast axis. To the west it is bounded by the Santa Lucia Range, while to the east are the Gabilan and Diablo Ranges. The valley is located in a tectonically active region, with the San Andreas Fault

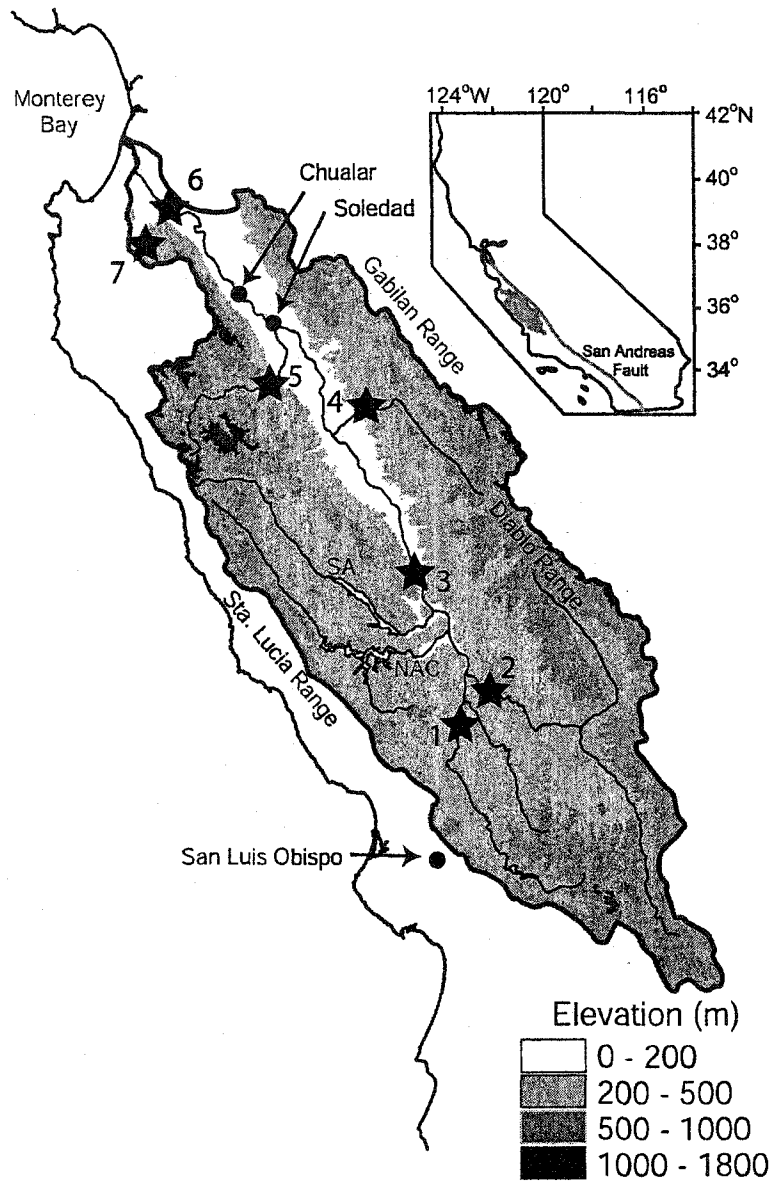


Figure 3-1: Topography of the Salinas watershed and the gauging stations used throughout this study. Stations are numbered from the headwaters to the mouth; 1) Salinas River at Paso Robles, 2) Estrella River nr Estrella, 3) Salinas River nr Bradley, 4) San Lorenzo Creek nr King City, 5) Arroyo Seco nr Soledad, 6) Salinas River nr Spreckels and 7) El Toro Creek nr Soledad. Two major reservoirs are indicated; SA: San Antonio and NAC: Nacimiento.

running parallel to the valley, northeast of the Gabilan Ranges. As such, the entire watershed is moving northward at between 3 – 6 cm/yr. Older granitic and metamorphic rocks in this basin are Santa Lucia and Gabilan ranges, and originated in the northwestern part of the Mojave Desert as a southern continuation of the Sierra Nevada (Kistler and Champion, 2001; Mattinson and James, 1985). They were uplifted and then dropped into deep marine conditions so as to become draped with marine deposits, known as the 10-million-year old Monterey Shale.

The more recent geologic history (Quaternary, < 2 ma) includes more active uplift of the mountain ranges and the sinking of the valley floor. This resulted in great thickness of alluvial sediments found in the valley (> 600 m in places; Hansen et al., 2002). The alluvial sediment inter-bedded with lenses and layers of mudstone from rapid marine transgression events has created the Salinas Valley deep aquifer system (Watson et al., 2003). The Santa Lucia Ranges continue to rise at a rate greater than 1 mm per year (Ducea et al., 2003), which coupled with rapid erosion leads to high sediment yields from this young landscape.

The climate in southern and central California is Mediterranean, with long, dry summers and short, wet winters. Highest rainfall occurs in the Santa Lucia Mountains to the west, with maximum mean annual precipitation reaching 1140 mm. The central and southern portions of the basin are semi-arid, with mean annual precipitation of only 300 mm.

In California, rivers are the dominant source for California beach sand (Hicks and Inman, 1987), with the bulk of the sand delivered to the coast at infrequent intervals by large floods that tend to last only a few days (Warrick and Milliman, in press). Only

during these winter floods do small ephemeral, subaqueous deltas form, followed by littoral reworking and redistribution during the remainder of the year. The mouth of the present-day Salinas River is only open during times of high flows; during low flow it is closed, forming the Salinas Lagoon. Water exits the lagoon through a floodgate on the north side of the lagoon, entering the Old Salinas River Channel and discharging through Moss Landing Harbor.

3.2 General Hydrology of the Watershed

The Salinas has been called the “upside-down river” (Fisher, 1945) both because of its northward river course and because much of the flow is subsurface in a shallow water-table aquifer. The floodplain and riverbed are underlain by extremely porous alluvium, and if a critical flow is not maintained, most of the water is lost to this aquifer. From the town of Soledad to the mouth of the river, the water table is nearly always disconnected from the streambed (Watson et al., 2003). The attributes of the major tributaries of the Salinas Basin are listed in Table 3-1 and shown in Figure 3-1. The principal flow direction is northwest, except for the San Antonio and Nacimiento Rivers, which flow southeast until they join with the mainstem.

The Salinas River Valley, like many agriculturally dominated regions, is facing a number of water related problems such as groundwater overdraft, inadequate water supply for recharge, saltwater intrusion into aquifers, flooding and water pollution by fertilizers and pesticides. Unlike most of the central and southern Californian regions, all water needs are currently met from within the watershed itself, with proposals for water export to surrounding municipalities. Irrigation is the dominant consumptive use of water, with much being withdrawn from the unconfined Salinas Aquifer (10 – 50 m

Table 3-1: Hydrologic statistics for USGS gauging stations throughout the watershed. Minimum daily average flow is not reported here, as it is 0 m³/sec (cms) for all of the stations examined.

	USGS Stn ID	Area (km ²)	Water years of operation	Number of years in operation	Max Daily Flow (m ³ /sec)	Year of max	Annual Mean Flow (m ³ /sec)	Annual Median Flow (m ³ /sec)	C _v of Daily Flows
Salinas @ Spreckels	11152500	10,760.0	1930 - 2000	70	2,690	1995	12.4	0.11	4.8
Salinas @ Bradley	11150500	6,566.0	1949 - 2000	51	3398	1995	14.3	7.1	3.1
Estrella nr Estrella	11148500	2,388.0	1955 - 1998	43	920	1969	0.97	0	10.3
Salinas @ Paso Robles	11147500	1,010.0	1940 - 2000	60	804	1995	3	0	4.9
El Toro Creek	11152540	82.6	1962 - 2000	38	19	1998	0.06	0.003	5.8
Arroyo Seco Nr Soledad	11152000	632.0	1902 - 2000	98	801	1958	4.8	0.8	3.4
San Lorenzo Nr King City	11151300	603.5	1959 - 2000	41	326	1969	0.5	0.04	6.4

below the surface; Watson et al., 2003). Even prior to groundwater withdrawals the river would be dry during the summer. Many of the tributaries lose large amounts of water to the permeable alluvium and do not connect with the mainstem but a few days a year. This is not atypical for rivers in semi-arid regions (Tooth, 2000).

The natural hydrologic setting of the valley has been greatly altered by agriculture. Prior to water withdrawal for irrigation, the lower reach of the river was very swampy and had numerous groundwater springs emanating from the surface aquifer (Fisher, 1945). Irrigation in the Salinas Valley began in the 1890's through withdrawals from the river via gravity; it wasn't until the late 1920's that there were widespread introduction of groundwater wells. This withdrawal of groundwater has led to the lowering of the water table so that it is disconnected from the stream channel. To combat the lowering of the water table due to groundwater pumping, two large dams were built in the mountains to provide flood control and summer release for groundwater recharge through streambed percolation. Nacimiento Dam was built in 1957, and San Antonio Dam in 1964 to provide summer discharges for groundwater recharge.

3.2.1 Hydrologic Data and Methods

3.2.1.1 Discharge

The United States Geologic Survey (USGS) has operated many stream gauges within the Salinas watershed. These sites measure river stage (height above a referenced datum), which is then converted to discharge using a stage-discharge rating curve. These stage-discharge rating curves are developed from coincident measurements of both stage and discharge at a site. Data are reported as daily average flow rates, and are published in annual water-year (October 1 – September 30) summaries, as well as online.

Operation and maintenance of the gauges are standardized and are described in Rantz et al. (1970).

Statistics for sub-watersheds are presented here, based on the historical discharge records from USGS river gauges throughout the basin (Table 3-1). Seven gauging stations were used, each having more than 35 years of continuous data (Figure 3-2) including both pre- and post-dam construction measurements. The maximum daily flow is the maximum "daily average flow" for the entire historical record of that station. The annual mean flow is the mean of the daily average flow values for the entire year, with the median presented for comparison. The coefficient of variance (C_v) is presented here as the standard deviation of daily averaged flows divided by the mean. This allows for comparison between sub-watersheds as it normalizes the standard deviation to the size of the mean daily averaged flow, which is dependent on the basin area. For some of the analyses, the discharge values were normalized by the area of the watershed the gauge represents, producing runoff in units of depth, allowing for the comparison between sub-watersheds of varying sizes. As many of these streams are intermittent, including the main stem of the river, no baseflow was removed from the records.

The Salinas River system exhibits very distinct seasonal streamflow patterns, which are dominated by winter storms. Over 50% of the annual runoff occurs during February and March (Figure 3-3), with the maximum daily mean flow in February corresponding with the maximum in percent of annual runoff (35%).

Hydrologic statistics for each station were computed and are presented in Table 3-1. The maximum daily mean flow ranged from a low of 11 m³/sec on the dry, lowland El Toro Creek to 1980 m³/sec near the mouth of the river (Spreckels). It is important to note

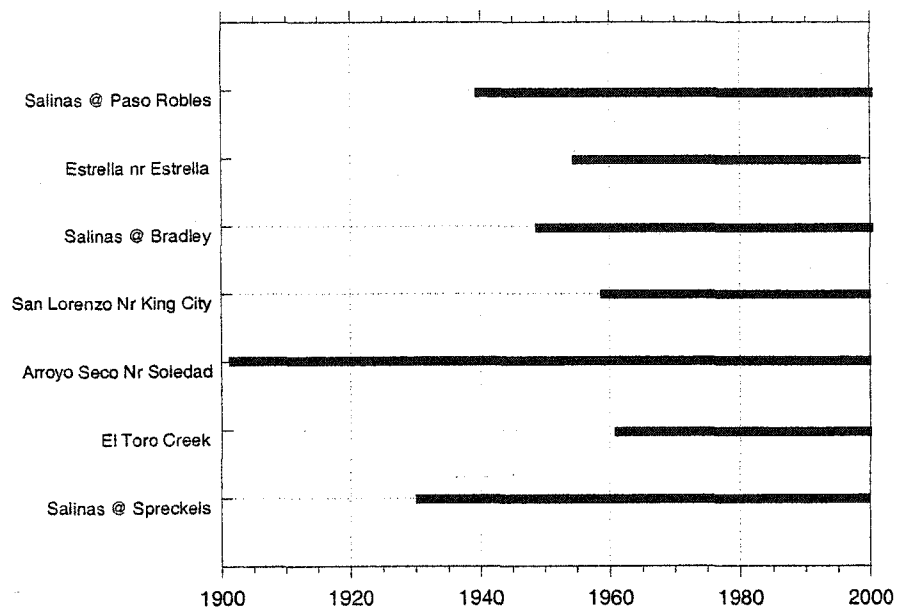


Figure 3-2: Period of record for the USGS stream gauging stations used in the analysis of the historical discharge from the Salinas River.

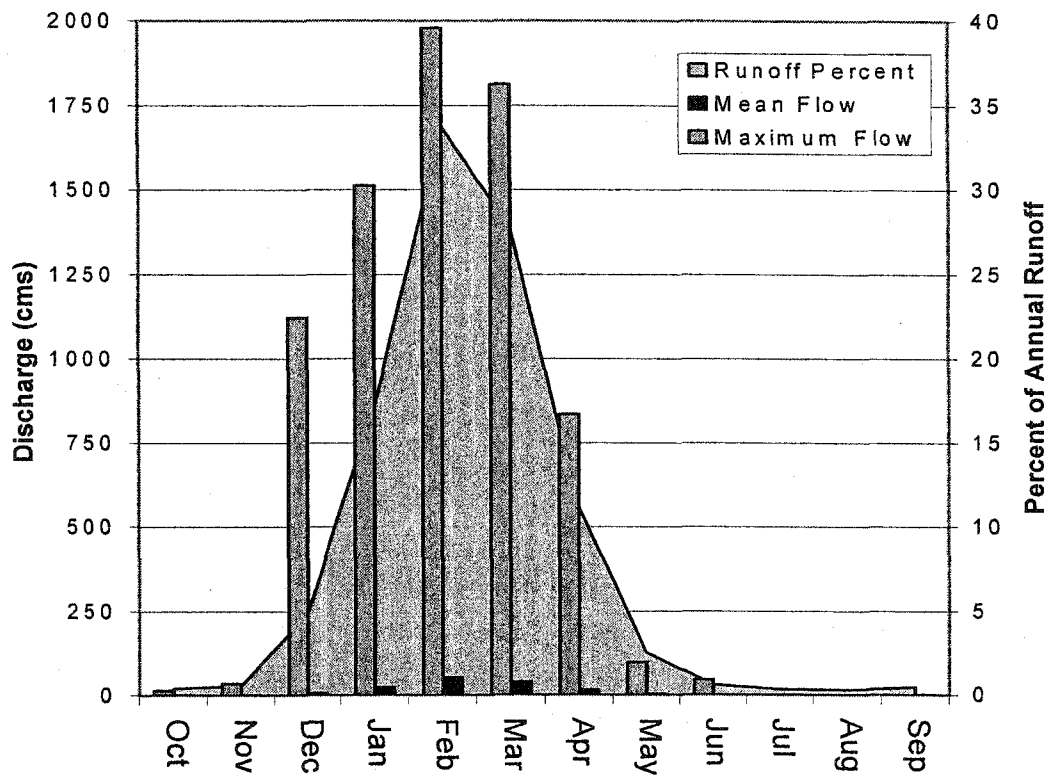


Figure 3-3: Monthly distribution of runoff, mean flow and maximum flow for the Salinas River. On average, over 75% of the discharge occurs during the months of December – March. With 50% occurring in the months of February and March.

that the year of the maximum flow was not the same basin wide. The floods of 1958, 1969, 1995 and 1998 are represented as the maximum daily mean flow of at least one of the stations. This is due to the variability between winter storms since some storms do not affect the entire watershed at the same time. The variability at the different stations is seen in the coefficient of variation, with the often-dry Estrella River having a C_v of 10.3 and the Salinas at Bradley having a low ratio of 3.1 due to releases from the San Antonio and Nacimiento reservoirs. The remaining variation values range between 3.4 and 6.4. Annual mean flows are quite low, ranging from 0.5 to 12.4 m³/sec due to the long dry season, which is also seen in the extremely low annual median flows (most < 1 m³/sec). The Bradley station has an anomalously high median discharge of 7.1 m³/sec that is due to summer and fall reservoir releases.

The objective of analyzing the mean daily flows was to understand the daily variability and magnitude of streamflow in the basin. The historical minimum daily mean flow at all of the stations is 0 m³/sec. The maximum daily mean flow mimics the same pattern as the mean (Figure 3-4), except for April – May (water days 190 – 240) due to extreme flood events in 1941 and 1983, which occurred late in the season, causing a step-like appearance in the maximum daily mean discharge time-series.

The flow duration curve is a cumulative frequency curve that represents the percent of time during which specific flows were equaled or exceeded throughout a given period of record. The curve summarizes the flow characteristics of a river without consideration for the historic sequence of flow events, and shows the integrated effects of climate, topography and geology on runoff. The flow duration curves were normalized by sub-basin area to allow comparison across the entire watershed. These daily runoff

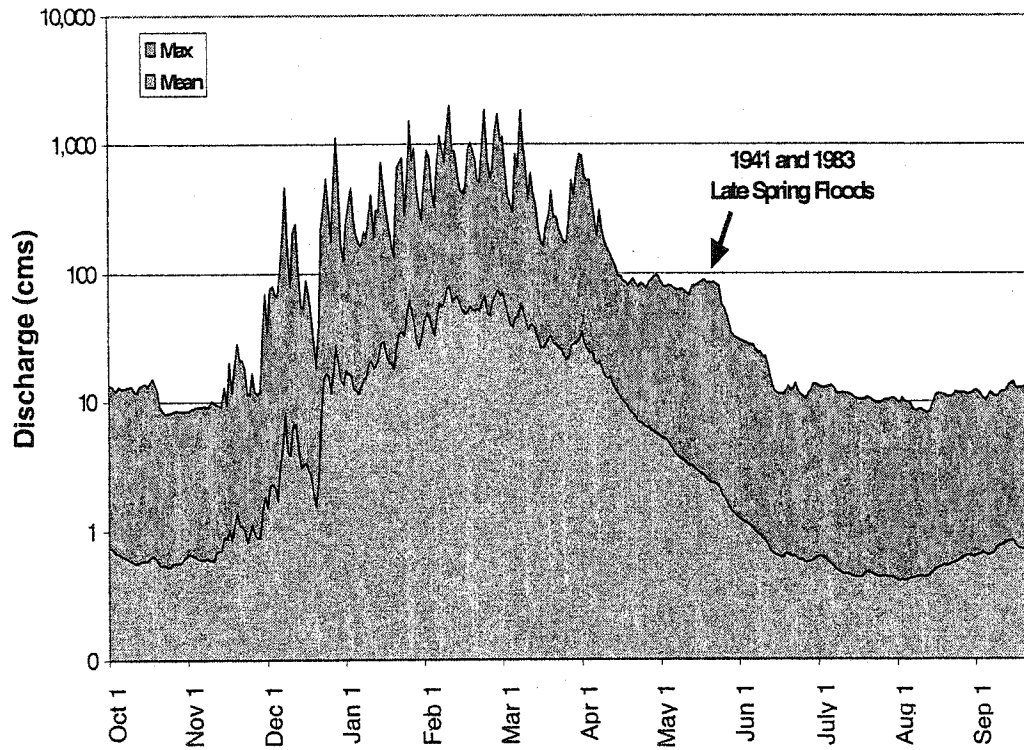


Figure 3-4: Historical maximum and mean daily average flow at Spreckels.

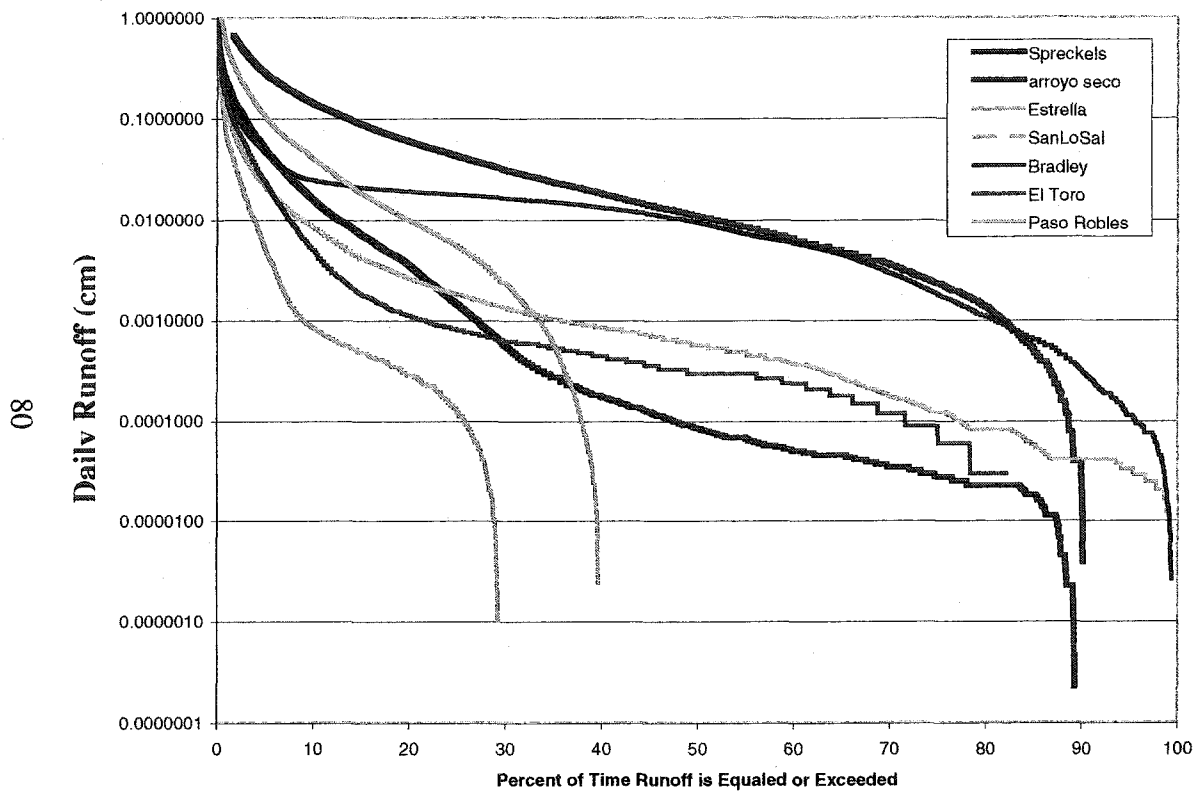
duration curves (Figure 3-5) show that the Arroyo Seco has the highest runoff, coupled with the Bradley station. These two records differ, however, in that Bradley has a very short and steep decrease in the top 10% of runoff values, and then a long and shallow curve over the majority of the record. This is indicative of the slow release of water from the Nacimiento and San Antonio dams, which aims to maintain discharge in the mainstem at approximately 15 m³/sec, or 0.2 mm of runoff at Bradley. The Arroyo Seco duration curve, on the other hand, is steeper and is influenced by direct runoff, rather than release from storage (either natural or anthropogenic). The gauging stations on the Estrella and at Paso Robles show very steep and short duration curves due to quick event runoff and extended periods of no surface flow (60-70% of the time). The duration curve for the Spreckels station has a relatively steep slope for much of the exceedence probabilities from direct runoff to the mainstem and the Arroyo Seco. All of the stations indicate ephemeral conditions, with none having any runoff at 100 % of exceedence.

The station at Spreckels shows the greatest range of mean daily runoff values, as indicated by a 20-to-80% exceedance ratio of 156 (Figure 3-5), with the rest of the stations showing approximately equal ratios, except for the storage-dominated Bradley station. Such high ratios indicate the extremes, both dry and wet, that are exhibited in the watershed.

3.2.1.2 Sediment

Although many U.S. rivers have been monitored for water discharge for as many as 100 years or more, sediment data are relatively few in number and have been decreasing for years (Lanfear and Hirsch, 1999). Suspended sediment measurements are collected as flow-weighted, depth-integrated samples across a stream section, and

Figure 3-5: Runoff duration curves for the seven USGS gauging stations used in the analysis of the Salinas River watershed.



	20%	80%	Ratio
Bradley	0.0192	0.0011	17
San Lorenzo	0.0026	0.0001	32
Arroyo Seco	0.0598	0.0014	44
El Toro	0.0011	0.00002	38
Spreckels	0.0035	0.00002	156

compiled into a single value (Guy and Norman, 1970). In contrast to discharge data, which are continuous or near continuous from stage-discharge recorders, suspended sediment concentration is typically collected manually at fixed intervals (or during events). In absence of these continuous sediment data, rating curves have been used to estimate suspended sediment loads of rivers. Sediment rating curves describe the average relation between water discharge and suspended sediment load for a location. The most commonly used sediment-discharge rating curve is an empirical relationship between suspended sediment load (L) and streamflow (Q). It is most often expressed as a power function (e.g., Campbell and Bauder, 1940; Walling, 1974; Walling, 1977):

$$L = aQ^b$$

where L is the suspended sediment discharge, Q is the water discharge, and a and b are regression coefficients found through least-squares regression on the logarithms of sediment and discharge.

Despite the widespread use of rating curves, many problems affect the accuracy of these methods. For example, there is a well recognized lack of established physical meaning of the rating curve coefficients (Asselman, 2000; Walling and Webb, 1981; Walling and Webb, 1988). Further, large errors are manifested in the underestimation of sediment load due to the statistical method used to fit the rating curve to the sampling data (Cohn et al., 1992; Ferguson, 1986; Ferguson, 1987; Jansson, 1985; Singh and Durgunoglu, 1989; Walling, 1977). The rating curve method, however, can be modified to reduce these errors (Ferguson, 1986; Ferguson, 1987). Such modifications include stratifying the data into seasonal or hydrologic groupings, developing various correction factors, using non-linear regression equations and using a smoothing method such as the

locally weighted scatter smoothing (LOWESS) technique (Asselman, 2000; Cleveland, 1979; Cohn et al., 1992; De Vries and Klavers, 1994; Duan, 1983; Ferguson, 1986; Hirsch et al., 1993; Walling and Webb, 1988).

The USGS has taken approximately 100 suspended sediment-discharge measurements at Spreckels, mostly during the 1970s, from which a discharge-sediment rating curve can be constructed. Care must be taken, however, in using this instantaneous rating curve with mean daily discharge data, the unit generally reported by the USGS. Because small, flashy rivers can have short-term (minutes to hours) discharge much greater than the mean daily value, and because the rating curve is a power function, using the mean daily discharge and the instantaneous rating curve almost inevitably will lead to a gross underestimation of actual sediment load during high flow events.

The USGS corrects for this problem following procedures outlined by Porterfield (1972). An instantaneous sediment-discharge rating curve is determined from measurements, which is then applied to the daily hydrograph to estimate the sediment concentration. This method allows for the time-weighted daily mean concentration to be computed either arithmetically or graphically. Once this mean concentration is determined, sediment load is calculated by multiplying the mean water discharge by the mean daily concentration.

We used a flow-stratified rating curve based on mean daily discharge and daily sediment loads reported by the USGS, since the latter had already been corrected by the Porterfield (1972) method. The nature of the river indicates that the majority of sediment transported by the river will occur during the few short flood events. To more accurately predict the suspended sediment load during high flows, a breakpoint of $200 \text{ m}^3/\text{sec}$ (the 2-

year flood) was used (Figure 3-6). The r^2 for the two rating curves are 0.91 for flows less than the breakpoint and 0.93 for those greater than the break point. To test the reliability of this rating curve, we calculated annual sediment loads for 1969 – 1979, years for which the USGS calculated loads. As seen in Figure 3-7, the agreement is excellent ($r^2=0.99$), with maximum difference between reported and estimated loads of ~10% for the two big years of sediment transport, 1973 and 1978. Given the uncertainties in measuring suspended sediment and in calculating daily and annual sediment loads, a 10% difference is more than acceptable.

3.3 Local Controls

Stream flow, and therefore sediment transport in the region is highly episodic. Yet delineating the controls on the magnitude and timing of delivery of both freshwater and sediment to the Monterey Bay requires an understanding of the interaction between local characteristics and the human management of the system. Local controls include, but are not limited to: interactions with the groundwater system of the basin, distribution of precipitation, littoral transport in the coastal zone, and alteration of the landscape by man to include land use changes and the construction of dams.

3.3.1 Groundwater System

The rivers of the Salinas watershed are only locally perennial. The extensive permeable alluvium allows for extensive water loss to the groundwater system over the course of the river and its tributaries. For most of the year, the tributaries are disconnected from the mainstem of the river, except during times of exceptional flow. The Monterey County Water Resources Agency controls the summer release of water from the two large reservoirs to optimize groundwater recharge for agriculture in the

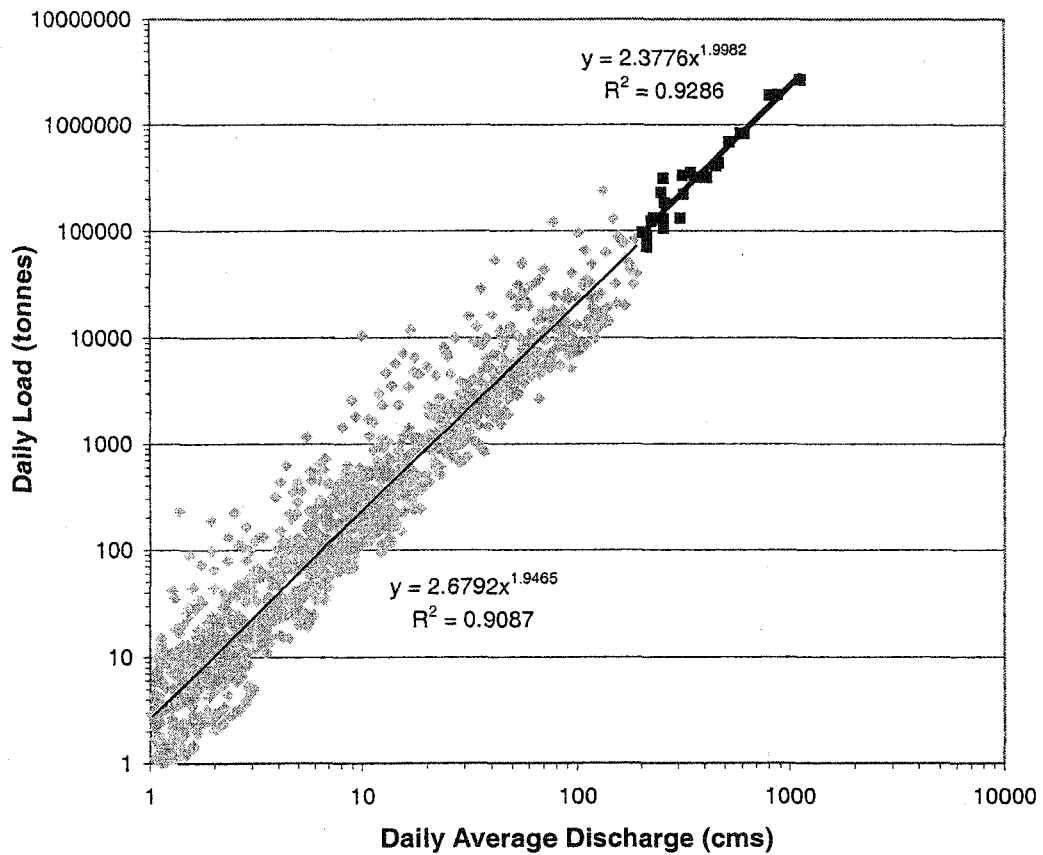
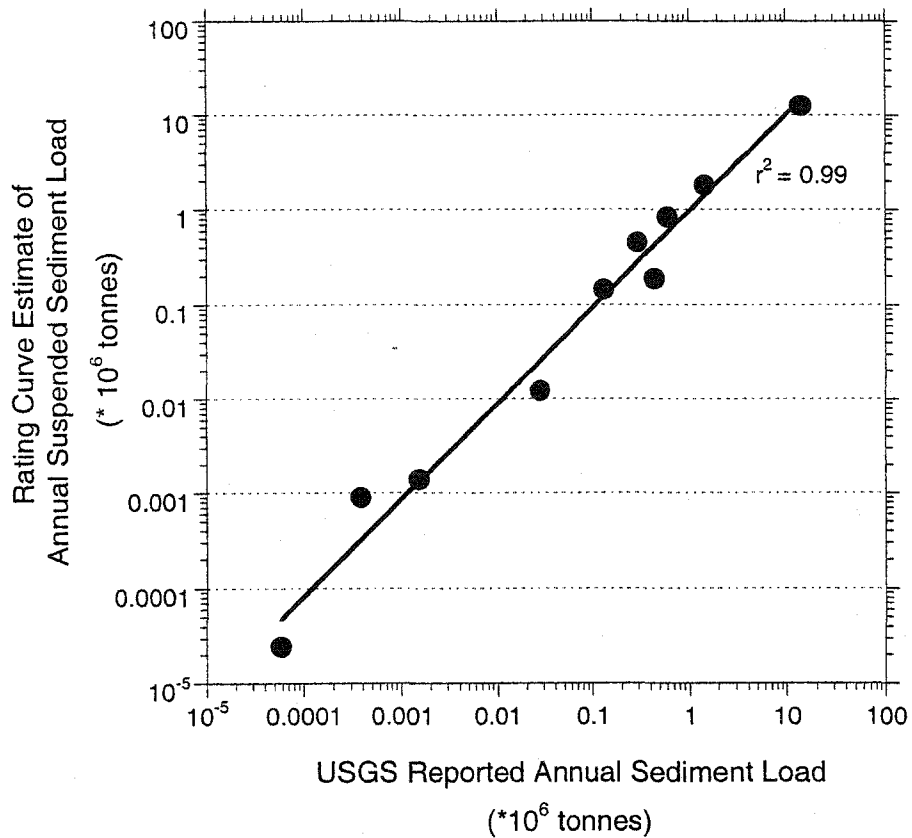


Figure 3-6: Sediment rating curve based on USGS daily load estimates 1969-1979. Only discharges greater than 1 m³/sec (cms) were considered. Rating curve was stratified for discharge greater-than and less-than 200 m³/sec. This rating curve was then used to estimate the historical sediment load of the Salinas River at Spreckels, it does not take into account erosion or deposition downstream of the Spreckels station.



	Reported USGS Annual Suspended Load (tonnes)	Rating Curve Estimated Annual Suspended Sediment Load (tonnes)
1970	130,188	143,633
1971	27,683	12,076
1972	1,503	1,383
1973	1,432,046	1,778,313
1974	599,903	821,026
1975	293,438	445,029
1976	375	902
1977	58	25
1978	13,793,561	12,557,712
1979	439,494	186,345

Figure 3-7: Comparison of estimated annual sediment loads and USGS reported sediment loads for the Salinas River at Spreckels. Estimated annual sediment loads were computed using a rating curve (Figure 3-7) derived from USGS reported daily sediment loads (<http://webserver.cr.usgs.gov/sediment/>).

lower valley. This loss of water to the groundwater system reduces the ability of the river to transport sediment from the upper reaches of the river to the mouth.

A simple water budget of the lower valley allows us to estimate the amount of water that enters the groundwater system. These annual budgets were constructed assuming surface storage downriver of Bradley was negligible. Annual groundwater recharge volumes were estimated using a mass balance equation for discharge volumes:

$$Q_B + Q_{AS} + Q_{SL} - Q_{SP} = Q_{\text{Recharge}} - Q_{\text{Runoff}}$$

where Q_B , Q_{AS} , Q_{SL} and Q_{SP} are the discharge volumes at Bradley, Arroyo Seco, San Lorenzo and Spreckels, respectively. Q_{Recharge} is defined as the volume of water entering the groundwater system from the river, and Q_{Runoff} the volume of water added to the Salinas mainstem through direct runoff below the station at Bradley. Average annual flow past Bradley is 0.45 km^3 . Adding in the flow from the Arroyo Seco (0.1 km^3) and the San Lorenzo (0.02 km^3) and then subtracting the historic average annual volume passing Spreckels (0.39 km^3) leaves a volume of 0.18 km^3 of water to account for the sum of groundwater recharge minus input from direct runoff in the lower valley. Average annual runoff in the lower valley was estimated to be 0.3 km^3 , giving a recharge volume of 0.48 km^3 . The summer reservoir releases equal 0.33 km^3 , leaving 0.15 km^3 of groundwater recharge during the winter months.

This water loss is also seen on shorter temporal and spatial scales. The Arroyo Seco drains the wettest part of the basin and contributes significantly to the total volume of water available for discharge at Spreckels. However, significant water loss is seen between the gauging station near Soledad and the one below the confluence with Reliz creek (Figure 3-8). The Arroyo Seco gauging station near Soledad is in a reach where the

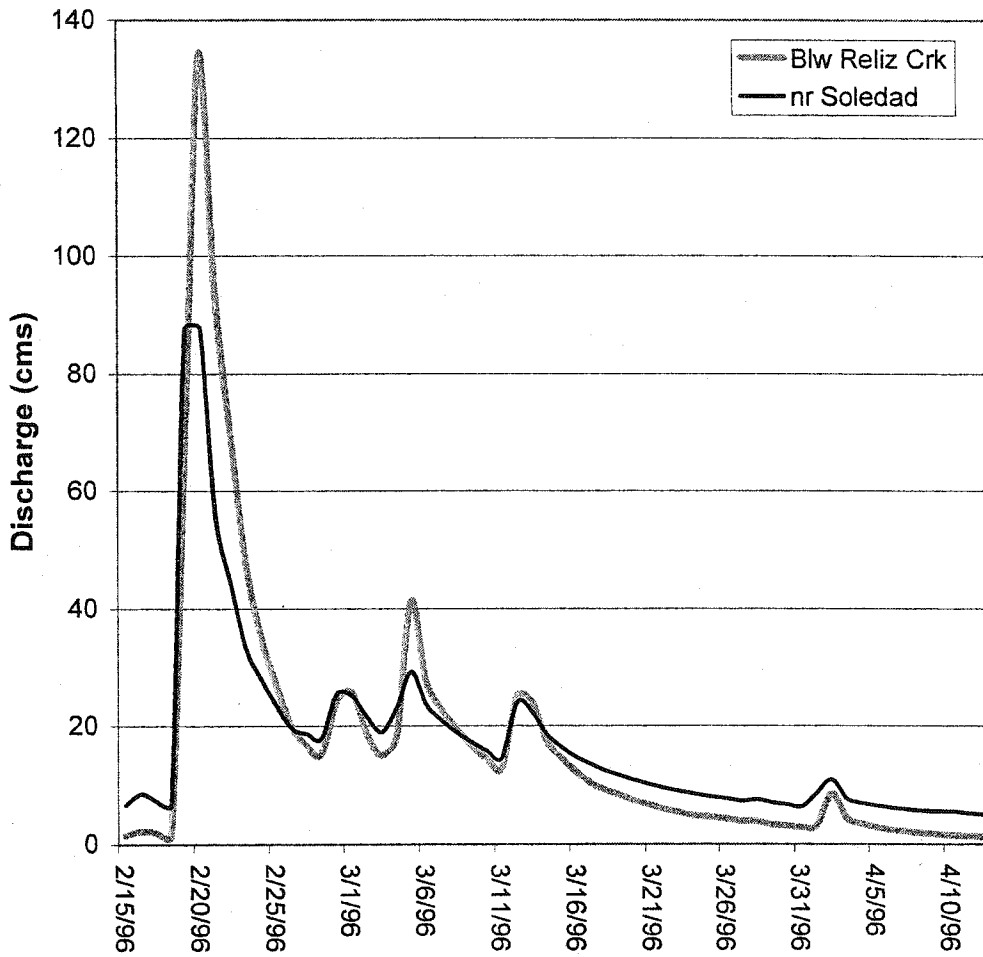


Figure 3-8: Water loss to groundwater system along the Arroyo Seco River. The Arroyo Seco River must cross a broad alluvial fan before reaching the mainstem of the Salinas River. The station nr Soledad is upriver from the alluvial fan, and the station below Reliz Creek is closer to the confluence of the Arroyo Seco and the Salinas River. It is only during high-flow events that water volumes increase from runoff and tributary input in this reach, rather than decrease. Much of the water is lost through infiltration during low flows. This threshold depends not only on the discharge of the river, but also on pre-existing conditions such as recent precipitation and soil moisture.

channel is confined by bedrock. Shortly after leaving this bedrock-confined region, the river discharges across a broad alluvial fan to the Salinas River. Depending on pre-existing conditions, recent rainfall, and soil moisture, the river can lose all of its volume prior to reaching the river. Earlier in the winter season, this is important if the “first flush” is not sufficient to reach the mainstem, because all the sediment carried by this event will be deposited on the alluvial fan before reaching the river. It is only during large events that the Arroyo Seco actually connects with the mainstem of the river.

3.3.2 Precipitation Distribution

The varying hydrologic conditions within the basin are dependent on the uneven distribution of precipitation across the basin, which is controlled by basin orientation and physiography (Figures 3-1 and 3-9). The highest rainfall occurs in the Santa Lucia Mountains to the west, with mean annual precipitation greater than 1000 mm. In contrast, the southeastern portion of the basin has a mean annual precipitation of only 300 mm. The sub-basins of the watershed have runoff values correlated with other sub-basins in similar precipitation regimes (Table 3-2). For example, flow at El Toro Creek is not strongly correlated with neighboring Arroyo Seco, but instead with the across valley San Lorenzo. Flow downstream at Spreckels, which acts as an integrator of the entire watershed, is significantly correlated to flow at all stations except Estrella (Table 3-2). This is due to the climatic isolation of the Estrella, which lies in a severe rain shadow. The orographic effect of the coastal mountains leaves very little moisture available to the Estrella, which much of the year is dry. Historical discharge records show that 70 % of the past 43 years there has been no flow in the tributary at all. When there is flow, it is very brief, with 98% of the historical record showing flow less than 10 m³/sec.

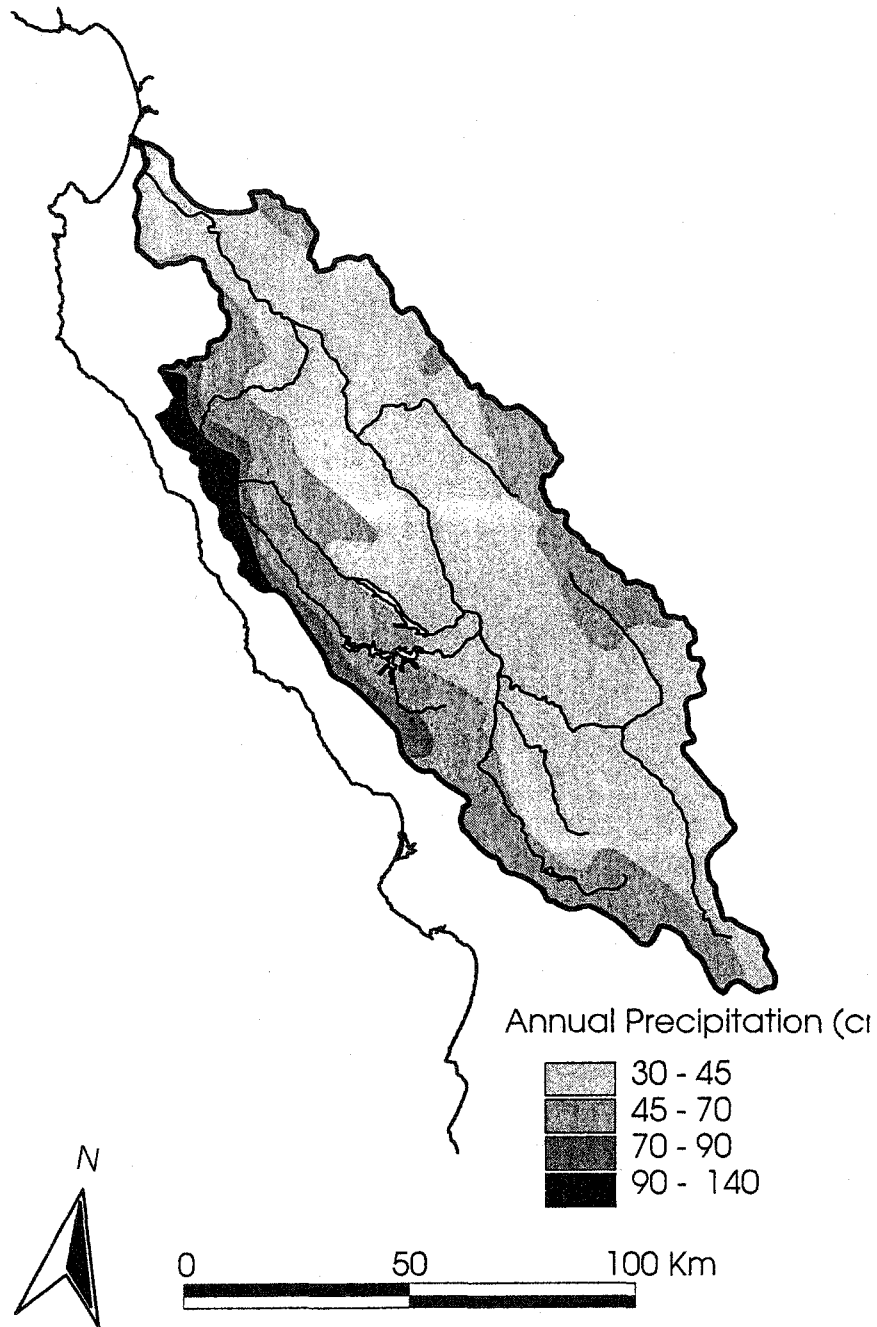


Figure 3-9: Distribution of annual precipitation in the Salinas watershed. High values in the western coastal mountains are transmitted to the mainstem through the Arroyo Seco and eventually through the San Antonio and Nacimiento reservoirs. The low values though not the majority of the basin result in the Salinas's mean precipitation of approximately 47 cm/year, defining it as a semi-arid river.

Table 3-2: Linear regression relations between the seven stations within the watershed. Data listed include regression slopes (m), r^2 and number of samples (n).

	Spreckels	Arroyo Seco	El Toro	San Lorenzo	Bradley	Estrella
Arroyo Seco	4.6507 0.6778 71					
El Toro	0.5844 0.7241 39	0.1044 0.5867 39				
San Lorenzo	0.582 0.7986 42	0.1052 0.6688 42	0.8868 0.7628 39			
Bradley	1.3954 0.6859 52	0.2613 0.7617 52	1.905 0.2766 39	2.1543 0.6126 42		
Estrella	0.3775 0.5395 44	0.0615 0.3637 44	0.6319 0.6371 37	0.7176 0.8098 40	0.2431 0.4583 44	
Paso Robles	2.3185 0.8498 57	0.4352 0.8218 57	3.3136 0.6409 35	3.7973 0.793 38	1.6317 0.8347 48	3.9917 0.2261 40

3.3.3 Salinas Lagoon

Another interesting local control on the delivery of sediment and water to the coastal ocean is the bar that closes off the river mouth, creating a lagoon. The formation of this bar is due to the persistent dominance of littoral transport over the river discharge. There is most likely some exchange of water between the Salinas River and the coastal ocean through the bar, but no sediment is delivered. This barrier to delivery is only removed when discharge is high enough to break through, or the local water resources agency weakens it with a bulldozer to prevent localized flooding. The volume of sediment stored in the lagoon available for transport by large floods is unknown; however, large changes (~2 m) in the bathymetry in one area of the lagoon was seen after the moderate floods in January 2001 (Watson et al., 2001).

3.3.4 Human Impact

Human alteration of the landscape can accelerate erosion rates, but impoundment of waterways can decrease sediment delivery. In the Salinas Valley the increased erosion on lands used for row crops and the fate of pesticides and fertilizers applied to these crops are dominant water quality issues. The flat northern valley around the city of Salinas is one of the world's most productive vegetable growing areas. In the middle and south valley, around King City and Paso Robles, large contiguous vineyards have been established in recent years. For lands converted from row crops, water conservation practices in these vineyards reduced the amount of water withdrawn from the groundwater system for irrigation. Grazing dominates the foothills, which are adjoined by steeper forested and scrub lands.

The three main reservoirs (Table 3-3) have a combined storage capacity of 0.9 km³. They impound approximately 2245 km², about 20% of the total watershed area. The smallest of the reservoirs, the Santa Margarita Reservoir, was created in 1941 by the building of the Salinas Dam to provide water to a local military training camp and the city of San Luis Obispo. It captures 290 km² of watershed, and has a storage capacity of 0.028 km³. It was run by the Army Corp of Engineers starting in 1947, and then transferred to the San Luis Obispo County Flood Control and Water Conservation District in 1965 through a lease agreement with the Army Corp of Engineers. It has an average annual release of 0.017 km³, which is distributed throughout the year under a requirement of the California State Water Resources Control Board (CSWRCB) to keep a “live stream” (observable surface flow) down river to the confluence of the Nacimiento River (CSWRCB permit # 5882).

The Nacimiento Reservoir was created by the construction of the Nacimiento Dam in 1957. With a storage capacity of 0.466 km³, it is the largest reservoir in the watershed. With an average annual release of 0.247 km³ it also serves as winter flood control and summer groundwater recharge (MCWRA, 2001). The need for summer water releases to recharge the groundwater system is a balancing act between releasing enough water to have flow the length of the river, without wasting water by allowing escape to the ocean.

The San Antonio Reservoir was built by Monterey County in 1965. It impounds 850 km² of watershed, and has a storage capacity of 0.413 km³. The San Antonio Dam is operated mainly for winter flood control as well as water conservation. The conservation of water is implemented by the slow release of winter runoff, through the dry summer

Table 3-3: Reservoirs located in the Salinas watershed. There are other smaller diversions of water, but these are the largest that have significant impact on the hydrologic system.

Reservoir	Watershed Area Impacted (km²)	Storage Capacity (km³)	Use	Avg. annual releases (km³)
Santa Margarita	290	.028	Water Supply	.017
San Antonio	850	.413	Water Conservation and Flood Control	.086
Nacimiento	850	.466	Water Conservation and Flood Control	.247

months, allowing for groundwater recharge. It has an average annual release of 0.086 km³ (MCWRA, 2001).

The inflow into the reservoirs is directly related to precipitation. During years of drought, reservoir levels drop, and it may take years for the reservoir to refill to pre-drought levels. This influences the amount of water available for summer release and groundwater recharge. The Salinas Watershed experienced severe drought in the late 1980's into the early 1990's (Figure 3-10) as well as two years of low precipitation from 1976-1977. The delay of transmittal of water via the alteration of the annual hydrograph and the trapping of sediment are the main effects of the reservoirs.

3.4 Global Controls

Variability in streamflow is ultimately controlled by regional climate, which in turn is related to larger-scale atmospheric and oceanic phenomena. Two recurrent global climate phenomena affecting the Pacific Ocean are particularly important for the hydrologic and climatic variability in the western United States.

- The El Niño Southern Oscillation (ENSO) has been shown to influence inter-annual variability of regional climates in many parts of the world, including severe drought in the southwest Pacific (Indonesia, Papua New Guinea and Australia), weakened monsoon over much of South Asia (Webster and Palmer, 1997), and the well-known flooding along the Pacific coast of South America.
- The Pacific Decadal Oscillation (PDO) is a decadal-scale variability in sea-surface temperature in the Northern Pacific that has been identified as a contributor to inter-decadal variability (Mantua et al., 1997) in the climate of western North America.

Both phenomena have quantitatively accepted indices that can be used to determine correlation with Salinas discharge. These indices are available online from the

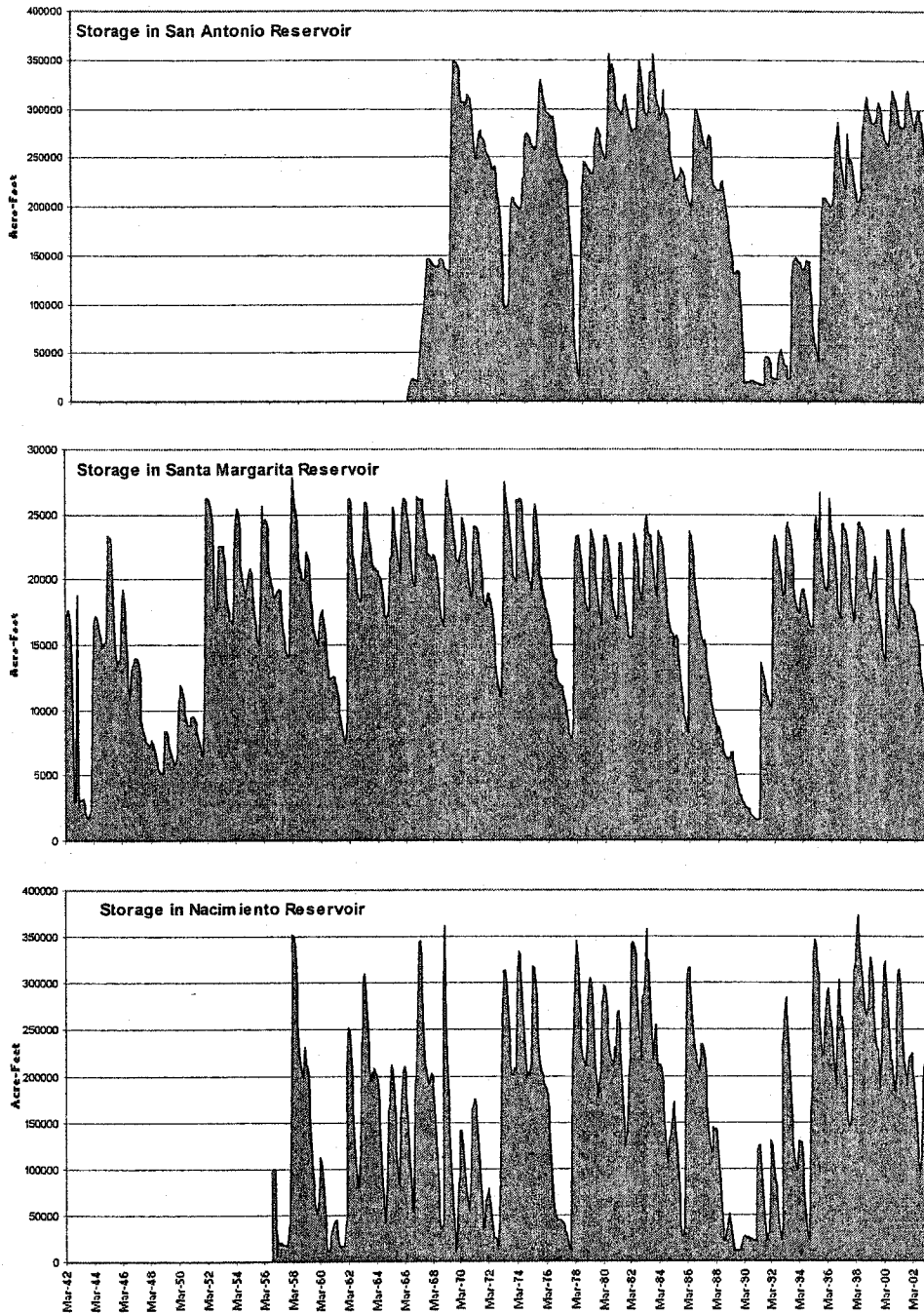


Figure 3-10: Historical records of storage in the three reservoirs in the Salinas watershed. A) Santa Margarita Reservoir, B) San Antonio Reservoir and C) Nacimiento Reservoir (Data from <http://cdec.water.ca.gov/misc/resinfo.html>, March 2003). Of note is the drought of the early 1990s, early 1970s and 1985.

National Oceanic and Atmospheric Administration (<http://www.cpc.ncep.noaa.gov>) and the University of Washington (ftp://ftp.atmos.washington.edu/mantua/pnw_impacts/INDICIES/PDO.latest).

3.4.1 El Niño-Southern Oscillation

Peruvian fisherman first used the term El Niño when discussing the warming of coastal sea temperatures, which lead to flooding and large drops in fish catches. This term is now used more generally to refer to the warming of the tropical Pacific waters, which occurs every 5-7 years, and persists for 1-2 years (Figure 3-11a). This phenomenon is composed of large-scale ocean-atmosphere interactions with equatorial dynamics (Neelin et al., 1998) in which the tropical warm pool is displaced to the east, causing shifts in precipitation and disruption of global climate patterns (Webster and Lukas, 1992). The opposite phase, La Niña, is characterized by stronger than normal trade winds and corresponding colder sea-surface temperatures. This is collectively referred to as the El Niño/Southern Oscillation. Each year is unique in its strength, duration and pattern – thus causing differing patterns of response on land. The Southern Oscillation Index (SOI) is a standardized measure of the difference in sea-level pressure between Tahiti and Darwin, Australia (Figure 3-11a). El Niño events are characterized by negative SOI values, while La Niña is characterized by positive SOI values.

Teleconnections between large-scale atmospheric circulation patterns and tropical precipitation fields can alter the probability of certain weather in a region, rather than causing a predictable change in the weather patterns (Palmer and Mansfield, 1986; Ropelewski and Halpert, 1987). Based on climatic records, the strongest effect of El Niño is over the North Pacific and North America (Ropelewski and Halpert, 1987), but El

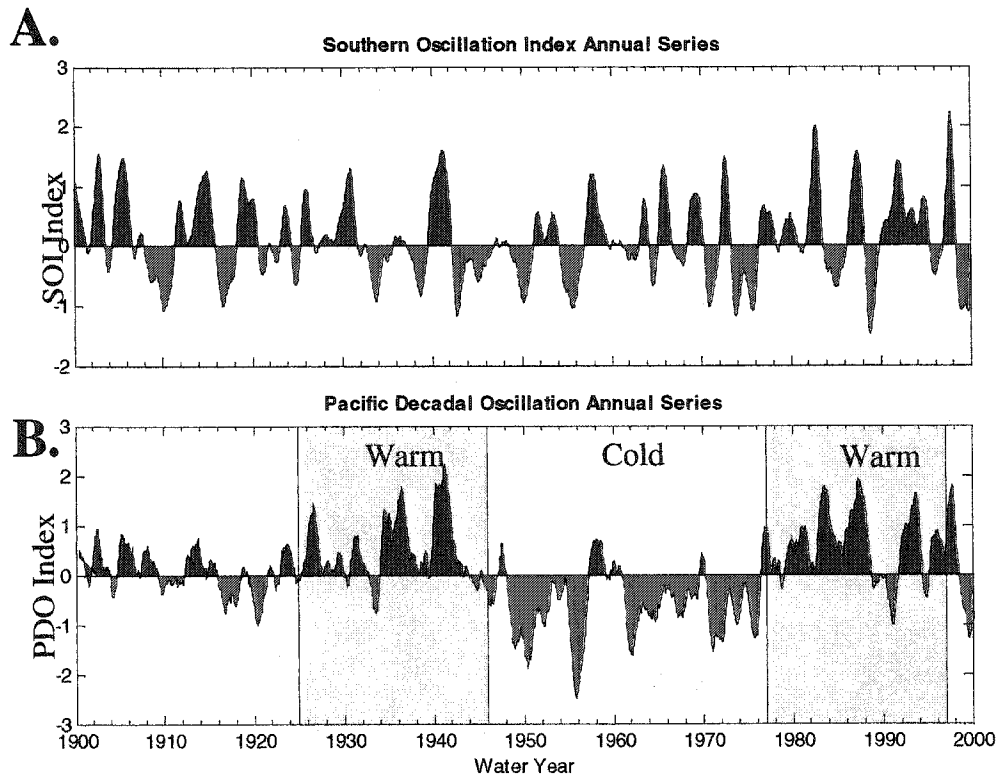


Figure 3-11: Global climatic signals affecting the Central Coast of California. A) Southern Oscillation Index (standardized Tahiti – standardized Darwin) standardized using the Trenberth (1984) method to maximize the signal and B) Pacific Decadal Oscillation.

Niño years of similar 'strength' do not have the same weather patterns, making prediction of specific effects of El Niño-related storms almost impossible. However, in general the probability of stronger winter storms is greatly increased over southern California during El Niño years (Dettinger et al., 2002).

The relationship between ENSO and precipitation has been well documented throughout the equatorial Pacific (Ropelewski and Halpert, 1987; Waylen and Caviedes, 1990; Woolhiser et al., 1993). The association between ENSO and river discharge naturally follows and has been documented throughout the world and the United States (Amarasekera et al., 1997; Cayan et al., 2000; Cayan and Webb, 1992; Dettinger et al., 2002; Gutierrez and Dracup, 2001; Redmond and Koch, 1991; Waylen and Caviedes, 1986).

3.4.2 Pacific Decadal Oscillation

The Pacific Decadal Oscillation was first described in 1996 by Steve Hare when examining salmon population fluctuations in the northern Pacific. It is defined by sea-surface temperature and pressure variations in the northern Pacific Ocean. PDO phases persist from 20-30 years (Mantua et al., 1997) and are characterized as being in 'warm phases' or 'cool phases'. During the warm phase, below average sea-surface temperatures are seen in the North Pacific and higher than average sea-surface temperatures are observed off the coast of North America. The standardized index for the PDO is defined as the leading principal component of sea-surface temperatures in the Pacific Ocean north of 20°N (Mantua et al., 1997). Mantua et al. (1997) have identified four periods of consistent PDO behavior characterized by a PDO of predominantly the same sign. Shifts in the PDO were seen in 1925, 1947 and 1977 (Figure 3-11b), with a

cool phase from 1947-1976 and warm phases from 1925 – 1947, and 1977 through the mid 1990s. There appears to have been a shift back to a cool phase around 1997, but more time is needed to make a definitive statement to this regard. Recent studies suggest that the PDO has an affect on North American climate, as well as the ENSO (e.g., McCabe and Dettinger, 1999).

3.4.3 Interaction with Salinas River

Streamflow in the Salinas watershed is clearly controlled by the supply of water from winter precipitation. For this study monthly streamflow values for the seven stations throughout the Salinas watershed were compared with the SOI and PDO. ENSO and PDO classifications are shown in Table 3-4, with the six categories defined for each of the water years (October through September). The ENSO classifications are based on the Nino 3.4 index of Trenberth (1997), with winter averages of SOI more than 0.5 standard deviations from the long-term mean classifying the water years into El Niño, Neutral, and La Niña categories.

Correlation coefficients were computed between the 3-month averaged SOI and annual streamflow from the Salinas River. A significant correlation is first seen in the June/July/August SOI, with the highest correlation seen in the winter SOI (December/January/February) (Figure 3-12). The rest of the analyses were therefore completed using the winter SOI. The river discharge at Spreckels is significantly greater during El Niño years than non-El Niño years ($p=0.0045$). The same relationship is seen with higher than average discharge during Warm-PDO than the Cool-PDO phases ($p=0.0361$) (Figure 3-13).

Table 3-4: Classification of Water Years in to six categories defined by SOI and PDO indices.

Cool PDO			Warm PDO		
El Nino	Neutral	La Nina	El Nino	Neutral	La Nina
1947	1946	1930	1940	1931	1938
1949	1954	1934	1941	1932	1939
1952	1957	1943	1942	1933	1982
1953	1963	1945	1944	1935	1997
1964	1965	1950	1958	1936	
1966	1968	1951	1959	1937	
1969	1972	1955	1970	1948	
1973	1975	1956	1978	1960	
1990	1979	1962	1983	1961	
1995	1991	1967	1987	1977	
		1971	1988	1980	
		1974	1992	1981	
		1976	1993	1984	
		1989	1998	1985	
		1999		1986	
		2000		1994	
				1996	

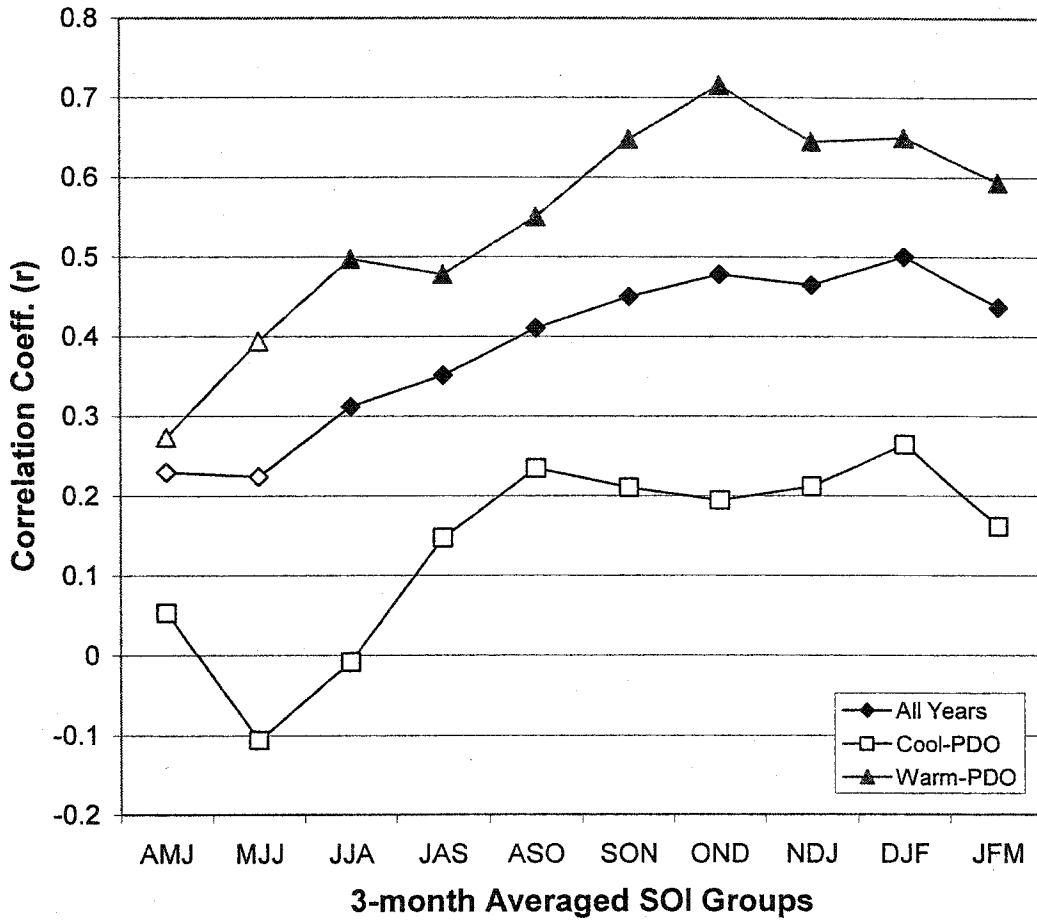


Figure 3-12: Correlation between 3-monthly averaged SOI and annual discharge of the Salinas River. Significant correlation is seen starting in the June/July/August SOI, with a maximum in the December/January/February SOI. Dividing the years into Warm and Cool PDO phases, no significant correlation is seen with the SOI during Cool PDO years, with maximum correlation in the October/November/December SOI in the Warm PDO phases. Filled makers indicate significance at p=0.005, non-filled indicates no significance.

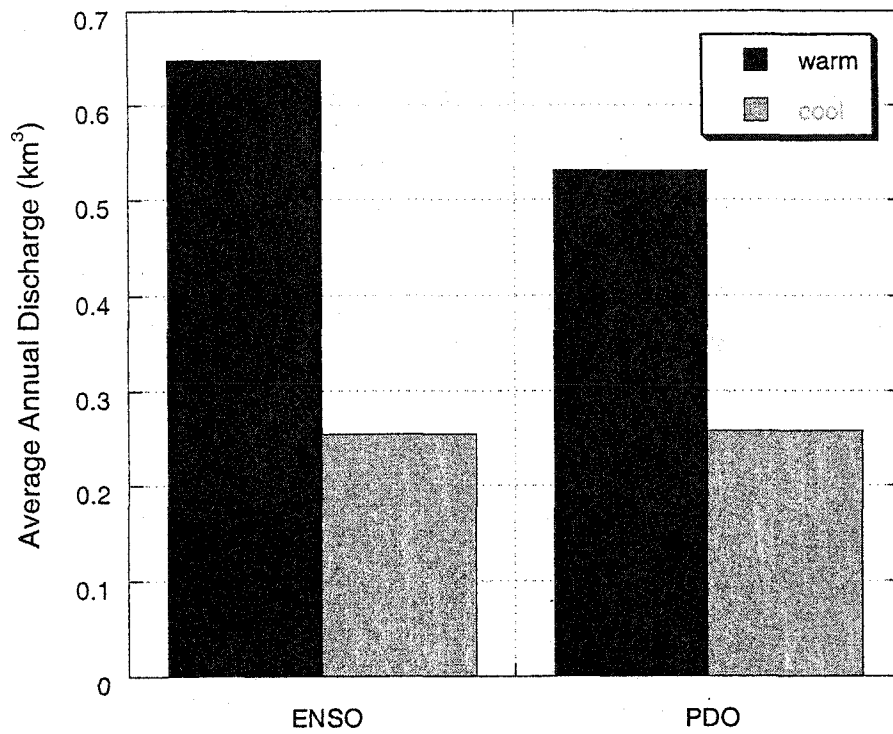


Figure 3-13: Relationship between the ENSO and PDO and annual discharge of the Salinas River. Warm ENSO years have a significantly ($p=0.0045$) higher annual discharge than cool ENSO years. The same relationship is seen in the PDO ($p=0.0361$).

The signature of both the ENSO and the PDO is clearly evident in the annual discharge from the Salinas River. By removing the mean annual value from the annual time series of runoff, stations throughout the basin indicate an above average discharge at the ENSO frequency (Figure 3-14). The PDO influence is also seen when we examine the last 70 years of historical discharge for the Salinas River at Spreckels (Figure 3-15). The average annual discharge during the cool phase of PDO is lower (0.26 km^3) than during the warm phase (0.53 km^3).

Inman and Jenkins (1999) first described the effects of this interaction between the PDO and ENSO as multidecadal wet and dry periods. This pattern has since been identified as the Pacific Decadal Oscillation, and is seen to affect the climate variability all along the west coast of North America (Mantua et al., 1997). Maximum flow years in the Salinas River seem to require both ENSO and PDO warm phases. Of the 10 years with the highest annual discharge, seven of them occurred during warm phase of the PDO, and of these five were also El Niño years.

The interaction between the PDO and the ENSO signals is seen when we further divide up the years into six different categories based on the atmospheric-oceanic phenomena (Table 3-4). The streamflow at the Spreckels gauge is significantly ($p=0.002$) higher than the average for water years that fall into both the warm ENSO and the warm PDO years. This is the only significant difference from the mean for the Spreckels station. This relationship is seen throughout the basin in all runoff regimes (Figure 3-15).

Inter- and intra-annual variability within the system is also affected by these phenomena. The annual discharge of the Salinas River shows much more variation in

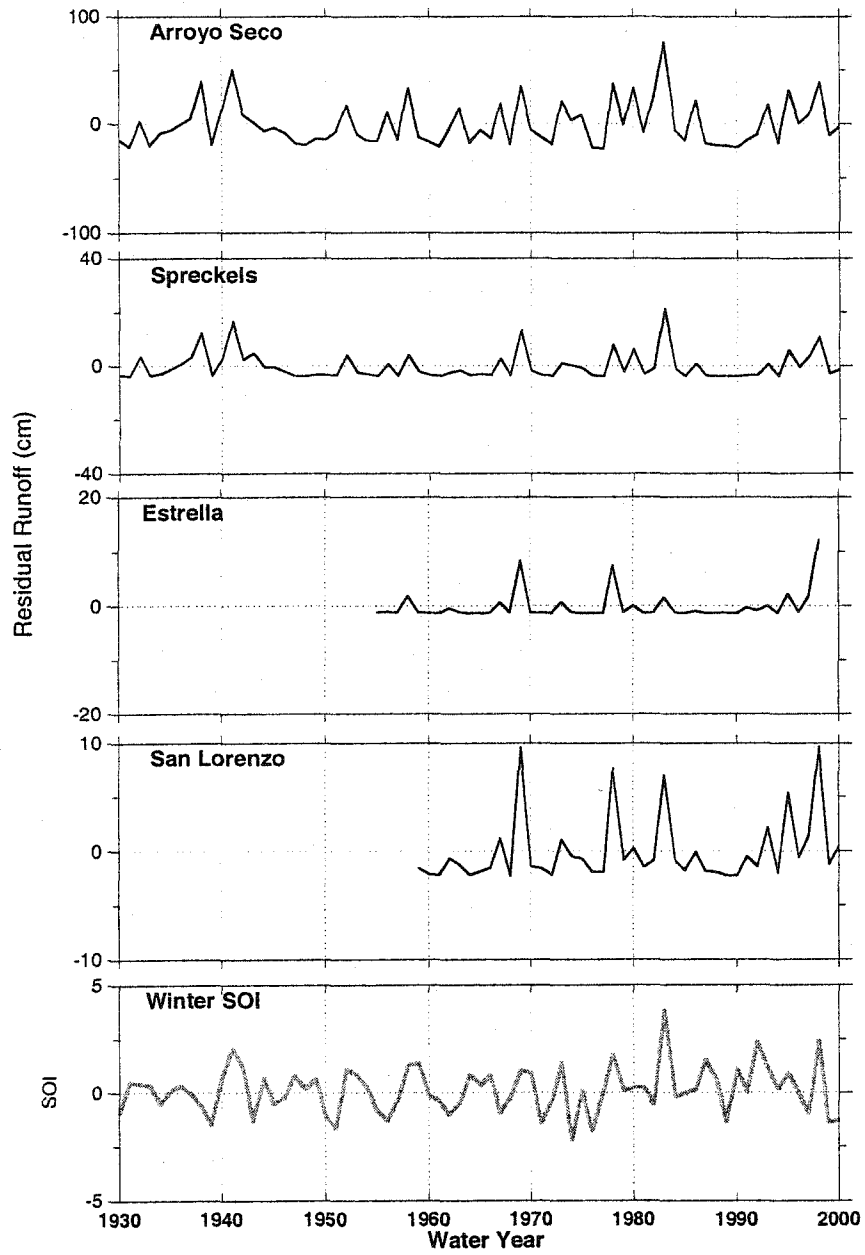
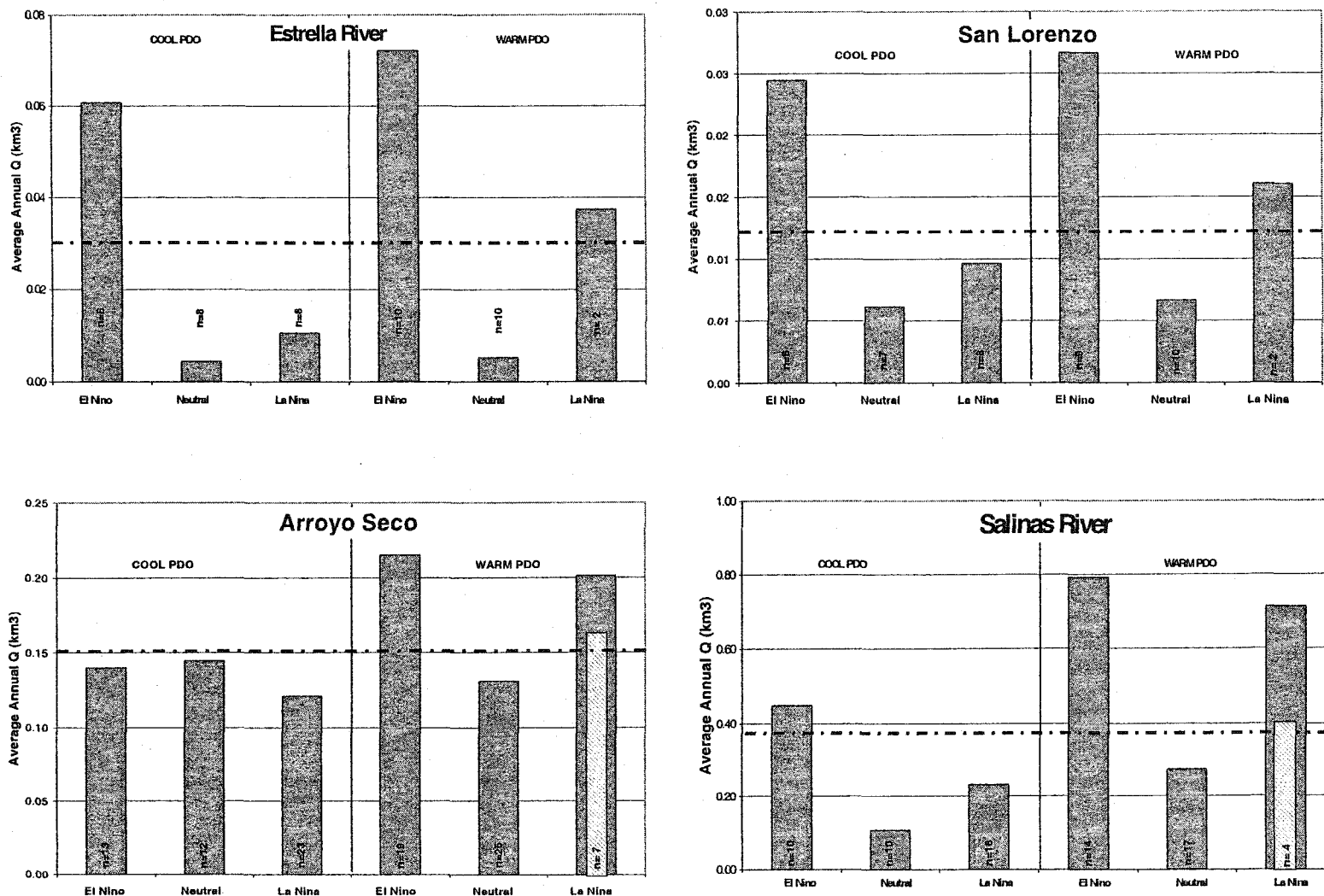


Figure 3-14: Annual residual runoff (annual runoff – mean annual runoff) for four stations in the Salinas watershed. The Arroyo Seco displays a strong relationship with the frequency of El Niño; the other stations display this same relationship, however with a lower magnitude. The Spreckels, Estrella and San Lorenzo stations show extended periods below average, punctuated by large flood events.

Figure 3-15: Annual discharge for various Salinas River tributaries relative to PDO and ENSO indices. All stations show significant difference between Warm-PDO-El Niño and the historical average (dashed line); Estrella ($p=0.0208$), San Lorenzo ($p=0.0275$) Arroyo Seco ($p=0.0139$) and Salinas at Spreckels ($p=0.002$). La Niña interior bar (light gray) is with anomalous water-year 1938 removed.



flow values during the warm phases of the PDO. This is further quantified by using the ratio of the maximum flow for each year to the mean flow for that year (Figure 3-16b). During the cold phases of PDO there is less intra-annual variation (lower ratio values), however, there is a much more pronounced inter-annual variation signal at the ENSO 5-7 year frequency.

3.5 Events

As with most semi-arid rivers, it is the flood events that define the annual mean discharge of the Salinas River (Figure 3-17). A high-volume year may result from extreme flood events, or overall higher precipitation throughout the winter and into spring. The years may be divided into groups based on annual discharge volume and the number and duration of events (Figure 3-18):

- Group 1: Dry Years –years that have little to no discharge
- Group 2: No Large Floods - not quite dry, but few (if any) events
- Group 3: Flashy years –medium to high total annual discharge, with flashy events (high peaks, short duration)
- Group 4: Wet years –high total annual discharge, extreme flood peak; wettest years also have wetter late springs

Annual instantaneous peak flows have ranged from 0.12 to 2690 m³/sec. The three largest instantaneous peaks on the Salinas River (near Spreckels) were recorded March 12, 1995 (2690 m³/sec), February 26, 1969 (2353 m³/sec), and February 12, 1938 (2124 m³/sec). While the public is concerned with large floods with recurrence intervals greater than 10 years, the 5- to 10-year events appear to play significant geomorphic roles in shaping the river. The annual exceedence probability was calculated using the Bulletin

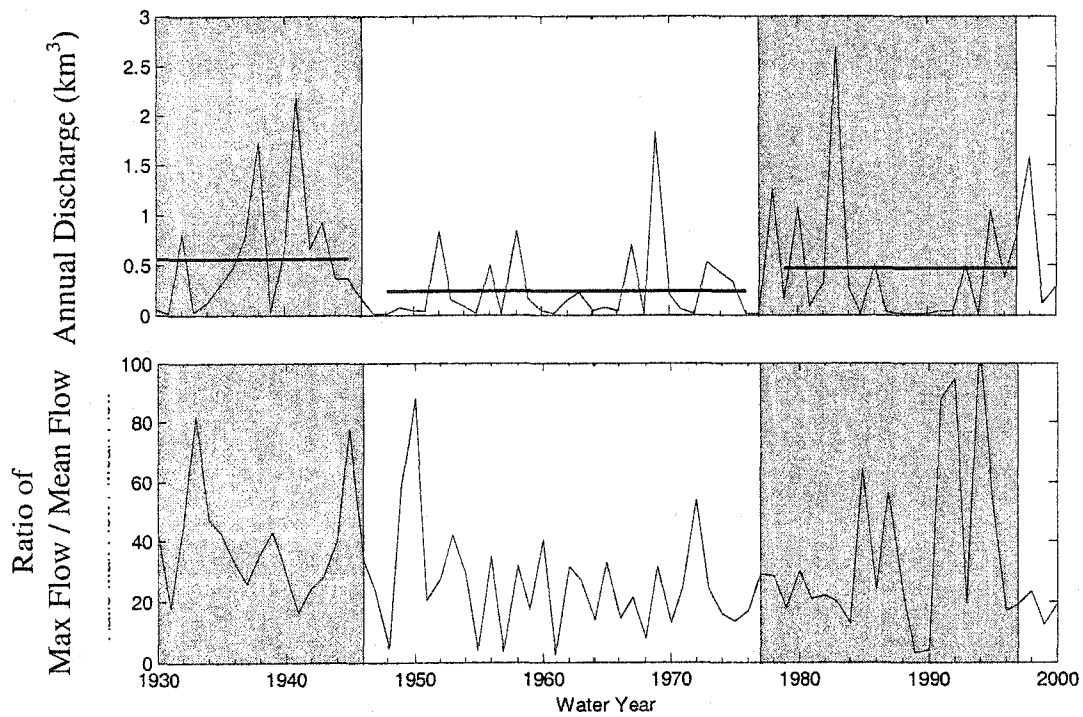


Figure 3-16: Annual time series for the Salinas River with Cool (white) and Warm (grayed) phases of the Pacific Decadal Oscillation indicated. Annual discharge (A) shows distinctly higher average annual discharge during the warm phase of the PDO, as well as larger intra-annual variation (B) as seen in the ratio of the maximum flow the mean flow for each year.

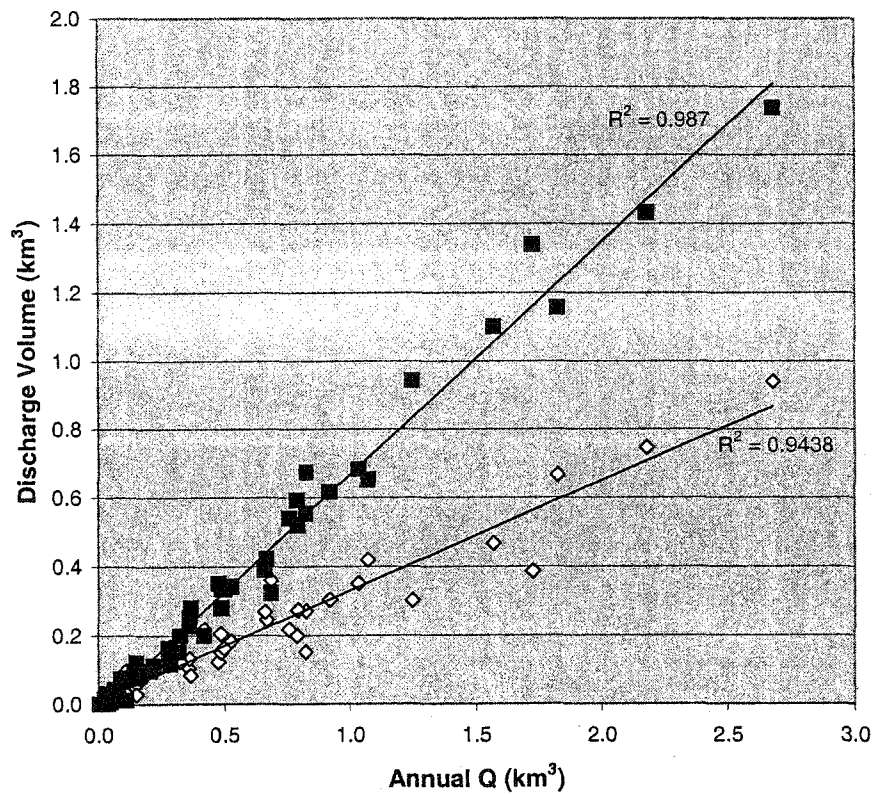
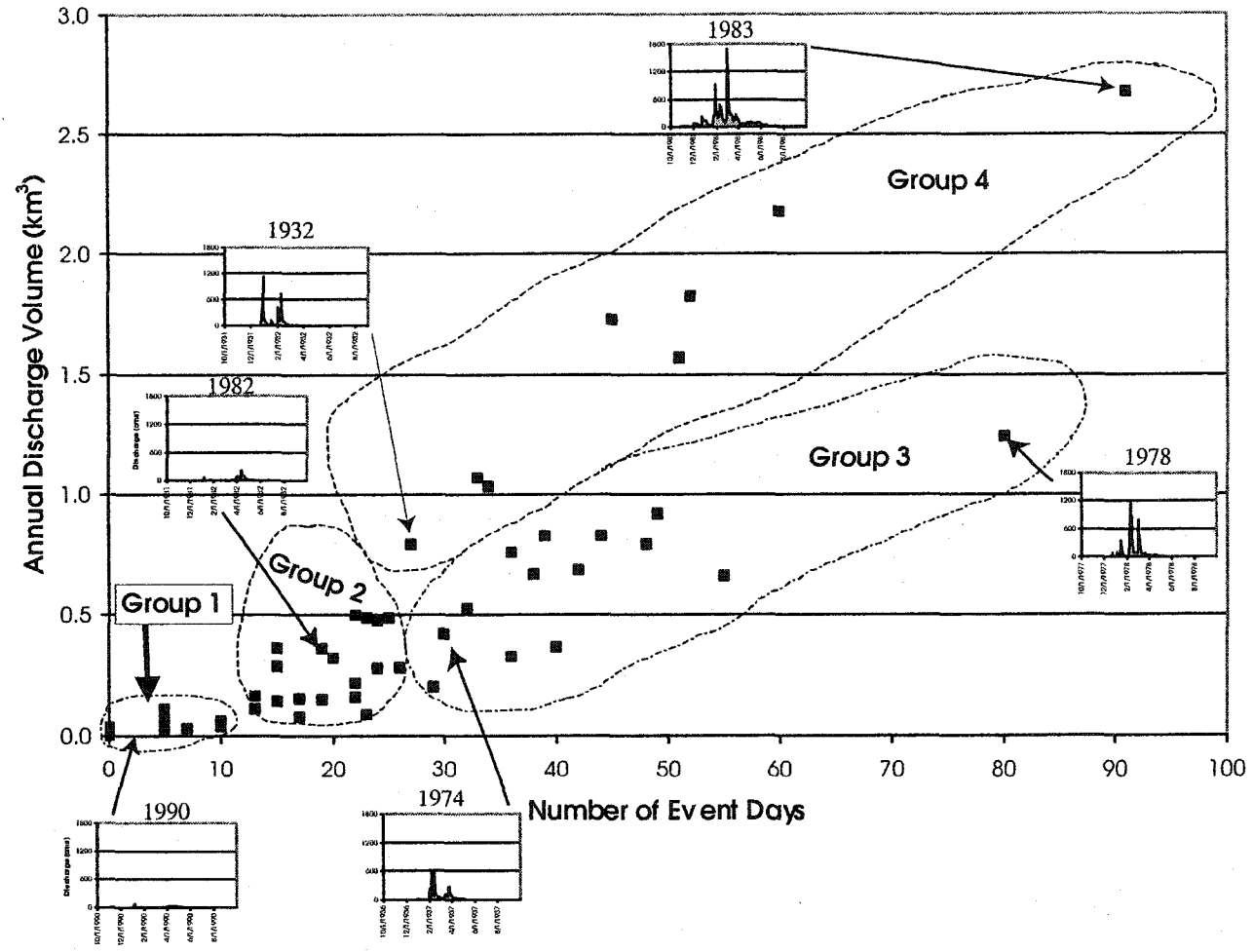


Figure 3-17: Annual event and non-event discharge volumes vs. total annual volume. The total annual discharge can be accurately predicted by examining the event discharge of the river. Events were defined by peaks at Spreckels $> 25 \text{ m}^3/\text{sec}$, and extend from 1 day prior to peak day, through 3 days following.

Figure 3-18: Division of water years into four groupings based on total annual discharge (km^3) and the number of event days in that water year. Some years with high numbers of event days have lower total annual discharge due to smaller events, than some years with short duration events, but very large floods.



17B guidelines (Hydrology Subcommittee of the Interagency Advisory Committee on Water Data, 1981). The procedure fits the logarithms of annual peak discharges to the Pearson Type III frequency distribution, known as the log-Pearson Type III distribution. A flood-frequency relationship is the relation of the magnitude of flood peak to the probability of exceedence (or recurrence intervals). The probability of exceedence is the chance a given flood magnitude is surpassed in any given year. For example, a 25-year flood has the probability of 0.04 of being exceeded in any given year. The Mean Annual Flood (MAF), defined as the flood with 2.33-year recurrence interval (Dunne and Leopold, 1978), is 264 m³/sec at Spreckels. The sample mean of annual peaks is 462 m³/sec, which is equivalent to the 3.2-year event. Normalizing the data by sub-basin area, the Mean Annual Runoff (2.33 year recurrence interval) for the seven gauges ranges from 37 mm at Spreckels to 365 mm at the Arroyo Seco station (Table 3-5). Those streams draining the drier northeastern portion of the basin record much lower values than those draining the wet southwestern portion. These recurrence intervals are helpful in predicting the probability of discharges of certain magnitudes. The episodicity of events in these sub-basins is represented by the ratio of the estimated 100-year flood to the MAF (Table 3-5). This shows that floods on the Estrella are extremely flashy in nature, with the discharge during these rare events being 30 times that of the mean annual flood. This is in contrast to the mouth of the river, where the ratio is only 7.

To examine the role of individual events in the watershed, event statistics were calculated and water budgets completed for specific events within the watershed. As we are interested ultimately in the discharge from the mouth, only events that manifest themselves in the flow record at the mouth were considered. An event on the river was

Table 3-5: Discharge (m³/sec) and runoff (mm) recurrence intervals for seven gauging stations in the Salinas watershed. The mean annual flood (MAF) is defined as the 2.33-year recurrence interval with mean annual runoff (MAR) being the MAF normalized to basin area. It is important to note that estimates are suspect for recurrence intervals greater than record length (n).

	USGS Stn ID	Area (km ²)	n	Log(Q) cfs			Recurrence Interval Peak Discharges (cms)							
				Mean	Std. dev.	Skew	Q2	Q5	Q10	Q25	Q50	Q100	MAF	Q100/MAF
Salinas @ Paso Robles	11147500	1,010	56	3.60	0.53	-0.96	136	319	452	611	719	815	191	4.25
Estrella nr Estrella	11148500	2,388	44	2.71	1.07	-0.12	15	114	322	948	1883	3454	109	31.55
Salinas @ Bradley	11150500	6,566	53	3.74	0.71	-0.54	178	622	1106	1928	2682	3541	424	8.34
San Lorenzo Nr King City	11151300	604	43	3.02	0.62	-0.23	31	101	181	329	478	663	68	9.63
Arroyo Seco Nr Soledad	11152000	632	96	3.83	0.39	-0.59	208	414	565	762	908	1052	267	3.92
El Toro Creek	11152540	83	40	1.88	0.71	-0.33	2	8	16	31	46	64	5	11.58
Salinas @ Spreckels	11152500	10,760	69	3.66	0.94	-1.12	194	819	1424	2256	2850	3391	460	7.37

	USGS Stn ID	Area (km ²)	n	Recurrence Interval as Runoff (mm)						
				R2	R5	R10	R25	R50	R100	MAR
Salinas @ Paso Robles	11147500	1,010	56	116	273	386	523	615	697	164
Estrella nr Estrella	11148500	2,388	44	5	41	116	343	681	1249	39
Salinas @ Bradley	11150500	6,566	53	23	81	145	253	352	465	55
San Lorenzo Nr King City	11151300	604	43	45	145	259	471	684	949	98
Arroyo Seco Nr Soledad	11152000	632	96	285	566	773	1042	1242	1438	365
El Toro Creek	11152540	83	40	24	91	171	325	483	679	58
Salinas @ Spreckels	11152500	10,760	69	15	65	114	181	228	272	36

defined as discharge peaks at the Spreckels gauge exceeding $25 \text{ m}^3/\text{sec}$. The event duration was defined as one day before the peak, the peak day and the following three days (a total of 5 days). Using this scheme, some of the classified events overlapped; even though they may have been distinct meteorological events, they were combined and considered one hydrologic event (e.g., Figure 3-19). These events were traced back through the watershed by using a lag of one day to all of the other gauging stations. This method allowed for event water budgets to be calculated throughout the watershed in a uniform fashion. At the Spreckels station, a total of 322 peaks were defined in this way. These were then grouped into 235 individual events in the water years 1930 - 2000.

The top 8 flood events on the Salinas River had event volumes greater than the mean total annual volume of 0.39 km^3 . These floods were in February 1938 (0.519 km^3), February 1998 (0.501 km^3), March 1983 (0.437 km^3), February 1941 (0.427 km^3), January 1969 (0.411 km^3), February 1978 (0.398 km^3), February 1969 (0.397 km^3), and March 1995 (0.395 km^3). In fact these eight events (64 days), accounted for 12.5 % of the cumulative 70-year discharge.

These flood events bring large amounts of sediment to the mouth as well. As sediment load increases as a power of discharge, these short-lived events are bound to carry catastrophic amounts of sediment to the coastal ocean. The same top eight events that accounted for 12 % of the historical discharge volume, account for nearly 40 % of the historical sediment load. The length of these events has been defined as at least 5 days, these events may be longer, and if extremely flashy, may contain days where discharge and loads are below normal, therefore it takes less than the 64 days to reach the 40% of the historical load. Sixteen of the top 20 events had sediment loads that were

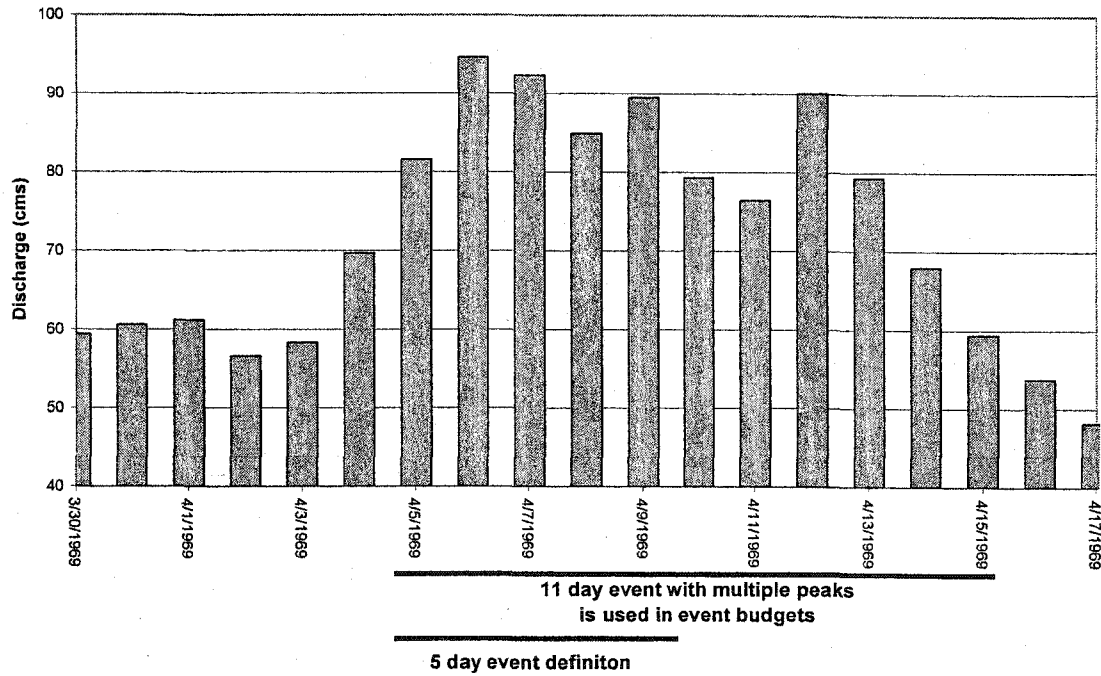


Figure 3-19: Example of combining meteorological events into a single hydrologic event for budget calculations. Overlapping events (defined as one day prior to peak, peak day and three days following peak) are combined together into a single event.

greater than the average annual sediment load of the river. The largest event, in early February of 1938, carried 5 times the average annual sediment load in only 8 days. These events define the annual load, with the largest floods on average accounting for greater than half of that year's load.

3.5.1 Hyperpycnal Flows

The rivers of southern California rivers are thought to discharge under hyperpycnal conditions during extreme El Niño related floods (Warrick and Milliman, in press). The nature of these small semi-arid coastal rivers is such that suspended sediment concentrations are extremely variable over the course of hours, with the majority of the daily sediment load occurring in just a few hours of a flood event. Using mean daily suspended sediment concentrations may mask the fact that a river has a suspended sediment concentration high enough to produce hyperpycnal flows from the river mouth (Warrick and Milliman, in press). The concentration needed to initiate river mouth generated hyperpycnal plumes has been debated (e.g., Johnson et al., 2001; Mulder and Syvitski, 1995; Wright et al., 1990) as it is influenced not only by fluvial sediment concentration but also interaction with seawater upon entering the ocean.

The USGS sediment database reports a maximum measured concentration of only 14.8 g/L for the Salinas River at Spreckels, but is lacking peak measurements during large flood events. The instantaneous sediment-discharge rating curve (created from USGS sediment database and Waananen, 1969; $C = 93.698 * Q^{0.7034}$) estimates the concentration for the maximum flow ever recorded (March 12, 1995; 2690 m³/sec) would be only 24 g/L, indicating that hyperpycnal flows are not likely from the Salinas River. However, Waananen (1969) measured a suspended sediment concentration of 34 g/L

during the February 1969 flood. The measurements during the 1969 flood, made every few hours of February 25, ranged from 12.6 – 34 g/L, indicating the short duration of high concentration flows.

It is important to note that all of these measurements were made at the Spreckels station (15 km from the mouth) and erosion in the lagoonal area during these large floods may supply enough sediment that these dense underflows may be possible. If hyperpycnal flows are generated at the mouth of the Salinas River, they are rare, short events.

3.6 Summary

Small mountainous rivers, especially those in semi-arid regions, are dominated by short-lived flood events. The Salinas River has had nearly 40% of its estimated historical sediment load delivered in just over 25 days (occurring during the 8 major events on the river) (Figure 3-20); however, in the same amount of time only 9% of the historical freshwater entered the ocean. The historical record indicates that in 30% of the record (7665 days) all of the freshwater and sediment is discharged, in large part reflecting the climatic signal, both seasonal and inter-annual. The need for large events to break through the river mouth bar is essential, for the ultimate release of floodwaters and sediment. Between breaches of the barrier, sediment is stored in the lagoonal area, and it is only during these large magnitude events that this area is scoured out, thus augmenting sediment delivery during floods.

The Salinas River watershed appears to be transport limited, with an ample supply of sediment available through most of the system. The limiting factor is the presence of sufficient water to transport the sediment to the mouth and to combat the loss of water to

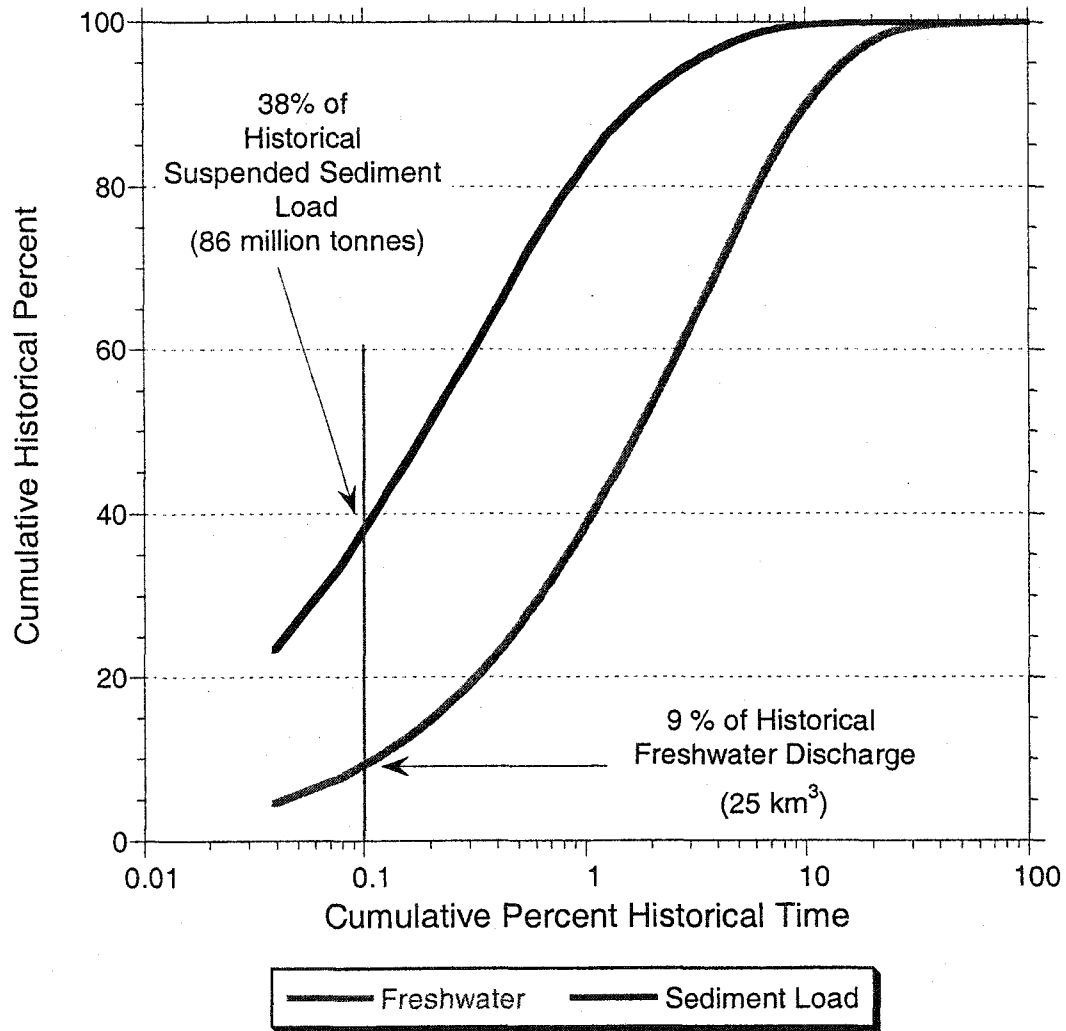


Figure 3-20: Historical event driven fluvial delivery from the Salinas River. In 1 % of the historical record (25 days), 38 % of the total sediment load and 9% of the total freshwater discharge may be accounted for. Essentially all (99%) of the sediment and freshwater passing Spreckels occurs in 6.8% (1773 days) and 25% (6573 days) of the time respectively. This is governed by the Mediterranean climate of the region, with no natural flow during the summer months.

groundwater recharge. This is especially important for the first flush events. If the first significant rainfall is insufficient to allow the rivers to cross the alluvial fans, the high load from the first flush is deposited on the fan, rather than transported to the mainstem. This increases the residence time for that sediment in the basin. This combined with increasing groundwater withdrawal has led to the river rarely gaining more water from runoff than is lost to groundwater water in its lower reaches (Figure 3-21) since 1947. The combination of decreased precipitation during the cool phase of the Pacific Decadal Oscillation (which switched in 1947) and increased demand on water has created this deficit in the water budget without a rebound when precipitation increased as we entered the warm phase of the Pacific Decadal Oscillation in 1977.

The role of the El Niño Southern Oscillation and the Pacific Decadal Oscillation is one of probability. The warm phase of ENSO increases the probability of a wet winter, as does the warm phase of the PDO. Therefore, years that are both warm ENSO and warm PDO are the ones that tend to have extreme water and sediment discharge from the Salinas River. A possible affect of global warming is increasing of extreme precipitation events (Karl and Knight, 1997). If this is true, then the timing and magnitude of sediment and water delivery to the Monterey Bay will change drastically.

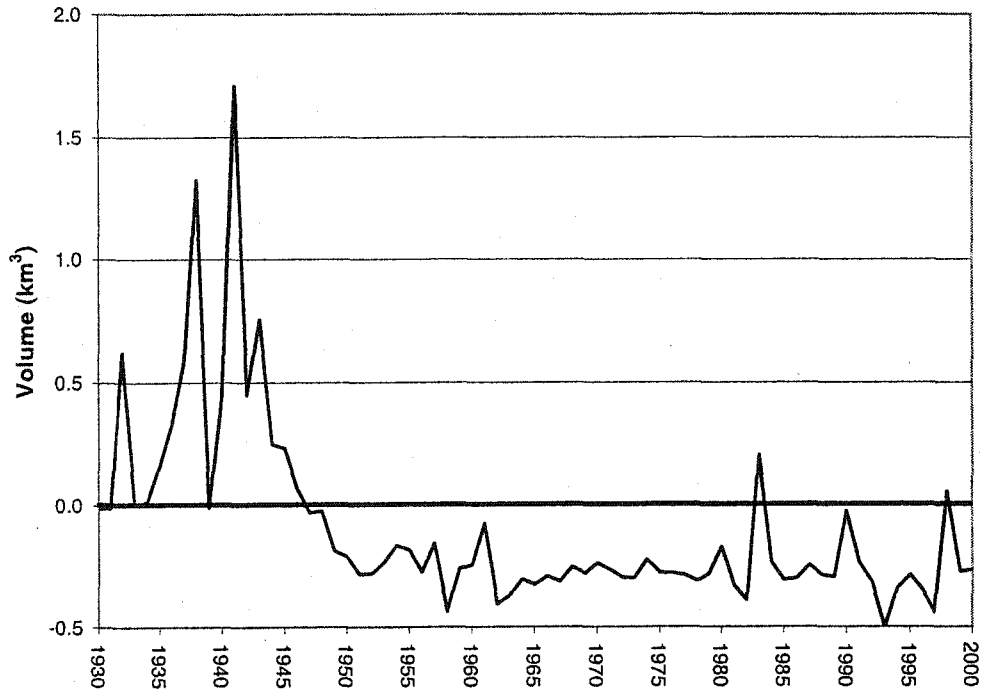


Figure 3-21: Difference in annual volume of water passing Spreckels, and that from upstream. Upstream volume was calculated as the volume entering from the San Lorenzo and Arroyo Seco Tributaries, added to that passing Bradley. With the increase groundwater pumping, the Salinas has become a losing river, with the rare wet years; rather than the opposite.

3.7 References:

- Amarasekera, K.N., Lee, R.F., Williams, E.R. and Eltahir, E.A.B., 1997. ENSO and the natural variability in the flow of tropical rivers. *Journal of Hydrology*, 200: 24-39.
- Asselman, N.E.M., 2000. Fitting and interpretation of sediment rating curves. *Journal of Hydrology*, 234: 228-248.
- Campbell, F.B. and Bauder, H.A., 1940. A rating-curve method for determining silt-discharge of streams. *EOS*, 21: 603-607.
- Cayan, D., Redmond, K. and Riddle, L., 2000. El Niño/La Niña and Extreme Daily Precipitation and Streamflow Values. www.wrcc.dri.edu/enso/percentile.html.
- Cayan, D.R. and Webb, R.H., 1992. El Niño/Southern Oscillation and streamflow in the western United States. In: H.F. Diaz and V. Markgraf (Editors), *El Niño - Historical and Paleoclimatic Aspects of the Southern Oscillation*. Cambridge University Press, pp. 58-68.
- Cleveland, W.S., 1979. Robust locally weighted regression and smoothing scatterplots. *Journal of the American Statistical Association*, 74(368): 829-836.
- Cohn, T.A., Caulder, D.L., Gilroy, E.J., Zynjuk, L.D. and Summers, R.M., 1992. The validity of a simple log-linear model for estimating fluvial constituent loads: An empirical study involving nutrient loads entering Chesapeake Bay. *Water Resources Research*, 28: 2353-2363.
- De Vries, A. and Klavers, H.C., 1994. Riverine fluxes of pollutants: monitoring strategy first, calculation methods second. *European Water Pollution Control*, 4: 12-17.
- Dettinger, M., Cayan, D. and Redmond, K., 2002. United States Streamflow Probabilities and Uncertainties based on Anticipated El Niño, Water Year 2003. 2003(May 20), D:\JournalArticles\Non-Journals\Dettinger_ElNino_Streamflow.pdf http://meteora.ucsd.edu/cap/flow2003_fcast.html.
- Duan, N., 1983. Smearing estimate: A nonparametric retransformation method. *Journal of the American Statistical Association*, 78(383): 605-610.
- Ducea, M., House, M.A. and Kidder, S., 2003. Late Cenozoic denudation and uplift rates in the Santa Lucia Mountains, California. *Geology*, 31(2): 139-142.
- Dunne, T. and Leopold, L.B., 1978. *Water in Environmental Planning*. W.H. Freeman, New York, 818 pp.

- Ferguson, R.I., 1986. River loads underestimated by rating curves. *Water Resources Research*, 22: 74.
- Ferguson, R.I., 1987. Accuracy and precision of methods for estimating river loads. *Earth Surface Processes and Landforms*, 12: 95-104.
- Fisher, A.B., 1945. *The Salinas Upside-Down River*. Farrar & Rinehart., New York, 316 pp.
- Fread, D.L., 1993. Flow Routing. In: M. D.R. (Editor), *Handbook of Hydrology*. McGraw-Hill, New York.
- Gutierrez, F. and Dracup, J.A., 2001. An analysis of the feasibility of long-range streamflow forecasting for Colombia using El Nino-Southern Oscillation indicators. *Journal of Hydrology*, 246: 181-196.
- Guy, H.P. and Norman, V.W., 1970. *Field Methods for measurement of fluvial sediment, Techniques of water-resources investigations; book 3 Applications of Hydraulics*. US Government Printing Office, Washington, D.C., pp. 59.
- Hansen, R.T. et al., 2002. Geohydrology of a deep aquifer system monitoring site at marina, Monterey County, California. *Water-Resources Investigations Report 024003*, U.S. Geological Survey, 36 pp.
- Hicks, D.M. and Inman, D.L., 1987. Sand Dispersion from an Ephemeral River Delta on the Central California Coast. *Marine Geology*, 77: 305-318.
- Hirsch, R.M., Helsel, D.R., Cohn, T.A. and Gilroy, E.J., 1993. Statistical treatment of hydrologic data. In: M. D.R. (Editor), *Handbook of Hydrology*. McGraw-Hill, New York.
- Hydrology Subcommittee of the Interagency Advisory Committee on Water Data, 1981. Guidelines for determining flood frequency. *Bulletin 17B*, U.S. Geological Survey : Office of Water Data Collection, Reston, VA, 183 pp.
- Inman, D.L. and Jenkins, S.A., 1999. Climate Change and the Episodicity of Sediment Flux of Small California Rivers. *Journal of Geology*, 107: 251-270.
- Jansson, M., 1985. A comparison of detransformed logarithmic regressions and power function regressions. *Geografiska Annaler*, 67 A: 61-70.
- Johnson, K.S., Paull, C.K., Barry, J.P. and Chavez, F.P., 2001. A decadal record of underflows from a coastal river into the deep sea. *Geology*, 29(11): 1019-1022.
- Karl, T.R. and Knight, R.W., 1997. The 1995 Chicago Heat Wave: How Likely Is a Recurrence? *Bulletin of the American Meteorological Society*, 78(6): 1107-1119.

- Kistler, R.W. and Champion, D.E., 2001. Rb-Sr whole-rock and mineral ages, K-Ar, Ar/Ar, and U-Pb mineral ages, and strontium, lead, neodymium, and oxygen isotopic compositions for granitic rocks from the Salinian terrane, California. Open File Report 01-453, U.S. Geological Survey, 84 pp.
- Lanfear, K.J. and Hirsch, R.M., 1999. USGS Study Reveals a Decline in Long-record Streamgages. EOS, 80(50): 605-607.
- Mantua, N.J., Hare, S.R., Yuan, Z., Wallace, J.M. and Francis, R.C., 1997. A Pacific Interdecadal Climate Oscillation with Impacts on Salmon Production. Bull. Am. Meteorol. Soc., 78(6): 1069-1079.
- Mattinson, J.M. and James, E.W., 1985. Salinian block U-Pb age and isotopic variations: Implications for the origin and emplacement of the Salinian terrane. In: D.G. Howell (Editor), Tectonostratigraphic terranes of the Circum-Pacific region. Earth Sciences Series. Circum-Pacific Council for Energy and Mineral Resources, pp. 215-226.
- McCabe, G.J. and Dettinger, M.D., 1999. Decadal variations in the strength of ENSO teleconnections with precipitation in the western United States. International Journal of Climatology, 19: 1399-1410.
- MCWRA, 2001. Draft Environmental Impact Report/Environmental Impact Statement for the Salinas Valley Water Project. 2002(January), http://www.co.monterey.ca.us/mcwra/deir_svwp_2001/INDEX.HTM.
- Milliman, J.D. and Syvitski, J.P.M., 1992. Geomorphic/Tectonic Control of Sediment Discharge to the Ocean: The Importance of Small Mountainous Rivers. Journal of Geology, 100: 525 - 544.
- Mosley, M.P. and McKerchar, A.I., 1993. Streamflow. In: M. D.R. (Editor), Handbook of Hydrology. McGraw-Hill, New York.
- Mulder, T. and Syvitski, J.P.M., 1995. Turbidity currents generated at river mouths during exceptional discharges to the world oceans. Journal of Geology, 103(3): 285-299.
- Neelin, J.D. et al., 1998. ENSO Theory. JGR Oceans, 103: 14,261-14,290.
- Palmer, T.N. and Mansfield, D.A., 1986. A study of wintertime circulation anomalies during past El Niño events using a high resolution general circulation model. II. Variability of the seasonal mean response. Quarterly Journal of the Royal Meteorological Society, 112(473): 639-660.

- Rantz, S.E., 1970. Urban Sprawl and Flooding in Southern California. Water in the Urban Environment Circular 601-B, USGS, Washington, 11 pp.
- Redmond, K.T. and Koch, R.W., 1991. Surface climate and streamflow variability in the western United States and their relationship to large scale circulation indices. *Water Resour. Research*, 27: 2381-2399.
- Ropelewski, C.F. and Halpert, M.S., 1987. Global and regional scale precipitation patterns associated with the El Niño / Southern Oscillation (ENSO). *Monthly Weather Review*, 115: 1606-1626.
- Singh, K.P. and Durgunoglu, A., 1989. Developing accurate and reliable stream sediment yields. IAHS-AISH Publication, 184: 193-199.
- Tooth, S., 2000. Process, form and change in dryland rivers: a review of recent research. *Earth Science Reviews*, 51: 67-107.
- Trenberth, K.E., 1997. The Definition of El Niño. *Bull. Amer. Met. Soc.*, 78: 2771-2777.
- Waananen, A.O., 1969. Floods of January and February 1969 in Central and Southern California. Open-File Report, USGS Water Resources Division, Menlo Park, CA, 223 pp.
- Walling, D.E., 1974. Suspended sediment and solute yields from a small catchment prior to urbanization. In: K.J. Gregory and D.E. Walling (Editors), *Fluvial processes in instrumented watersheds; studies of small watersheds in the British Isles*. Inst. Brit. Geogr., London, UK, pp. 169-192.
- Walling, D.E., 1977. Assessing the Accuracy of Suspended Sediment Rating Curves for a Small Basin. *Water Resources Research*, 13(3): 531 - 538.
- Walling, D.E. and Webb, B.W., 1981. The reliability of suspended sediment load data, in: *Measurement of erosion and transport of sediments*. IAHS-AISH Publication, 133: 177-194.
- Walling, D.E. and Webb, B.W., 1988. The reliability of rating curve estimates of suspended sediment yield; some further comments. IAHS-AISH Publication, 174: 337-350.
- Warrick, J.A. and Milliman, J.D., in press. Hyperpycnal sediment discharge from semi-arid southern California rivers—implications for coastal sediment budgets. *Geology*.
- Watson, F. et al., 2003. Salinas Valley Sediment Sources. Watershed Institute Report WI-2003-06, California State University Monterey Bay, 239 pp.

- Watson, F., Newman, W., Anderson, T., Alexander, S. and Kozlowski, D., 2001. Winter Water Quality of the Carmel and Salinas Lagoons, Monterey, California:2000/2001WI-2001-01, The Watershed Institute Earth Systems Science and Policy California State University Monterey Bay, 42 pp.
- Waylen, P.R. and Caviedes, C.N., 1986. El Niño and annual floods on the North Peruvian littoral. *Journal of Hydrology*, 89(1-2): 141-156.
- Waylen, P.R. and Caviedes, C.N., 1990. Annual and seasonal fluctuations of precipitation and streamflow in the Aconcagua River basin, Chile. *Journal of Hydrology*, 120(1-4): 79-102.
- Webster, P. and Lukas, R., 1992. TOGA COARE: The coupled ocean atmosphere response experiment. *Bull. Am. Meteorol. Soc.*, 73: 1377-1416.
- Webster, P.J. and Palmer, T.N., 1997. The past and the future of El Niño. *Nature*, 390: 562-564.
- Woolhiser, D.A., Keefer, T.O. and Redmond, K.T., 1993. Southern oscillation effects on daily precipitation in the southwestern U.S. *Water Resources Research*, 29: 1287-1295.
- Wright, L.D. et al., 1990. Processes of marine dispersal and deposition of suspended silts off the modern mouth of the Huanghe (Yellow River). *Continental Shelf Research*, 10: 1-40.

Chapter 4: Long-term Sediment Storage on the Monterey Bay Continental Shelf

4.1 Introduction

A range of diverse processes control delivery of terrestrial sediment to the continental shelves. The dispersal and long-term accumulation of riverine sediment has been well studied near many river mouths (e.g., Nittrouer and Kuehl, 1995; Eel River: Drake, 1999; Wheatcroft et al., 1997 and Ganges-Brahmaputra: Kuehl et al., 1997). These systems are defined by their sediment sources, transport pathways, and sediment sinks. The interplay between sediment supply, physical energy regime (winds, tides, waves) as well as the regional geology determines the nearshore and coastal geomorphology (Orton and Reading, 1993; Wright and Coleman, 1972).

The climate and geomorphology of watersheds play key roles in determining sediment supply from rivers (Milliman and Syvitski, 1992). Sediment yield from small rivers draining tectonically active margins are some of the highest (e.g., Milliman et al., 1999). The supply of sand-sized sediment to the littoral zone of California, for example, is estimated to be 75 – 90% riverine with the remaining proportion from bluff erosion (Best and Griggs, 1991). Floods play a key role in this delivery, especially from small mountainous rivers (Brown and Ritter, 1971; Wheatcroft et al., 1997; Warrick and Milliman, in press; Chapter 3).

4.1.1 Salinas Shelf

This paper discusses the role of the Salinas River in the long-term sediment budget of Monterey Bay. Monterey Bay is located approximately 115 km south of San Francisco, California (Figure 4-1). A symmetrical open embayment, mostly shallower than 100 m and a shelf width of only 6 km, the bay shelf is a typical wave-cut platform formed during the Holocene transgression (Bradley and Griggs, 1986).

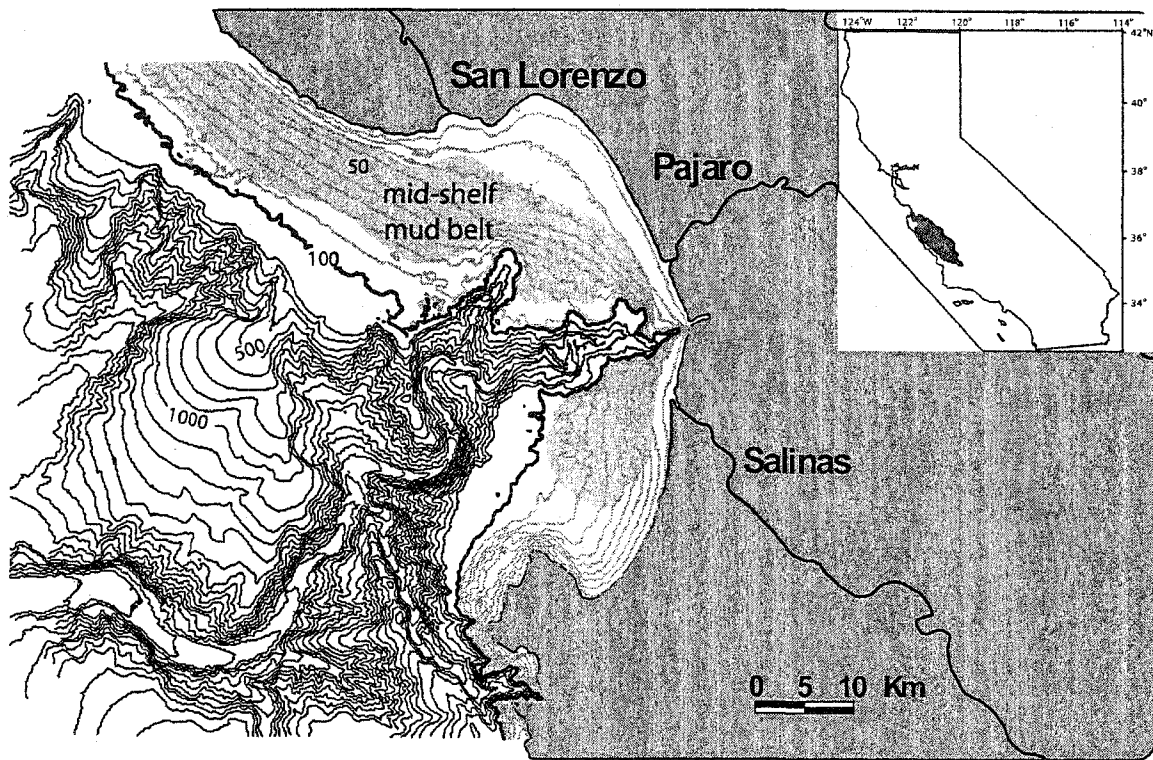


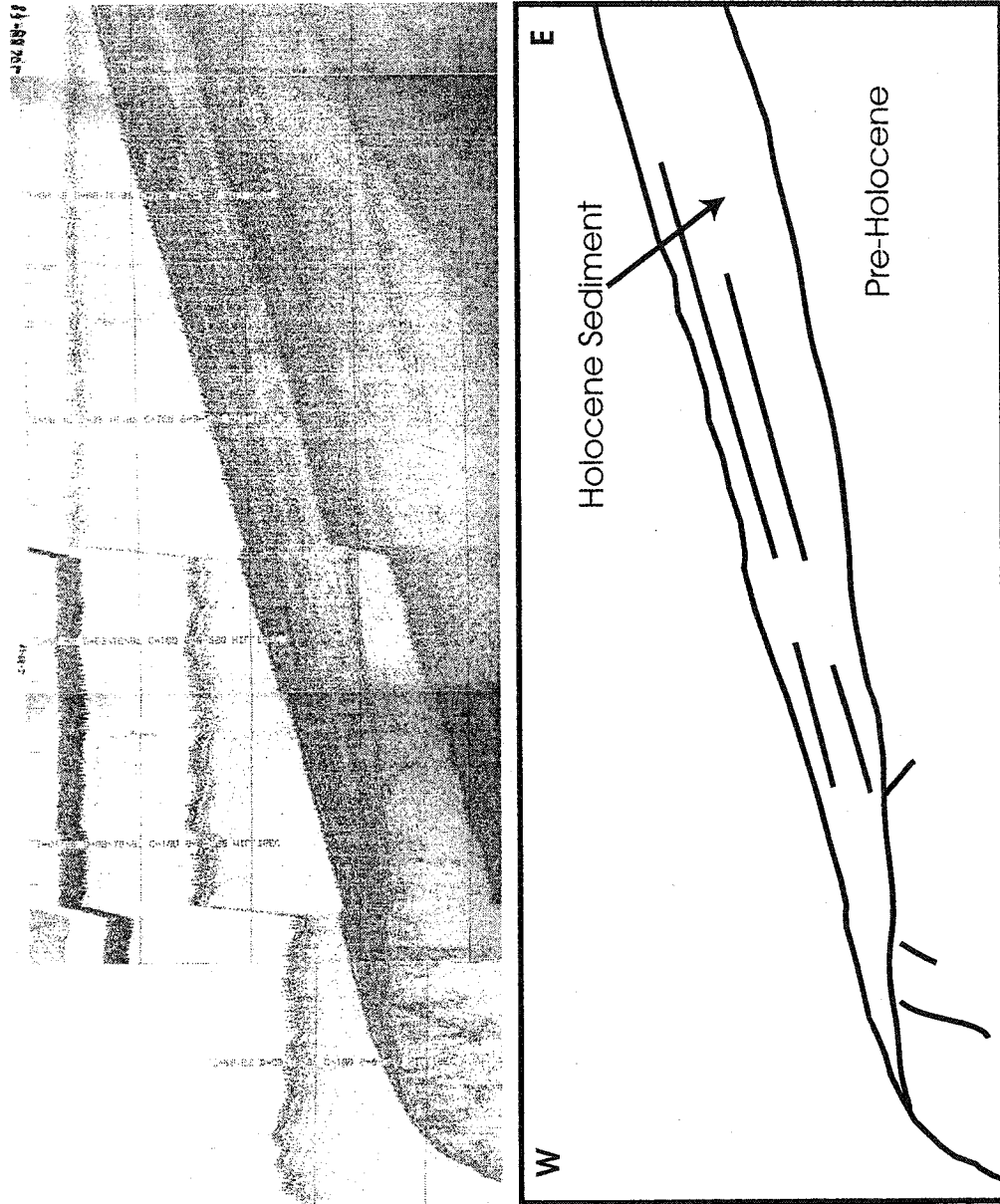
Figure 4-1: Location of Monterey Bay and bathymetric map showing dominance of the Monterey Bay Submarine Canyon, major rivers draining to the bay and location of mid-shelf mud belt. Contour interval is 10m to 100m water depth, then 100m.

It is characterized by relatively low relief, and isobaths more or less parallel to the shoreline, except near the mouth of the present day Salinas River where there is a subaqueous sediment lobe. The bay is bisected by the large Monterey Bay submarine canyon, which reaches almost to shore. The shoreline of the southern half of the bay is composed of broad sandy beaches, many backed by large aeolian sand dunes. This is in contrast to the high cliffs and flat-topped terraces found along the northern shoreline.

Predominant direction of wave approach is from the northwest, with winter swell from the southwest (2-3m; Tait and Revenaugh, 1998). This allows the northern part of the bay protection from waves from the northwest, and the far southern part of the bay protection from southwest swell. Shelf circulation is mainly driven by coastal upwelling and wind forcings. The tides in the bay are semi-diurnal and average approximately 1.6 m.

Both the northern and the southern shelves are characterized by mid-shelf (40 – 90 m water depth) fine-grained sediments (Eittreim et al., 2002a; Figure 4-1). Medium sands are found in the near-shore (< 20 m water depth) and near the shelf break (~ 90 m). The high-energy near-shore environment does not allow for long-term deposition of fine-grained sediment, and it is thought that tidal interaction with the canyon lip does the same at the shelf break (Cacchione and Drake, 1986). Sand and gravels found near the shelf break originate from outcropping beds (Chin et al., 1988; Eittreim et al., 2002a) (Figure 4-2).

Figure 4-2: Seismic line 87-88 showing sediment wedge from mouth of Salinas River into the Monterey Submarine Canyon.



4.1.2 Delivery System

The region has a Mediterranean climate, receiving 90% of its rainfall between the months of November and March. Storms tend to be intense and short-lived, with mean annual rainfall of 1000 mm in the coastal mountains and 300 mm in the lower valley. The Salinas River is the most important source of sediment to the Monterey Bay. The northern shelf receives sediment inputs from the San Lorenzo River, Soquel Creek, the Pajaro River, coastal erosion and littoral drift around the headland. Some fine-grained material from the Salinas may reach the northern shelf during flood events via a surface plume, but it is assumed no littoral transport crosses the head of the canyon (Best and Griggs, 1991). Much of the sediment is delivered episodically from these small steep coastal rivers. The Salinas River displays considerable inter-annual variability. For example, water year 1969 had an annual suspended sediment load of 25.6 million tonnes, which exceed the cumulative load of the previous 25 years. Larger events were more frequent from 1978 through the late 1990's, with an annual load in 1983 of 28.4 million tons being greater than the previous 10 years of suspended sediment discharge combined. This increase in frequency is associated with the increased affect of El Niño along the Central Coast during warm phases of the Pacific Decadal Oscillation (Inman and Jenkins, 1999; Chapter 3). These years of high discharge are dominated by short-lived flood events as is the case in most of the coastal California watersheds (Borgeld, 1985; Griggs and Hein, 1980; Helley and LaMarche, 1973; Leithold, 1989; Mertes and Warrick, 2001; Milliman and Syvitski, 1992; Wheatcroft et al., 1997). These floods are the dominant delivery method of sediment to the shelf.

During 1983, 50 % of the annual suspended sediment load was delivered in only 4 days. In fact, more than 60% of the annual suspended load typically is delivered within 5 or fewer days each year. It is important to note that during low-flow years transported sediment does not reach the ocean, as a river mouth bar closes the river mouth and is only removed when flood flows are reached. Instead, the sediment is temporarily deposited behind the river mouth bar in the Salinas lagoon.

Historically the mouth of the Salinas River has been dynamic, switching over a wide north-south swatch, including sharing a mouth with the Pajaro River 12 km north of the present day river mouth (Figure 4-3). Schwartz et al. (1986) state that the present river mouth was formed during the large winter storms of 1909, and was maintained by farmers and local government agencies to protect their fertile farmland. The Old Salinas Channel still carries water during low flow periods, especially when the river mouth bar is in place, allowing water to leave the Salinas Lagoon via the Moss Landing Harbor. During high flow periods, the gates are closed to allow for water pressure to build behind the river mouth bar to facilitate breaching (usually conducted when river flow approaches $20 \text{ m}^3/\text{sec}$, but this is dependent on tidal and wave conditions as well; Watson et al., 2001).

This paper will discuss the role of the Salinas River in the long-term sediment budget of the Monterey Bay. That is, I will address the fate of Salinas-derived sediments, both short- and long-term. These results suggest that very short-term deposition, followed by removal occurs on the shelf. This implies that Monterey Canyon is an active transport corridor for the majority of Salinas River sediment.

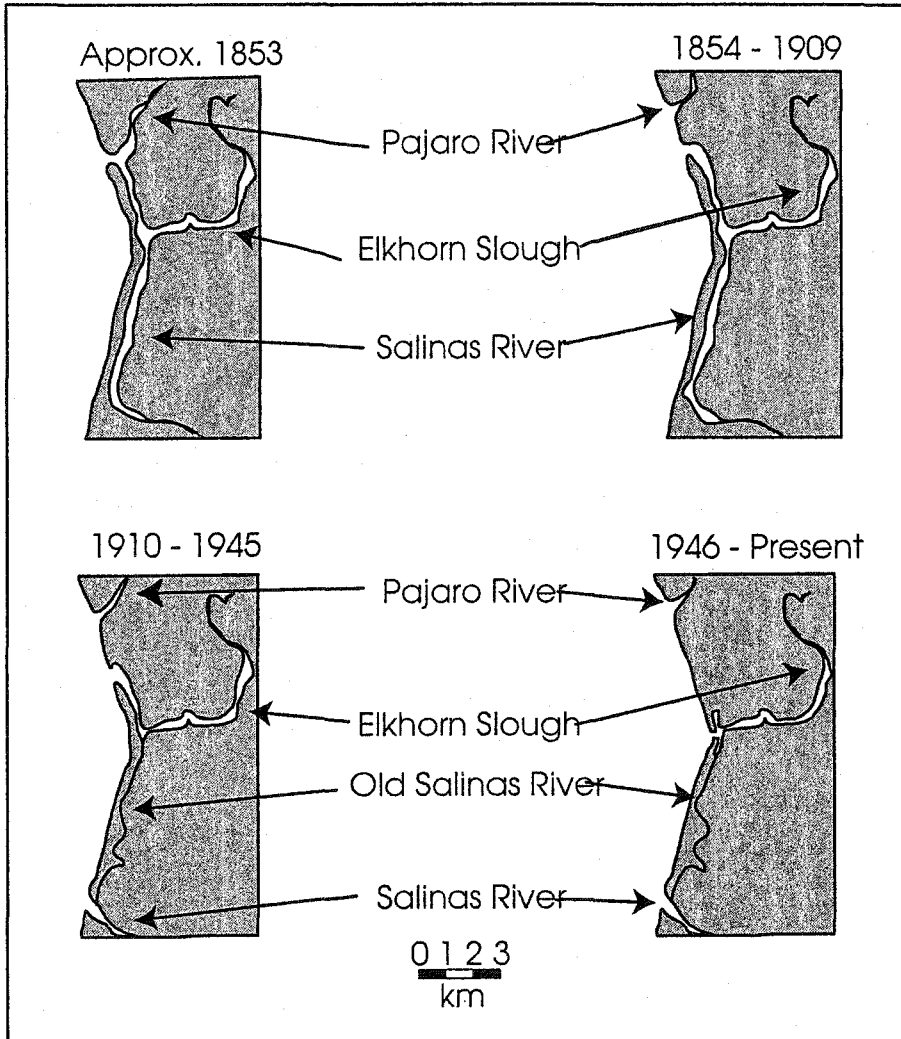


Figure 4-3: Geomorphic setting of the Pajaro River, Elkhorn Slough, the Old Salinas River Channel and the present day Salinas River Mouth (after Schwartz et al., 1986).

4.1.3 Methods

Modern sediment input from the Salinas River was estimated using sediment-discharge rating curves and 70 years of discharge data from the USGS gauging station near Spreckels (Chapter 3). Daily sediment load values for days with mean daily discharge greater than $1 \text{ m}^3/\text{s}$ were used to calculate the rating curve (<http://webserver.cr.usgs.gov/sediment/>). This rating curve was then applied to the historical discharge record (1930 – present) to estimate annual and historical sediment loads from the Salinas River.

In 1992 the federal government designated over $16,000 \text{ km}^2$ of ocean offshore of the central coast of California as the Monterey Bay National Marine Sanctuary (MBNMS). In order to characterize the seafloor geology of the sanctuary, the United States Geological Survey (USGS) was tasked with mapping the seafloor in this region. The southern shelf of Monterey Bay was included in this large survey project. In September of 1997, the USGS collected high-resolution seismic-reflection data of the Monterey Bay seafloor. Approximately 160 trackline kilometers of seismic data were collected from the southern shelf using a HUNTEC boomer operating in the 2 – 2.4 kHz range (Figure 4-4).

Archived data from three other USGS cruises conducted in the early 1980's also were used (Chin et al., 1988). These data were collected using a single-plate EG&G Uniboom, filtered between 600-1400 Hz and a double-plate EG&G Uniboom filtered between 500 – 1500 Hz.

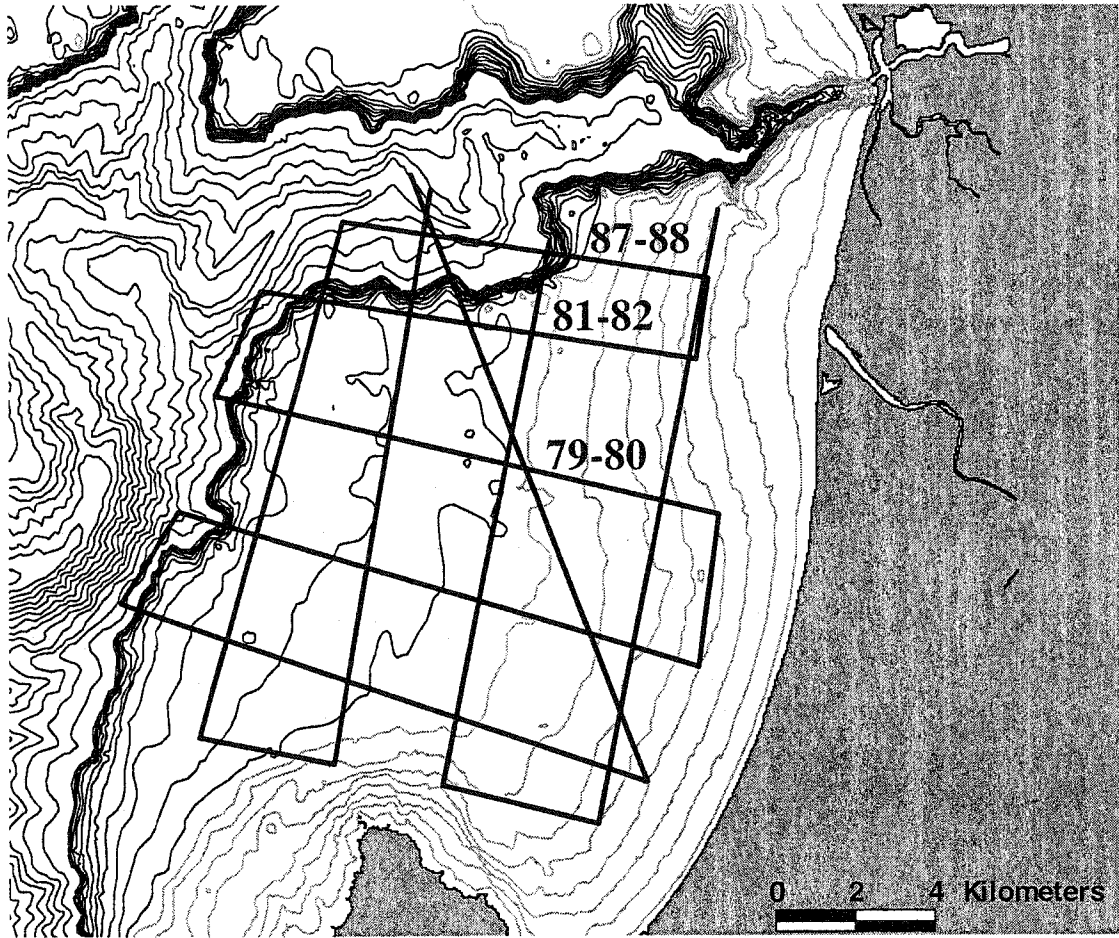


Figure 4-4: Tracklines of HUNTEC high-resolution seismic cruise. Numbered lines are cited in other figures.

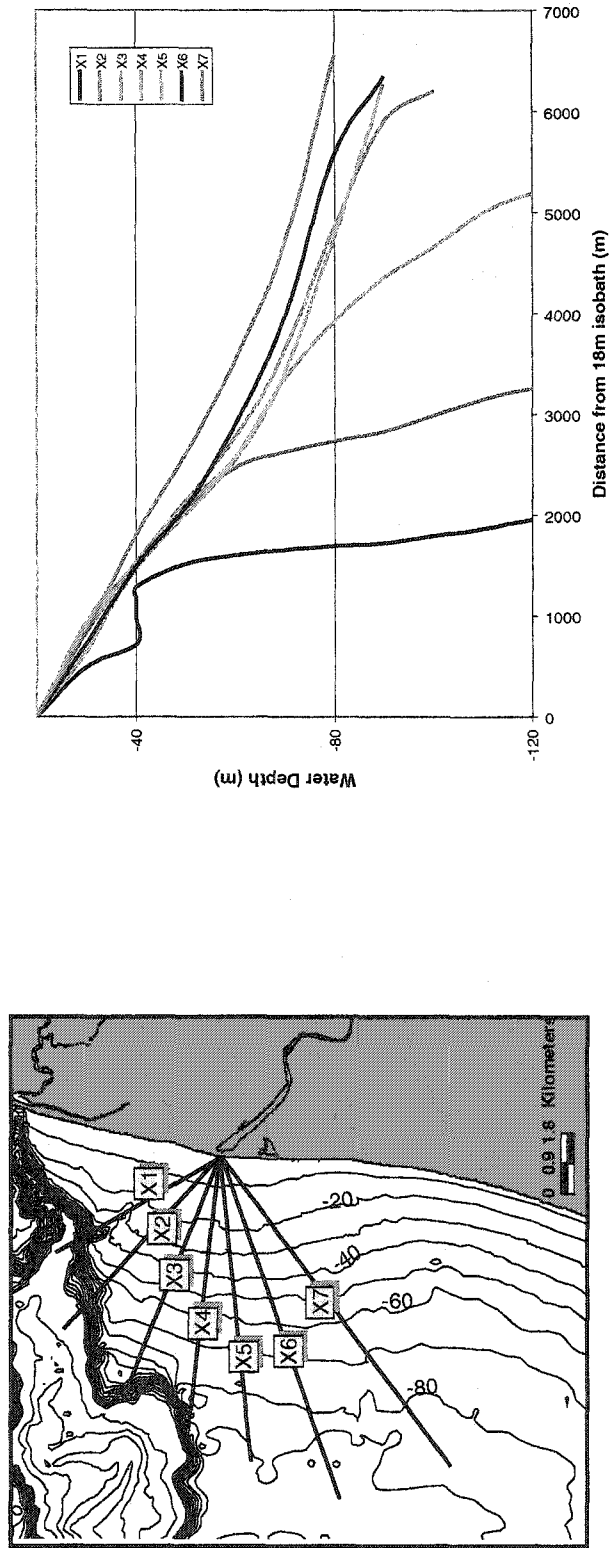
4.2 Results and Discussion

The Salinas outer-shelf is characterized by little modern sediment cover; outcropping strata are noted on many seismic profiles (Figure 4-2). The inner shelf is dominated by the deltaic topography off the Salinas River mouth, covering an area of approximately 75 km², the remainder of the southern shelf is sediment starved. The slope of the seafloor in this region is uniform over the entire deposit, with a steeper slope close to shore (from 20 - 30 m water depth) gradually flattening to the shelf-break (Figure 4-5). The only part of the sediment lobe that does not demonstrate this pattern is the most northerly portion that has a much steeper slope directly into the canyon head.

4.2.1 Long-term Sediment Storage

The high-resolution seismic profiles revealed an erosional unconformity in all of the seismic profiles on the southern shelf, overlain by a thick lense of sediment with parallel to sub-parallel reflectors separating acoustically transparent layers. This unconformity is easily identified as the underlying reflectors are angled and truncated. This is likely the result of erosion during the last marine transgression (Anima et al., 2002; Chin et al., 1988; Greene, 1977; Mullins et al., 1985), meaning that all sediment deposited above this unconformity is Holocene in age. This is supported by ¹⁴C dates at the base of the sediment layer of 14.8 ka Cal BP (Eittreim et al., 2000; Eittreim et al., 2002b). Paleo-channels like those seen on the northern shelf (Anima et al., 2002) are not seen on the southern shelf, possibly indicating that the Salinas River did not drain across the shelf during the low stand.

Figure 4-5: Bathymetric profiles from the mouth of the Salinas River across the sediment lobe on the southern shelf.



Profiles of the erosional surface along shore-normal lines (79-80 and 82-81) show a distinct change in slope at approximately 90 meters water depth (Figure 4-6). The profiles collected in 1997 did not go inshore enough to see the break in slope Chin et al. (1988) describe at 50 m water depth. The change in slope at 90 m is also documented on the northern shelf and interpreted as a wave-cut terrace that was drowned quickly due to a rapid rise in sea-level approximately 14.8 ka Cal BP (Anima et al., 2002). Grossman et al. (2002) have found a sharp contact in vibracores from the northern shelf that separates marine carbonate-rich sands and gravels from the terrigenous silts and clays. The marine facies has abundant inter-tidal to sub-tidal molluscs (used to date the flooding of the shelf around 14.8 ka cal BP). The bottom of the silt and clay facies is estimated to be $11.0 \pm .3$ ka Cal BP (Grossman et al., 2002), caused by abrupt changes in the depositional environment. The Holocene sediment volume for the southern shelf was determined by combining the seismic profile data from Chin et al. (1988) with the newly acquired data. All sediment above the unconformity was included, and assumed to be Holocene in age (Figure 4-7). The volume of sediment stored on the southern shelf was estimated to be $1.1 * 10^9 \text{ m}^3$.

Climatic conditions along the California coast show dramatic differences between the early Holocene and the late Holocene. The modern climatic pattern of cool summers, and relatively warm and wet winters was established between 5.2 and 3.2 ka cal BP (Barron et al., 2003). Prior to that, the sea-surface temperatures were significantly cooler, and pollen records indicate warmer, drier conditions in much of the western United States (Fritz et al., 2001). Using Grossman et al.'s 2002 estimate of mud accumulation starting 11 ka cal BP, and the climatic transitions indicated from

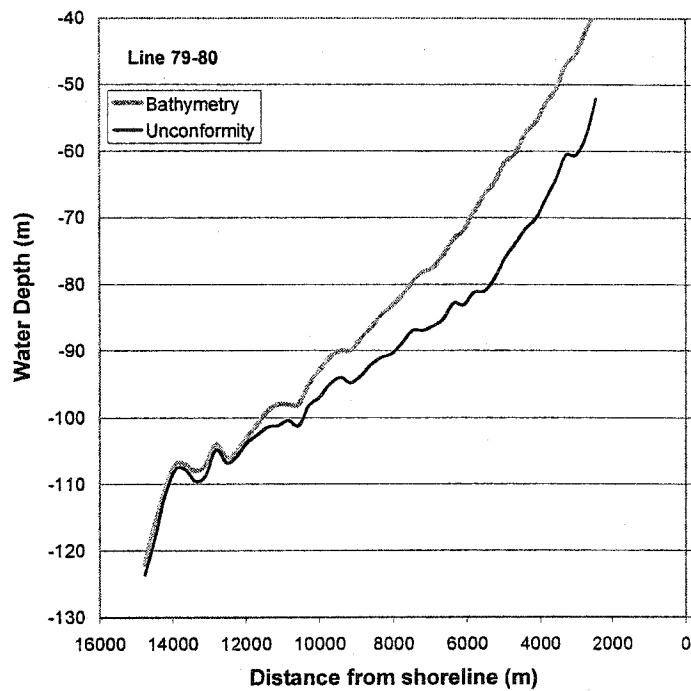
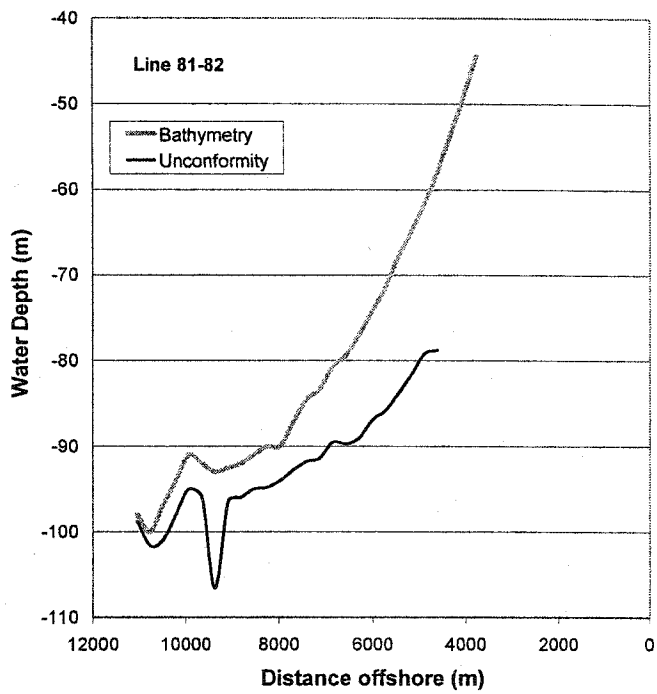


Figure 4-6: Profiles of shore-normal seismic lines, showing bathymetry and the angular unconformity.

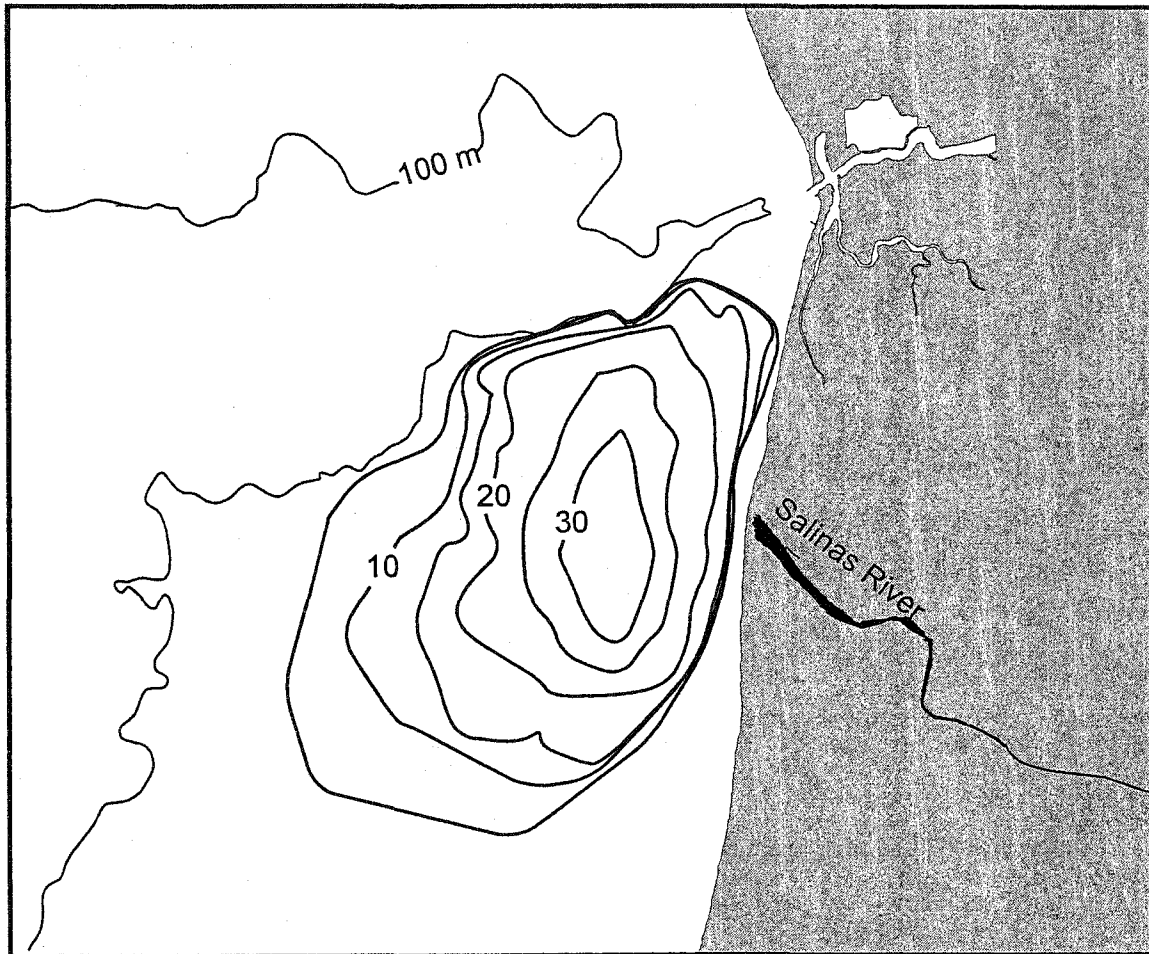


Figure 4-7: Isopach map of Holocene sediment accumulated on the southern shelf of the Monterey Bay. Holocene sediment thickness in meters, 100m isobath shown to delineate the shelf-break and canyon.

offshore cores, historical estimates were extrapolated for the last 11,000 years to determine total sediment input to Monterey Bay. Assuming a dry sediment weight of 1600 kg/m^3 , chosen to be consistent with Eittreim et al. (2002b) and Best and Griggs (1991), the average annual sediment load of the Salinas River is $1.9 * 10^6 \text{ m}^3$.

Historical sediment input rates were extrapolated over the last 5 ka, however for the 6 ka between shelf inundation and establishment of modern climatic conditions, the extent of load reduction is not known. A range of sediment input was then calculated between the minimum (absolutely no input from the rivers) and the maximum (equal to modern rates) of Holocene sediment input. This results in an estimated Holocene sediment input from the Salinas River of $9.4 - 20.7 * 10^9 \text{ m}^3$. This first order estimate indicates that only 5 - 12 % of the sediment can be accounted for by storage on the southern shelf (Table 4-1). This situation is in contrast with that on the north shelf, where Eittreim et al. (2002b) find the Holocene volume to be $3.6 * 10^9 \text{ m}^3$. With an estimated input of $600,000 \text{ m}^3$ (2002b) of sediment from the rivers and direct input along the coastline, total Holocene input ranges from $3 - 6.6 * 10^9 \text{ m}^3$ suggesting that the northern shelf deposits represent approximately 55 - 120 % of the total terrigenous input.

This north-south disparity at first might suggest that there has been considerable northward escape of Salinas sediment, presumably when the river's mouth was north of the Monterey Canyon. However, there are several reasons for doubting this. First, during floods a river is more likely to seek its shortest path to the sea, not meander along a longer path; this suggests that during floods the Salinas probably broke through the beach bar and discharged at or near its present location.

Table 4-1: Long-term storage and sediment delivery to Monterey Bay. Stored sediment accounts for an estimated 17 - 38% of total estimated sediment discharged to the Monterey Bay in the past 11 ka. Estimated for maximum (modern rates for entire 11 ka) and minimum (no input prior to 5 ka BP).

Shelf	Long-Term Storage (m³)	Modern Estimated Annual Sediment Delivery (m³/yr)	Minimum Holocene Estimated Sediment Delivery (m³)	Percent of Holocene Accounted For using Minimum Estimate	Maximum Holocene Estimated Sediment Delivery (m³)	Percent of Holocene Accounted For using Maximum Estimate
North	3.6 * 10 ⁹	600,000	3 * 10 ⁹	120 %	6.6 * 10 ⁹	55 %
South	1.1 * 10 ⁹	1.88 * 10 ⁶	9.4 * 10 ⁹	12 %	20.7 * 10 ⁹	5 %
Total	4.7 * 10⁹	2.48 * 10⁶	12.4 * 10⁹	38 %	27.3 * 10⁹	17 %

This supposition is supported by the fact that the only evidence of a modern Salinas-derived delta seen on either the north or south shelf is off the present-day mouth.

Moreover, if the river had emptied north, it seems likely that some or all of the sediment might have discharged directly or indirectly into the Monterey Canyon, thereby being lost to the northern shelf.

The presence of the subaqueous sediment lobe off the mouth of the Salinas River indicates that the majority of the sediment discharged from the river has occurred from the present day location of the mouth. However, even if we accept the possibility of northward discharge of the Salinas river, the combined Holocene sediment cover on the shelf of Monterey Bay is only $4.7 * 10^6 \text{ m}^3$, compared to fluvial input of $12.4 - 27.3 * 10^9 \text{ m}^3$ (Table 4-1), giving a long-term storage of only 17 – 38 %. Changes in regional climate have been addressed in this estimate, however the effect of human alteration of the landscape has not. The increase of intensive agriculture and grazing in the Salinas Valley may have caused an increase in the sediment load of the river, however the construction of dams and the removal of streambed sediment for economic as well as flood abatement purposes has decreased the sediment load of the river. It is thought that the magnitude of the increases and decreases of the anthropogenic changes are of the same order of magnitude, and were therefore not considered in this estimate.

4.2.2 Short-Term Sediment Storage

Modern patterns may help us to understand the ultimate fate of fluvial sediment in Monterey Bay. During storm events, strong onshore winds set up longshore currents that converge at the head of Monterey Canyon. The accompanying waves may cause resuspension of bottom sediment, allowing for transport canyon-ward (Griggs and Hein,

1980). It is also during these winter storms when large amounts of precipitation fall on the basin.

Flooding in early March of 1995 introduced nearly $7.5 * 10^6 \text{ m}^3$ of suspended sediment to the shelf (82 % of the 1995 annual load). This was the fourth largest sediment discharge event of the historical record. Sampling of the shelf in the first half of April (USGS Cruise ID: M-1-95-MB), 2-3 weeks following the flood, revealed the presence of a distinctive sandy-silt layer atop the ambient clayey silts on the middle shelf (Figure 4-8). However, sampling was not extensive enough to delineate the entire flood deposit. Where sampled, this mud layer was less than 2 cm in thickness, and if we overestimate the flood layer by assuming it was deposited over the entire southern mudbelt, it accounted for $1.4 * 10^6 \text{ m}^3$, which suggests that only about 30% of the sediment discharged from the Salinas River was stored on the shelf.

Box cores collected from the southern shelf in September of 1995 (7 months after the large flood; USGS Cruise ID: P-2-95-MB, Figure 4-8) contained what appears to be a homogenous mud layer, approximately 1 cm in thickness, suggesting a possible redistribution of the flood deposit since April. However, once again box cores are not extensive enough to delineate the extent of this deposit.

Lewis et al. (2002) report ^{210}Pb -derived maximum sediment accumulation rates in this region of 1.5 mm/year. If this is representative for the entire mudbelt, it would indicate that 6% of the historic annual sediment discharged from the Salinas River is stored on the southern shelf. The northern shelf on the other hand appears to have an excess of stored sediment, with estimates from ^{210}Pb accumulation rates

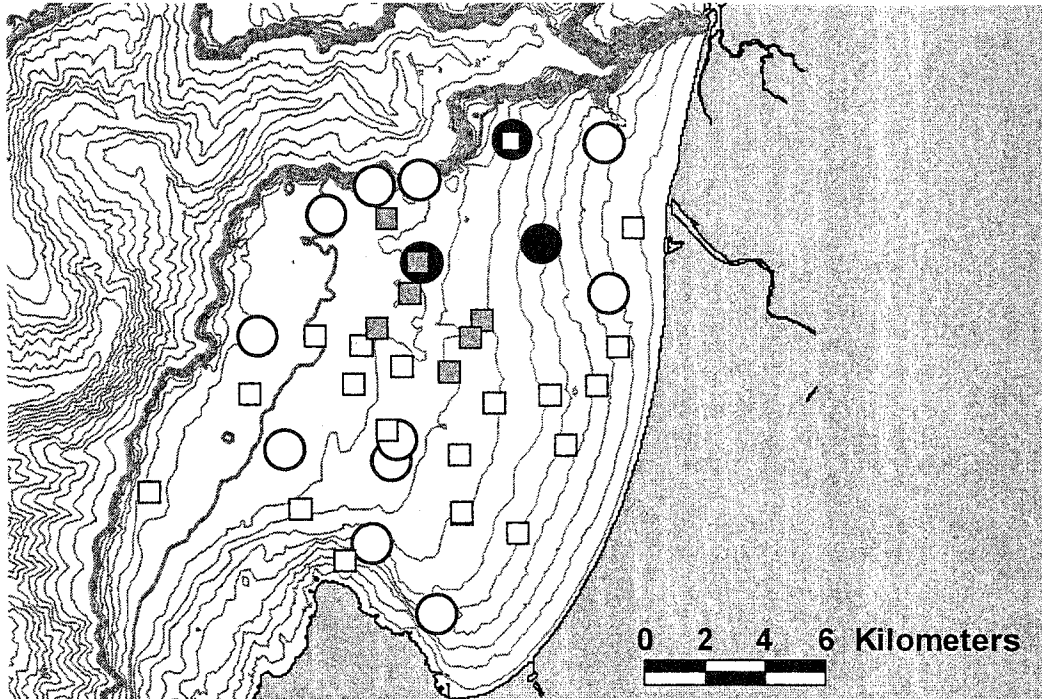


Figure 4-8: Map showing location of box cores collected during April and September of 1995. Flood layer was seen in 3 cores from April (○-box core with no flood layer, ●-box core with flood layer), and 7 cores from September (□-box core with no flood layer, ■ - box core with flood layer). Sampling scheme did not allow for full delineation of flood deposits on either cruise. It is important to note the lack of mud in the nearshore during the April cruise, sediment either was resuspended and removed from this in the 2 weeks between the flood and sampling, or fine-grained sediment could not deposit due to high energy conditions.

indicating almost 2 times the annual input is stored on the shelf (from Eittrheim et al., 2002). Considering the bay as a whole, 50% of the estimated annual baywide input is stored on the shelf (Table 4-2).

The samples collected immediately after the 1995 flood indicate some flood deposit on the shelf, but may have missed the magnitude of the initial deposit. Moorings in the Monterey Submarine Canyon recorded highly turbid, fresher and warmer water passing through the canyon at depth approximately 4 days following the large flood (Johnson et al., 2001). It is thought that sediment resuspension from the shelf created dense turbid bottom plumes that escaped the shelf into the canyon at this time. The removal of sediment from the shallow shelf to the deep ocean via the canyon has been documented by massive failures at the head of the canyon (Okey, 1997), whereas the Johnson et al. (2001) observations suggest a dense underflow from the resuspension of flood deposits. Normark and others (1999) document a lack of fine-grained sediment in the main channel of the fan, indicating that there has been active flow down canyon, and DDT has been found in sediments out to a water depth of 3000 m (Paull et al., 2002), indicating modern delivery of sediment to the deep offshore portions of the canyon.

One possible transport pathway not yet discussed is the generation of river mouth hyperpycnal plumes. During floods on small mountainous rivers, suspended sediment concentrations in river water may be high enough to enter the ocean as dense bottom flows (Mulder and Syvitski, 1995; Warrick and Milliman, in press). The Salinas River has very few suspended sediment concentration measurements, especially during times of high floods. Waananen (1969) reports concentrations of

Table 4-2: Short term modern sediment accumulation estimates for the Monterey Shelf. The northern shelf is capturing all of the sediment input from local rivers, as well as sediment from a more distal source (Eittreim et al., 2002), while the southern shelf is storing only a fraction of the Salinas River input. Overall, modern accumulation rates seem to indicate that short-term accumulation accounts for less than 50% of estimated annual inputs.

Shelf	^{210}Pb Accumulation Rate (mm/yr)⁽¹⁾	Short-Term Accumulation (m³/yr)	Modern Estimated Sediment Delivery (m³/yr)	Percent Accounted For
North	2.5	$1.1 * 10^6$ ⁽²⁾	600,000	180 %
South	1.5	$0.11 * 10^6$	$1.9 * 10^6$	6 %
Total		$1.2 * 10^6$	$2.48 * 10^6$	48 %

Notes:

1. from Lewis et al., 2002
2. from Eittreim et al., 2002

34 g/L during the late February 1969 flood. This measurement was taken before the peak of the flood was reached, indicating that even higher concentrations may be possible. Such high concentrations may generate bottom flows that could allow sediment delivery directly to the canyon, bypassing the shelf entirely.

A quick first order examination of the velocity of river-mouth generated hyperpycnal plumes was done using the Chezy equation, which balances the role of gravity and friction and is expressed as:

$$\alpha * B = C_d * u_{grav}^2$$

where α is the sine of the bottom slope, u_{grav} is the velocity of the plume, C_d is the drag caused by friction on the bottom and B is the depth-integrated buoyancy of the hyperpycnal layer. The buoyancy may be calculated as:

$$B = g s \int_0^{\delta} c' dz$$

where g is the acceleration of gravity, s is the weight of siliceous sediment relative to seawater, δ is the plume thickness, and c' is the sediment volume concentration. We assumed a river mouth of 5 m depth and a drag coefficient of 0.003 (M. Scully, per comm.). Using this equation with variable sediment concentration from 24 – 44 g/L and the most direct down slope paths to the canyon, cross-shelf travel times range from 20 – 35 minutes (Table 4-3). This simplified equation highlights that if flood events discharge hyperpycnal plumes, much or most of the sediment might move across the shelf and into deeper water in a matter of minutes to hours. This provides additional support for the theory put forth by Johnson and others (2001) that their

Table 4-3: First order approximations on travel velocities and time to escape for hypothetical Salinas River mouth generated hyperpycnal plumes. Sediment concentrations ranging from 24 – 44 g/L were used, along with a Coefficient of Drag (C_d) of 0.003 and a river mouth depth of 5 meters. Escape via hyperpycnal plume would be on the order of minutes to hours.

	Distance to Shelfbreak (km)	α	B (24 g/L)			B (34 g/L)			B (44 g/L)		
			U_{grav} (m/s)	Time to Shelf Edge (minutes)	U_{grav} (m/s)	Time to Shelf Edge (minutes)	U_{grav} (m/s)	Time to Shelf Edge (minutes)			
path1	4	0.0250	0.7322	2.4701	27	1.0373	2.9400	23	1.3424	3.3445	20
path2	4.8	0.0208	0.7322	2.2549	35	1.0373	2.6839	30	1.3424	3.0531	26
path3	6.2	0.0371	0.7322	3.0087	34	1.0373	3.5811	29	1.3424	4.0738	25

observed underflows are due to resuspension, rather than river mouth generated hyperpycnal plumes.

4.3 Summary

Estimates of sediment storage on the shelf of Monterey Bay indicate that between 24 and 48 % of the sediment discharged from local rivers is retained. Eittrheim et al. (2002b) indicated that modern sediment budgets reveal that the north shelf was currently capturing all of the sediment delivered from local rivers, while the southern shelf modern accumulation only accounts for a small fraction of total load (6-7%). Overall, this system is mostly a bypassing system, with the Monterey Submarine Canyon presumably acting as a conduit of sediment to the deep ocean. This movement of sediment through the canyon must be quite frequent as the canyon receives a large portion of sediment from the Salinas River, as well as 400,000 m³ from littoral transport and the head of the canyon is not filling up, and much clean sand is seen in the axis of the canyon (Paull et al., 2003). Flushing events have been observed in the canyon (Okey, 1997; Paull et al., 2003), which must move the majority of the sediment through the canyon, especially since mean tidal currents in the canyon are not strong enough to transport much sediment seaward (Xu et al., 2002).

It has been estimated in large drainage basins that a substantial portion of fluvial sediment is sequestered in the lower floodplain of rivers, downstream of the last gauging station. Goodbred and Kuehl (1999), for instance have estimated 20-30% storage in the lower Bengal delta. While it seems highly unlikely that such a small and flashy river as the Salinas could store 30% of the sediment load measured at Spreckels, 15 km from the coast, even a loss of this magnitude would still mean that more than 70% of the Spreckels

load escapes the shelf. This is consistent with what is seen on the northern California shelf, where an estimated 25 % of sediment is stored on the shelf (Wheatcroft et al., 1997), the rest escaping the shelfbreak.

The importance of the large magnitude escape of sediment to the deep ocean may be far reaching. In these regions, delivery of sediment and sediment-associated material (e.g., carbon and nutrients) to the deep ocean may be fostering a unique biogeochemical system in the nearby deep-sea. The modern input of anthropogenic materials, such as fertilizers and pesticides may have large impacts on these systems. Shallow-water systems also could be impacted if the sediment is temporarily stored prior to ultimate removal to the deep-sea. With possible residence times of hours to weeks, the positive effects of nutrient delivery and the negative effects of anthropogenic pollutant delivery may be tempered in these regions.

If narrow active margins dominated by floods allow bypassing of sediment to the deep ocean, this may change the way we think about the carbon cycle. Berner (1982) states that over 80% of carbon burial takes place on deltas and shelves, if much of the carbon delivered by small rivers on active coastlines is bypassing the shelf, this may affect the quantification of the shelf as such a large carbon reservoir. A quick escape to the deep sea means little remineralization and higher than expected percentages of terrestrial carbon in slope and deep-sea sediment. Prahl and others (Prahl et al., 1994; Prahl and Muehlhausen, 1989) have seen this in cores from the shelf, slope and basin off the mouth of the Columbia River, with widespread terrestrial carbon found offshore into the hemipelagic Cascadia Basin.

Further work should be conducted on the shelf to quantify the residence time of flood deposits on the shelf and determine the timing and magnitude of sediment delivery to the canyon. If conducted concurrently with monitoring in the canyon it would allow for the quantification of sediment delivery from the rivers to the deep-sea.

4.4 References

- Anima, R.J., Eittreim, S.L., Edwards, B.D. and Stevenson, A.J., 2002. Nearshore morphology and late Quaternary geologic framework of the northern Monterey Bay Marine Sanctuary, California. *Marine Geology*, 181: 35-54.
- Barron, J.A., Heusser, L., Herbert, T. and Lyle, M., 2003. High-resolution climatic evolution of coastal northern California during the past 16,000 years. *Paleoceanography*, 18(1).
- Berner, R.A., 1982. Burial of organic carbon and pyrite sulfur in the modern ocean: Its geochemical and environmental significance. *American Journal of Science*, 282: 451-473.
- Best, T.C. and Griggs, G.B., 1991. A Sediment Budget for the Santa Cruz Littoral Cell, California, From Shoreline to Abyss. SEPM Special Publication No. 46, pp. 35-50.
- Borgeld, J.C., 1985. Holocene Stratigraphy and Sedimentation on the Northern California Continental Shelf. Ph.D. dissertation, University of Washington, 177 pp.
- Bradley, W.C. and Griggs, G.B., 1986. Form, genesis, and deformation of central California wave-cut platforms. *Geological Society of America Bulletin*, 87: 433-449.
- Brown, W.M., III and Ritter, J.R., 1971. Sediment Transport and Turbidity in the Eel River Basin, California. Water Supply Paper 1986, USGS, 70 pp.
- Cacchione, D.A. and Drake, D.E., 1986. Nepheloid layers and internal waves over continental shelves and slopes. *Geo-Marine Letters*, 6: 147-152.
- Chin, J.L., Clifton, H.E. and Mullins, H.T., 1988. Seismic Stratigraphy and Late Quaternary Shelf History, South-Central Monterey Bay, California. *Marine Geology*, 81: 137 - 157.
- Drake, D.E., 1999. Temporal and spatial variability of the sediment grain-size distribution on the Eel Shelf: the flood layer of 1995. *Marine Geology*, 154: 169-182.
- Eittreim, S.L., Anima, R. and Stevenson, A.J., 2002a. Seafloor geology of the Monterey Bay area continental shelf. *Marine Geology*, 181: 3-34.
- Eittreim, S.L., Edwards, B.D. and Anima, R.J., 2000. Mid-shelf mudbelt in northern Monterey Bay (abstract). *Trans. Am. Geophysical Union* 81 (suppl.), 682.

- Eittrheim, S.L., Xu, J.P., Noble, M. and Edwards, B.D., 2002b. Towards a sediment budget for the Santa Cruz Shelf. *Marine Geology*, 181(1-3): 235-248.
- Fritz, S.C., Metcalf, S.E. and Dean, W.E., 2001. Holocene climate of the Americas inferred from paleolimnological records. In: V. Markgraf (Editor), *Interhemispheric Climate Linkages (Present and Past Interhemispheric Climate Linkages in the Americas and Their Social Effects)*. Academic, San Diego, California, pp. 241-264.
- Goodbred, S.L. and Kuehl, S.A., 1999. Holocene and modern sediment budgets for the Ganges-Brahmaputra river system: Evidence for highstand dispersal to floodplain, shelf and deep-sea depocenters. *Geology*, 27(6): 559 - 562.
- Greene, H.G., 1977. *Geology of the Monterey Bay region*. Open File 77-718, USGS.
- Griggs, G.B. and Hein, J.R., 1980. Sources, Dispersal and Clay Mineral composition of fine-grained sediment off central and northern California. *Journal of Geology*, 88: 541-566.
- Grossman, E.E., Eittrheim, S.L., Field, M.E. and Edwards, B.D., 2002. Mid-Shelf mud Deposition During the Holocene Transgression on the Monterey Bay, California Shelf, EOS Trans. AGU Fall Meet. Suppl. 83(47) Abstract OS71D-0318.
- Helley, E.J. and LaMarche, V.C., 1973. Historic flood information for northern California streams from geological and botanical evidence. Professional Paper 485-E, USGS.
- Inman, D.L. and Jenkins, S.A., 1999. Climate Change and the Episodicity of Sediment Flux of Small California Rivers. *Journal of Geology*, 107: 251-270.
- Johnson, K.S., Paull, C.K., Barry, J.P. and Chavez, F.P., 2001. A decadal record of underflows from a coastal river into the deep sea. *Geology*, 29(11): 1019-1022.
- Kuehl, S.A., Levy, B.M., Moore, W.S. and Allison, M.A., 1997. Subaqueous delta of the Ganges-Brahmaputra river system. *Marine Geology*, 144(1-3): 81-96.
- Leithold, E.L., 1989. Depositional processes on an ancient and modern muddy shelf, northern California. *Sedimentology*, 36: 179-202.
- Lewis, R.C. et al., 2002. Accumulation rate and mixing of shelf sediments in the Monterey Bay National Marine Sanctuary. *Marine Geology*, 181: 157-169.
- Mertes, L.A.K. and Warrick, J.A., 2001. Measuring flood output from 110 coastal watersheds in California with field measurements and SeaWiFS. *Geology*, 29(7): 659-662.

- Milliman, J.D., Farnsworth, K.L. and Albertin, C.S., 1999. Flux and fate of fluvial sediments leaving large islands in the East Indies. *Journal of Sea Research*, 41: 97 - 107.
- Milliman, J.D. and Syvitski, J.P.M., 1992. Geomorphic/Tectonic Control of Sediment Discharge to the Ocean: The Importance of Small Mountainous Rivers. *Journal of Geology*, 100: 525 - 544.
- Mulder, T. and Syvitski, J.P.M., 1995. Turbidity currents generated at river mouths during exceptional discharges to the world oceans. *Journal of Geology*, 103(3): 285-299.
- Mullins, H.T., Nagel, D.K. and Dominguez, L.L., 1985. Tectonic and Eustatic Controls of Late Quaternary Shelf Sedimentation along the Central California (Santa Cruz) Continental Margin: High-Resolution Seismic Stratigraphic Evidence. *Sedimentary Geology*, 45: 327-347.
- Nittrouer, C.A. and Kuehl, S.A. (Editors), 1995. Special Issue: Geological Significance of Sediment Transport and Accumulation on the Amazon Continental Shelf. *Marine Geology*, V. 125, no.3/4, 175-399 pp.
- Normark, W.R., 1999. Late Pleistocene channel-levee development on Monterey submarine fan, central California. *Geo-Marine Letters*, 18: 179 - 188.
- Okey, T.A., 1997. Sediment flushing observations, earthquake slumping and benthic community changes in Monterey Canyon head. *Continental Shelf Research*, 17(8): 877 - 897.
- Orton, G.J. and Reading, H.G., 1993. Variability of deltaic processes in terms of sediment supply, with particular emphasis on grain size. *Sedimentology*, 40: 475-512.
- Paull, C.K., Greene, H.G., Ussler, W., III and Mitts, P.J., 2002. Pesticides as tracers of sediment transport through Monterey Canyon. *Geo-Marine Letters*, 22: 121-126.
- Paull, C.K., Ussler, W., III, Greene, H.G. and Keaten, R., 2003. Caught in the act: the 20 December 2001 gravity flow event in Monterey Canyon. *Geo-Marine Letters*, 22: 227-232.
- Prahl, F.G., Ertel, J.R., Goni, M.A., Sparrow, M.A. and Eversmeyer, B., 1994. Terrestrial organic carbon contributions to sediments on the Washington margin. *Geochimica et Cosmochimica*, 58(14): 3035-3048.
- Prahl, F.G. and Muehlhausen, L.A., 1989. Lipid Biomarkers as Geochemical Tools for Paleooceanographic Study. In: W.H. Berger, V.S. Smetacek and G. Wefer

- (Editors), *Productivity of the Ocean: Present and Past*. John Wiley and Sons Limited, pp. 271-289.
- Schwartz, D.L., Mullins, H.T. and Belknap, D.F., 1986. Holocene Geologic History of a Transform Margin Estuary: Elkhorn Slough, Central California. *Estuarine, Coastal and Shelf Science*, 22: 285-302.
- Tait, J.F. and Revenaugh, J., 1998. Source-Transport Inversion: An application of geophysical inverse theory to sediment transport in Monterey Bay, California. *Journal of Geophysical Research*, 103: 1275-1283.
- Waananen, A.O., 1969. Floods of January and February 1969 in Central and Southern California. Open-File Report, USGS Water Resources Division, Menlo Park, CA, 223 pp.
- Warrick, J.A. and Milliman, J.D., in press. Hyperpycnal sediment discharge from semi-arid southern California rivers—implications for coastal sediment budgets. *Geology*.
- Watson, F., Newman, W., Anderson, T., Alexander, S. and Kozlowski, D., 2001. Winter Water Quality of the Carmel and Salinas Lagoons, Monterey, California:2000/2001 WI-2001-01, The Watershed Institute Earth Systems Science and Policy California State University Monterey Bay, 42 pp.
- Wheatcroft, R.A., Sommerfield, C.K., Drake, D.E., Borgeld, J.C. and Nittrouer, C.A., 1997. Rapid and widespread dispersal of flood sediment on the Northern California margin. *Geology*, 25(2): 163-166.
- Wright, L.D. and Coleman, J.M., 1972. River Delta Morphology: Wave Climate and the Role of the Subaqueous Profile. *Science*, 176: 282-284.
- Xu, J.P. et al., 2002. Distribution and transport of suspended particulate matter in Monterey Canyon, California. *Marine Geology*, 181: 215-234.

Chapter 5: Summary

5.1 Summary

The purpose of this dissertation is to describe the controls on delivery of fluvial sediment to the coastal oceans. The global perspective is presented, as well as an in-depth look at the local scale. Understanding the controls on the magnitude and timing of sediment delivery to the coastal ocean is important when describing the role of rivers in the biological, chemical, physical and geological systems found in the coastal zones.

A database of approximately 1500 rivers was assembled to allow for global estimates of fluvial delivery of water and sediment to the coastal ocean. The estimates were made by extrapolating data from monitored rivers, usually the larger rivers, to adjacent unmonitored basins. This allowed for an estimate of 35,000 km³ of freshwater discharge, $4 * 10^6$ t/yr of dissolved solids and $18.6 * 10^6$ t/yr of suspended sediment delivered annually to the coastal oceans.

Large rivers such as the Amazon, Huangehe (Yellow River) and Ganges River provide a large portion of this global estimate. However, global delivery of fluvial water and sediment, both suspended and dissolved, is dominated by southeast Asia (Figure 1-5). Over 30% of the global freshwater discharge to the oceans is estimated to originate in southeast Asia and Oceania. This same region of the world is responsible for over 30% of the dissolved solid input and an astounding 70% of the suspended sediment. This is in part due to the presence of the Ganges and Brahmaputra rivers, as well as the large Chinese rivers in this region, but is mainly due to the unique climatic, geologic and geomorphic character of the smaller rivers in

this region. The young volcanic rock, combined with the large quantity of rainfall produce large sediment loads.

The importance of small rivers draining mountainous coastlines was emphasized in this study. These small watersheds do not provide large amounts of storage for either water or sediment compared with larger rivers, allowing for quick transport from headwaters to the coastal ocean. Although larger rivers have greater discharge and sediment loads, the yields (load normalized to basin area) of smaller rivers, especially those draining mountainous coastlines, may be magnitudes larger (Figure 1-3) (Milliman and Syvitski, 1992).

The Salinas River was the focus of an in-depth study on the controls on a small (11,000 km²), semi-arid watershed. This river discharges into the Monterey Bay (Central California) an average of 0.4 km³ of water and 3.3 tonnes of sediment per year. The annual precipitation is less than 30 cm for much of the basin, with some of the higher mountainous regions getting almost 1 meter of rainfall each year. All significant rainfall in the watershed falls during the winter months. The Salinas River was chosen to examine local controls on delivery because there is a significant historical dataset from monitoring efforts throughout the basin, and it is known to be similarly affected by global phenomena, such as El Niño, as the well-studied southern California rivers. Basin scale control on the discharge of the river is dominated by the underlying geology as well as the anthropogenic changes to the watershed. The Nacimiento and San Antonio dams have reduced winter flows, and allowed for summer releases into the river. The releases are scheduled to allow for flow into the

lower reaches of the river to maximize water-table recharge along the course of the river.

Despite the highly controlled nature of the Salinas River, the winter discharge is dominated by events, with large, quick increases in flow from short-lived, intense precipitation events. The frequency of these events is in turn determined by the oceanic and atmospheric conditions present offshore. Historically, large flood events on the Salinas River almost entirely correlate with El Niño events, with the exception of the large flood in 1938. However, not all El Niño years produce large flood events. The probability of a large flood on the Salinas River is determined by the interaction of the El Niño/Southern Oscillation (ENSO) with the Pacific Decadal Oscillation (PDO). The coinciding of warm phases of both of these large-scale phenomena produces significantly higher annual discharges than any other combination of the climatic phenomena.

The local and global controls determine the timing and magnitude of delivery of both freshwater and sediment to the Monterey Bay. Estimating the sediment load of the river from historical gauging records allows us to determine the role the Salinas River plays in the sediment budget of the Monterey Bay. The coastal environment of the bay is unique in that the Monterey Submarine Canyon bisects the bay including the littoral zone, limiting the exchange of sediment between the southern and northern shelves. This is particularly interesting because the Salinas River is estimated to discharge approximately 3 times the sediment onto the southern shelf as the creeks and rivers entering the northern half of the bay. This is in contrast to the long-term storage of sediment, because the northern shelf has 3 times the amount of sediment

sequestered than the southern shelf. This discrepancy in the long-term sediment budget indicates the uncertainties that exist in our estimates of sediment delivery to the Monterey Bay throughout the Holocene.

The estimate of Holocene sediment discharge from the rivers and creeks of the bay indicate that between 17 and 38% of the sediment is stored on the shelf. The northern shelf is a trapping shelf, while the southern shelf appears to allow for the bypassing of sediment. However, the transport pathways of sediment escape are currently unknown. Some evidence points to high-concentration sediment flows down the canyon from resuspension of flood deposits on the shelf (Johnson et al., 2001). Hyperpycnal flows from the river mouth may also be generated during the largest of the floods. Regardless of the method, modern transport to the deep-ocean via the canyon is supported by the presence of DDT to depths of > 3000m in the Monterey Canyon (Paull et al., 2002).

In the future, more studies on short-term processes need to be conducted to accurately determine the modern transport pathways. Further delineating the pathways on the shelf, as well as the interaction of the river with the Salinas Lagoon, is important to quantifying the sediment delivery, transport and storage in the Monterey Bay. This combined with further studies to better estimate Holocene sediment delivery will improve both the short- and long-term sediment budgets of the Monterey Bay.

5.2 References:

- Johnson, K.S., Paull, C.K., Barry, J.P. and Chavez, F.P., 2001. A decadal record of underflows from a coastal river into the deep sea. *Geology*, 29(11): 1019-1022.
- Milliman, J.D. and Syvitski, J.P.M., 1992. Geomorphic/Tectonic Control of Sediment Discharge to the Ocean: The Importance of Small Mountainous Rivers. *Journal of Geology*, 100: 525 - 544.
- Paull, C.K., Greene, H.G., Ussler, W., III and Mitts, P.J., 2002. Pesticides as tracers of sediment transport through Monterey Canyon. *Geo-Marine Letters*, 22: 121-126.

VITA

Katherine L. Farnsworth was born in Vallejo, California, on November 8, 1970. After completing high school at King City Secondary School, in King City, Ontario, Canada, she attended DePauw University in Greencastle, Indiana. After receiving her B.A. in Geography and Computer Science in 1993, she enjoyed a year of travel and expanded her transcript with classes at Middle Tennessee State University. She then entered the School of Marine Science at the College of William and Mary in Williamsburg, Virginia in the fall of 1994. Completing her M.S. in Marine Science in the spring of 1997, she accepted a position working at the School of Marine Science. She entered the doctoral program at the College of William and Mary, School of Marine Science in January 1999.